Chem Soc Rev

Chemical Society Reviews

www.rsc.org/chemsocrev

Volume 42 | Number 14 | 21 July 2013 | Pages 5981–6202

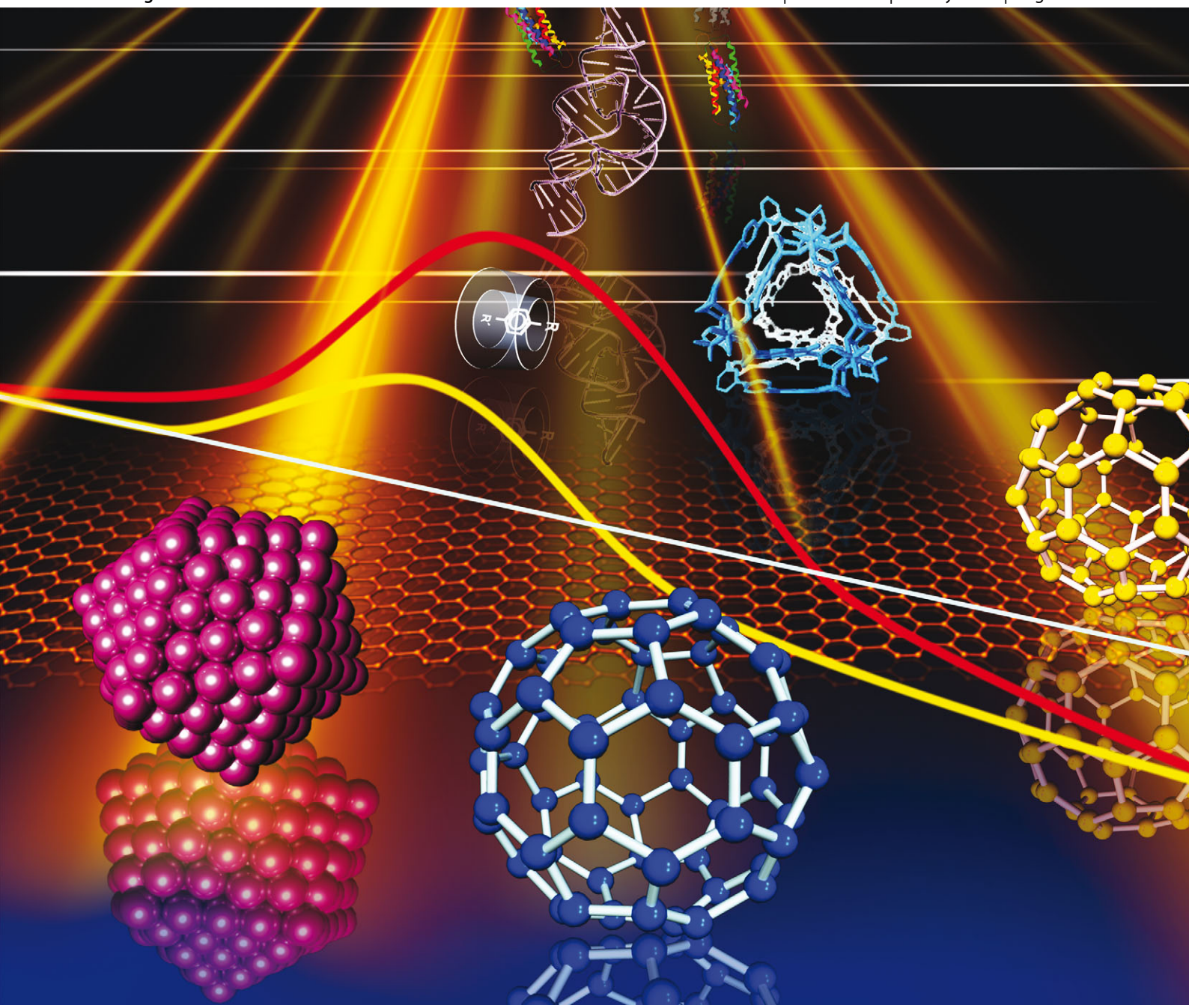

ISSN 0306-0012

RSC Publishing

REVIEW ARTICLE

Hui Wei and Erkang Wang

Nanomaterials with enzyme-like characteristics (nanozymes): next-generation artificial enzymes

0306-0012(2013)42:14;1-5

Chem Soc Rev

RSC Publishing

REVIEW ARTICLE

View Article Online
View Journal | View Issue

Cite this: *Chem. Soc. Rev.*, 2013, **42**, 6060

Nanomaterials with enzyme-like characteristics (nanozymes): next-generation artificial enzymes†

Hui Wei*‡ and Erkang Wang*

Received 28th November 2012

DOI: 10.1039/c3cs35486e

www.rsc.org/csr

Over the past few decades, researchers have established artificial enzymes as highly stable and low-cost alternatives to natural enzymes in a wide range of applications. A variety of materials including cyclodextrins, metal complexes, porphyrins, polymers, dendrimers and biomolecules have been extensively explored to mimic the structures and functions of naturally occurring enzymes. Recently, some nanomaterials have been found to exhibit unexpected enzyme-like activities, and great advances have been made in this area due to the tremendous progress in nano-research and the unique characteristics of nanomaterials. To highlight the progress in the field of nanomaterial-based artificial enzymes (nanozymes), this review discusses various nanomaterials that have been explored to mimic different kinds of enzymes. We cover their kinetics, mechanisms and applications in numerous fields, from biosensing and immunoassays, to stem cell growth and pollutant removal. We also summarize several approaches to tune the activities of nanozymes. Finally, we make comparisons between nanozymes and other catalytic materials (other artificial enzymes, natural enzymes, organic catalysts and nanomaterial-based catalysts) and address the current challenges and future directions (302 references).

1. Introduction

Artificial enzymes, the term coined by Ronald Breslow for enzyme mimics,[1] is a very important and exciting branch of biomimetic chemistry which is inspired by nature and aims to imitate the essential and general principles of natural enzymes using alternative materials.[2,3] Over the past few decades, researchers have established artificial enzymes as highly stable and low-cost alternatives to natural enzymes in a wide range of applications. Cyclodextrins, metal complexes, porphyrins, polymers, supramolecules and biomolecules (such as nucleic acids, catalytic antibodies and proteins) have been extensively explored to mimic the structures and functions of natural enzymes through various approaches.[1–17] To date, remarkable progress has been made in the field of artificial enzymes (Fig. 1), and several monographs and numerous excellent reviews have been published.[2–4,18–34]

Recently, some nanomaterials, such as fullerene derivatives, gold nanoparticles, rare earth nanoparticles and ferromagnetic nanoparticles, have been found to exhibit unexpected enzyme-like activity.[35–48] Since then, considerable advances have been made in this area due to the tremendous progress in nano-research and the unique characteristics of nanomaterials.[49–53] These nanomaterial-based artificial enzymes (nanozymes) have already found wide applications in numerous fields, including biosensing, immunoassays, cancer diagnostics and therapy, neuroprotection, stem cell growth, and pollutant removal. The term "nanozymes" was initially coined by Scrimin, Pasquato and co-workers to describe their thiol monolayer protected gold clusters with outstanding ribonuclease-like activity.[39] Here, we adopt the term and extend it to nanomaterials with enzyme-like activities. Although the progress and achievements of classic artificial enzymes have been thoroughly reviewed in the literature, no comprehensive review has been devoted to nanozymes.[51–63] To highlight the significant progress of nanozyme research, this review discusses various nanomaterials that mimic natural enzymes and their mechanisms, kinetics and numerous applications. Different approaches to tune the activities of nanozymes are summarized. We also compare nanozymes to other catalytic materials (such as other artificial enzymes, natural enzymes, organic catalysts and nanomaterial-based catalysts). Finally, we discuss the current challenges facing nanozyme technologies and future directions to realize their great potential. Note: although nanozymes include artificial hydrolytic enzymes and others, the current review mainly focuses on redox-based nanozymes, the intrinsic enzyme-like activities of which are from

State Key Laboratory of Electroanalytical Chemistry, Changchun Institute of Applied Chemistry, Chinese Academy of Sciences, Changchun, Jilin 130022, China. E-mail: weihui@nju.edu.cn, ekwang@ciac.jl.cn

† Electronic supplementary information (ESI) available: See DOI: 10.1039/c3cs35486e

‡ Current address: Department of Biomedical Engineering, College of Engineering and Applied Sciences, Nanjing University, Nanjing, Jiangsu, 210093, China.

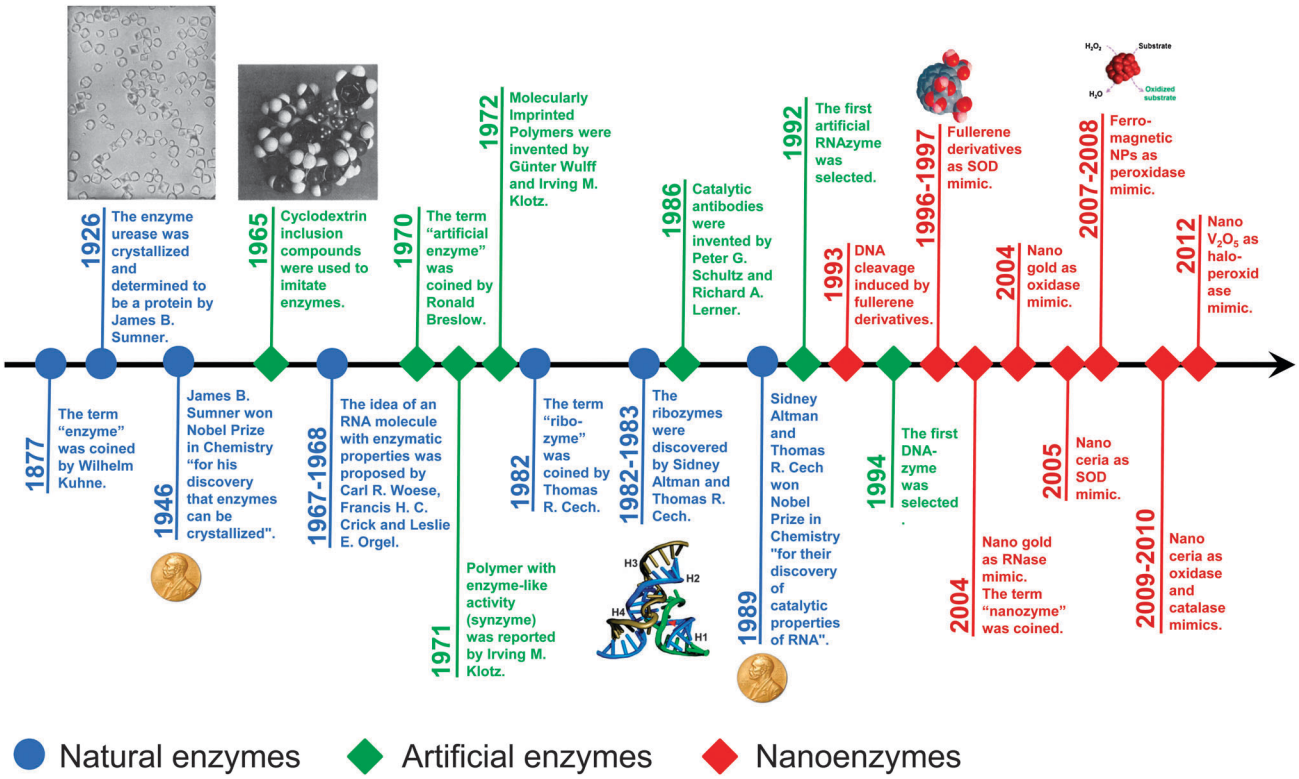

Fig. 1 A brief timeline for the development of artificial enzymes (natural enzymes are also listed for comparison) (see Table S1, ESI† for related references).

the nanomaterials cores instead of the functional groups present on the protecting shells.

Readers are referred to the monographs and reviews for more comprehensive information regarding other artificial enzymes rather than nanozymes (note: due to the space limit, only a small number of references are cited).[2–4,17–32,64–67]

2. Nanomaterials as nanozymes to mimic natural enzymes

At first glance, it seems counterintuitive to imitate natural enzymes with nanomaterials since they are so different in many ways. For example, most natural enzymes, which are proteins,

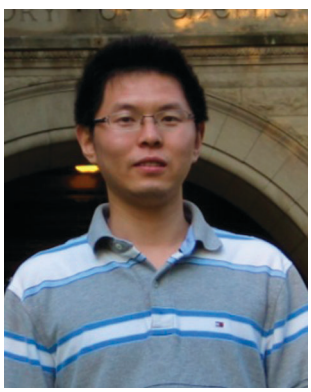

Hui Wei

Hui Wei is a Professor in College of Engineering and Applied Sciences at Nanjing University. He joined Nanjing University after postdoctoral training with Professors Yi Lu and Shuming Nie, respectively. He received his BS degree from Nanjing University in 2003, where he carried out undergraduate research with Professor Xinghua Xia. In the same year he joined Professor Erkang Wang's group at Changchun Institute of Applied Chemistry, Chinese Academy of Sciences, and received his PhD degree in 2008. He has published over 30 papers in peer-reviewed international journals. His work has been cited more than 1500 times with an H-index of 24. His research interests are focused on functional nanomaterials and new methodology for analytical and biomedical applications.

Erkang Wang

Erkang Wang is a Professor of Chemistry at Changchun Institute of Applied Chemistry, Chinese Academy of Sciences. He is Academicians of the Chinese Academy of Sciences and the Third World Academy of Sciences. He obtained his BS degree from University of Shanghai in 1952 and his PhD degree from Czechoslovak Academy of Sciences in 1959 under the direction of Professor J. Heyrovsky (Nobel Laureate). He has published over 690 papers in peer-reviewed journals. His work has been cited more than 15 000 times with an H-index of 62. His research interests lie in the fields of nanomaterials/nanotechnology, biosensors, electrochemistry and electrochemiluminescence.

have exact amino acid sequences and thus well-defined tertiary structures. On the other hand, most nanomaterials are not atomically uniform due to size and shape variations.[68] Proteins are also considered as soft materials while nanomaterials can be hard with crystalline cores.[68] However, they share certain similarities, such as overall size, shape and surface charge, which enable nanomaterials to mimic natural enzymes.[68] In this section, we will survey various nanomaterials that can mimic natural enzymes.

2.1 Cerium oxide-based nanomaterials

Cerium oxide (ceria) is well known for its highly catalytic performance in various applications due to the presence of mixed valence states of Ce^{3+} and Ce^{4+}, and the presence of oxygen vacancies.[51,53,69] Oxygen vacancies compensate the reduction of positive charge by Ce^{3+} and thus stabilize the chemically active Ce^{3+} oxidation state. The redox couple can switch between each state in a $CeO_2 \leftrightarrow CeO_{2-x} + x/2O_2$ ($Ce^{4+} \leftrightarrow Ce^{3+}$) recycle process, which is the key to the catalytic activity.[51,53] Moreover, nanoceria has dominant Ce^{3+} and oxygen vacancies on its surface due to a large surface-to-volume ratio. Early studies have shown that cerium complexes have many biological applications. For example, cerium(III) nitrate decreased superoxide content and thus promoted the germination of aged rice seed.[70] Thus, it was reasonable to investigate the superoxide oxidase (SOD) mimetic activity of nanoceria for catalytic removal of superoxide radicals. The seminal study by Seal *et al.* showed that vacancy-engineered nanoceria indeed protected normal cells but not tumor cells from radiation-induced damage (Fig. 2).[41] The protective role of the nanoceria was attributed to the elimination of radiation-induced free radicals, which were hypothesized to occur through catalyzation *via* a $Ce^{3+} \rightarrow Ce^{4+} \rightarrow Ce^{3+}$ regeneration process. The differential protecting capabilities in normal cells *vs*. tumor cells might be due to the fact that chromatin in tumors was more loosely packed and thus exposed more bases for free-radical attack.[41] Following this early work, numerous studies have confirmed the enzyme (including SOD, catalase, oxidase, *etc.*) mimetic properties

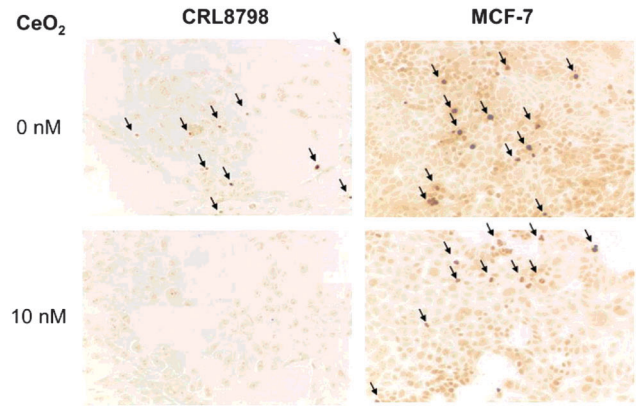

Fig. 2 Nanoceria with SOD mimicking activity could prevent normal human breast cell line (CRL8798) but not a human breast tumor cell line (MCF-7) from radiation induced damage. Reprinted with permission from ref. 41. Copyright (2005) American Chemical Society.

$$2O_2^{\bullet -} + 2H^+ \xrightarrow{SOD} H_2O_2 + O_2 \quad (1)$$

Scheme 1 The reaction catalyzed by SOD.

of nanoceria and have shown promising biomedical applications for scavenging radicals both *in vitro* and *in vivo*.[43,51,53,71–108] Here, we discuss the enzyme mimetic properties of nanoceria and their applications.

2.1.1 Nanoceria as SOD mimics. SOD catalyzes the dismutation of superoxide anions into hydrogen peroxide and molecular oxygen (Scheme 1). Superoxide anion, one of the reactive oxygen species, has been known to cause tissue injury and associated inflammation. Previous research has revealed that SOD play protective roles in the removal of superoxide anions. Due to the limits of native SOD (such as short term stability and high cost), significant efforts have been made to develop SOD mimics.[23,59,64] For example, a manganese-containing biscyclohexylpyridine complex, M40403, has been developed for this purpose.[64] Inspired by the work from Seal and co-workers, recent studies have showed that nanoceria exhibits interesting and promising SOD activity.[43,71,73,76,80,88,91,102]

No direct evidence was presented to support the redox regeneration mechanism in the early study.[41] In a later study, Seal *et al.* performed a competitive assay against cytochrome *c*, which indicated the SOD mimicking activity of the nanoceria.[73] The superoxide anion elimination capability of the nanoceria was also confirmed by electron paramagnetic resonance (EPR) measurements.[76] The results showed that nanoceria with a higher ratio of Ce^{3+}/Ce^{4+} has better activity.[73] They also observed the formation of hydrogen peroxide, which is one of the products of the SOD catalyzing reaction. The kinetics measurement showed that the nanoceria with a size of 3–5 nm was more efficient as a SOD mimic than a native CuZn SOD (with rate constants of 3.6×10^9 M^{-1} s^{-1} and $(1.3–2.8) \times 10^9$ M^{-1} s^{-1}, respectively). A dismutation mechanism similar to Fe- and Mn-SOD was proposed (Fig. 3a).[73] An alternative mechanism was also proposed as shown in Fig. 3b.[53] None of them clearly involved the auto-regeneration process of Ce^{3+} on nanoceria, though the second mechanism indicated that nanoceria with a higher ratio of Ce^{3+}/Ce^{4+} should have higher activity. If an auto-regeneration process indeed occurred, the ratio of H_2O_2 to O_2 would be larger than 1. This could be tested and verified experimentally in the future. Computational studies would also help to clarify the detailed mechanism when combined with further experimental results.

Though initial studies suggested that nanoceria could also eliminate hydroxyl radicals,[43,72] later EPR measurements demonstrated that nanoceria does not have such hydroxyl radical elimination capability.[76] This also suggested that nanoceria has some specificity towards superoxide radicals dismutation.

Applications. SOD mimics play important roles in many redox-active processes, such as scavenging reactive oxygen species, acting as anti-inflammatory and anti-oxidation agents, and promoting stem cell growth. Below, several selected examples are discussed to show the wide and promising applications of nanoceria based SOD mimics.

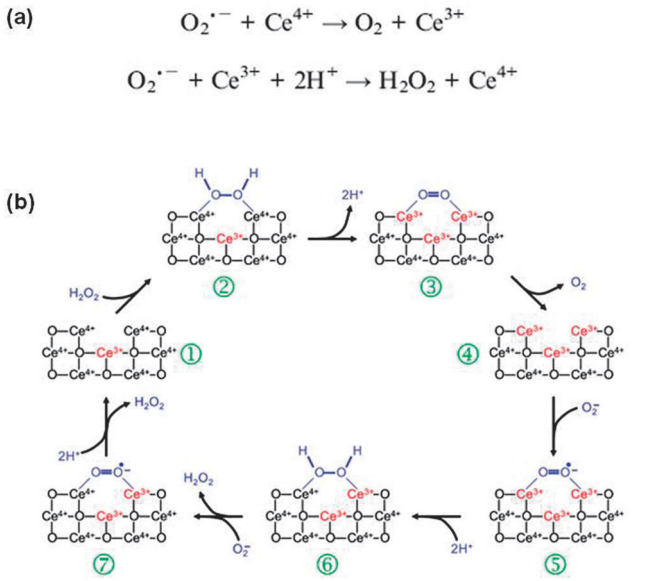

Fig. 3 Proposed mechanisms of nanoceria based SOD mimic: (a) reprinted with permission from ref. 73; copyright (2007) Royal Society of Chemistry; (b) reprinted with permission from ref. 53; copyright (2011) Royal Society of Chemistry.

(a) Anti-inflammatory effects. Similar to native SOD, nanoceria-based nanozymes exhibit anti-inflammatory effects due to the presence of mixed valence and oxygen defects, rendering them as highly efficient catalysts. Hirst and co-workers reported the anti-inflammatory properties of nanoceria.[84] Using J774A.1 murine macrophage cells as a model, they demonstrated that the nanoceria were benign and were internalized by the cells. Chemiluminescent and fluorescent measurements demonstrated that the nanoceria was able to decrease ROS production in J774A.1 cells. They further showed that nanoceria inhibited the production of the free radical nitric oxide, a critical mediator of inflammation when over-expressed. They also claimed that the nanoparticles did not cause any *in vivo* lesions in mice when different doses were administered intravenously, but did not further investigate the *in vivo* activity of the nanozymes.

(b) Antioxidants. Nanoceria-based SOD mimics have also been investigated as antioxidants. The antioxidant effects and the biological antioxidant mechanisms of nanoceria were examined by gradual doping of Sm^{3+}.[91] Since the doping decreased the Ce^{3+} concentration without affecting oxygen vacancies, the study confirmed that the Ce^{3+}/Ce^{4+} redox reactions were responsible for the nanozymes' outstanding biological activities.[91] When encapsulated within a ferritin cage, Liu *et al.* showed that the ROS-scavenging activity of 4.5 nm nanoceria was enhanced.[99] The presence of a ferritin shell also facilitated cellular uptake and improved their biocompatibility. A recent study showed that nanoceria was able to protect cardiac progenitor cells (CPCs), a promising cell source for cardiac regeneration, from hydrogen peroxide-induced cytotoxicity for one week.[100] The observed protective effects was attributed to the nanozyme's self-regenerating antioxidant mechanism involving the Ce^{3+}/Ce^{4+} redox cycles.

(c) Promotion of stem cell growth. Polymeric biomaterials have been extensively used in tissue engineering (such as in directing the growth of stem cells) because of their unique properties. Hybrid materials formed by incorporating inorganic materials into a polymeric matrix have even more promising advantages, such as novel functionalities, enhanced biocompatibility and improved mechanical and chemical properties. In their interesting study, Mandoli and co-workers showed that when nanoceria was fabricated together with PLGA scaffolds, the as-prepared hybrids exhibited enhanced mechanical properties.[87] They further cast the hybrids onto pre-patterned molds and demonstrated that the composite scaffold could align murine-derived cardiac and mesenchymal stem cells growth with enhanced bioactivity and better adhesion (Fig. 4). They then elucidated the potential mechanism by comparing the nanoceria composites to PLGA films without nanoceria and PLGA films with nanostructured TiO_2. Though nanostructured TiO_2 also induced directional cell growth, the cell proliferative activity was lower than the activity observed for nanoceria-loaded PLGA. Since the Ce^{3+}/Ce^{4+} redox pair of nanoceria is recyclable while the Ti^{3+}/Ti^{4+} redox pair of TiO_2 is not, the improved performance of the nanoceria hybrids was attributed to the nanoceria's anti-oxidation properties.

(d) Neuroprotection. Nanoceria as a SOD mimic also exhibited neuroprotective activity.[43,72,92] In Chen and co-workers' seminal study, they showed that the pretreatment of cultured retinal neuron cells with nanoceria eliminated the accumulation of hydrogen peroxide-induced reactive oxygen intermediates.[43] More importantly, their animal studies have firmly demonstrated that the nanozymes protected rat retina photoreceptor cells from light-induced degeneration after intravitreal injection (Fig. 5). Surprisingly, the nanozymes still exhibited protective activity towards photoreceptor cells even when administrated after the light exposure. Again, the reactive oxygen intermediate-scavenging activity was attributed to the switchable feature of the Ce^{3+}/Ce^{4+} redox pair. Later studies showed that the nanozymes' neuroprotective activity could be realized in other systems, such

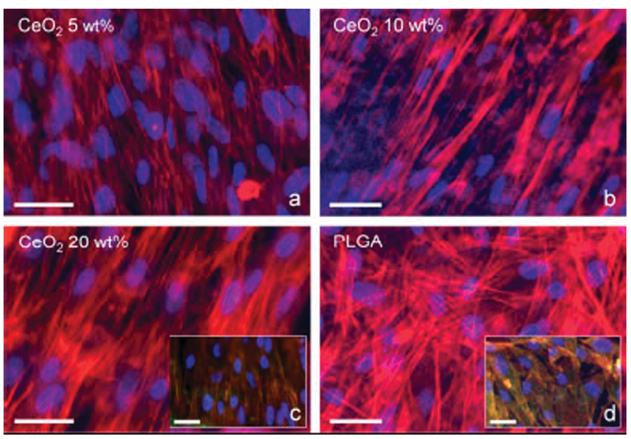

Fig. 4 Stem cell aligned growth induced by nanoceria in PLGA scaffolds. Reprinted with permission from ref. 87. Copyright (2010) John Wiley and Sons.

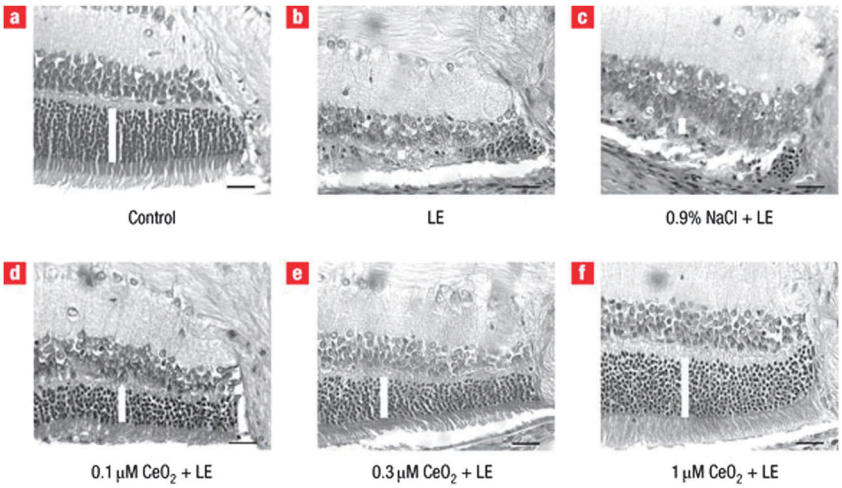

Fig. 5 Intravitreal injection of nanoceria protected rat retina photoreceptor cells from light-induced degeneration. Reprinted with permission from ref. 43. Copyright (2006) Nature Publishing Group.

as adult rat spinal cord neuron and other diseases of the central nervous system.[72]

(e) Other applications. Nanoceria-based SOD nanozymes have been studied for other interesting applications as well. As mentioned above, vacancy engineered nanoceria were able to protect normal human breast cells (but not breast tumor cells) from radiation-induced cell death, suggesting a new application in radiation oncology.[41] Using diabetic rats as a model system, a recent study also showed that the combination of nanoceria and sodium selenite was more effective than either alone in reducing diabetes-induced oxidative stress.[109]

2.1.2 Nanoceria as catalase mimics. Catalase catalyzes the decomposition of hydrogen peroxide into molecular oxygen and water (Scheme 2). Hydrogen peroxide, as the stable end product of superoxide radicals' dismutation (Scheme 1), plays a dual role in biological systems. It can be either a signaling molecule or a non-radical reactive oxygen species.[51] Though hydrogen peroxide itself is stable and less active, it can be converted into highly active and detrimental hydroxyl radical through Fenton chemistry. In nature, catalase is employed as the most efficient enzyme for the conversion of hydrogen peroxide to less active oxygen. Researchers have found that numerous metal oxide (such as nanoceria), as well as metal, nanomaterials exhibit intrinsic catalase activity.[88,95,110,111]

Inspired by the fact that some SOD mimics, such as manganese porphyrins, can also convert hydrogen peroxide into oxygen and water as catalase mimics, Self and co-workers performed a careful study to explore the catalase-like property of nanoceria.[88] The results established that catalase-like activity was dominant for nanoceria with a low Ce^{3+}/Ce^{4+} ratio while SOD-like activity was dominant for nanoceria with a high Ce^{3+}/Ce^{4+} ratio. In a later review from Ghibelli *et al.*, a possible molecular mechanism was proposed (Fig. 6).[53]

$$2H_2O_2 \xrightarrow{\text{Catalase}} 2H_2O + O_2 \quad (2)$$

Scheme 2 The reaction catalyzed by catalase.

So far, there have been no studies reporting the application of a nanomaterial-based catalase mimic.

2.1.3 Nanoceria as oxidase mimics. For reactions catalyzed by oxidase, a substrate is oxidized by molecular oxygen, which can be converted into either water or hydrogen peroxide (or even superoxide radical in some cases) (Scheme 3). For certain substrates, oxidation can result in a color change, which makes them ideal agents for detection purposes. Recent studies have shown that certain nanomaterials can imitate the catalytic activity of oxidase.[40,42,81,90,102,111–119]

As discussed above, nanoceria acts as an efficient anti-oxidant since it can be either a SOD mimic or a catalase mimic, depending on the Ce^{3+}/Ce^{4+} ratio.[88] Studies by Perez and co-workers have revealed that nanoceria can have additional functionality, reporting nanoceria with oxidase-like activity.[81,90] The oxidase mimetic activity of the biocompatible dextran-coated nanoceria towards several colorimetric substrates (ABTS, DOPA and TMB) was studied at acidic pH (Fig. 7).[81] The activity of oxidase instead of peroxidase was confirmed since no H_2O_2 was

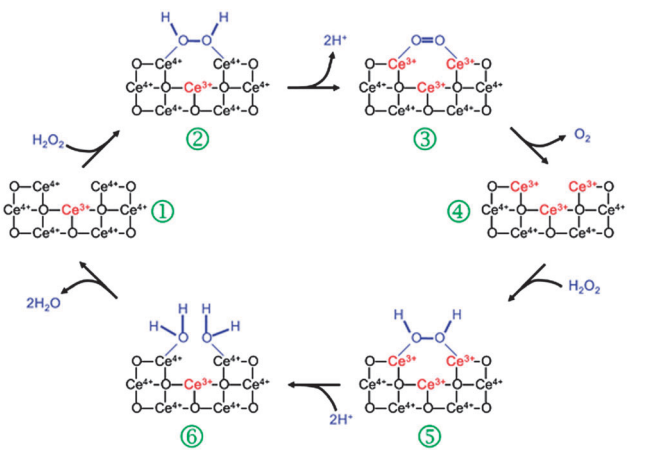

Fig. 6 Proposed mechanism of nanoceria based catalase mimic. Reprinted with permission from ref. 53. Copyright (2011) Royal Society of Chemistry.

$$A_{red} + O_2 + H_2O \xrightarrow{\text{Oxidase}} A_{ox} + H_2O_2 \quad (3a)$$

$$A_{red} + O_2 \xrightarrow{\text{Oxidase}} A_{ox} + H_2O \quad (3b)$$

$$A_{red} + O_2 \xrightarrow{\text{Oxidase}} A_{ox} + O_2^{\cdot -} \quad (3c)$$

Scheme 3 The reactions catalyzed by oxidase.

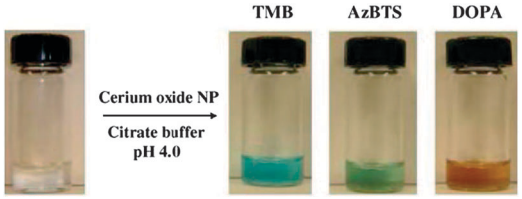

Fig. 7 Nanoceria as nanozyme to mimic oxidase. The oxidase mimetic property of the nanoceria was demonstrated by oxidizing colorimetric substrates (TMB, ABTS and DOPA) to form colored products at pH 4.0. Reprinted with permission from ref. 81. Copyright (2009) John Wiley and Sons.

added. This activity was found to be highly dependent on pH, size, and the coating of the nanoceria. The kinetics studies agreed well with the pH-, size-, and coating thickness-dependent activities (*i.e.*, lower pH, smaller size, and thinner coatings on the nanozymes led to higher activities). Based on measured values, the nanozymes had a faster rate constant ($1–7 \times 10^{-7}$ M^{-1} s^{-1} of the nanozyme *vs.* 1×10^{-8} M^{-1} s^{-1} of HRP).

Applications

(a) Immunoassays. Similar to traditional enzyme-linked immunosorbent assays (ELISA), several immunoassays using oxidase nanozyme mimics were developed for the detection of important targets, such as tumor cells.[81,90] Perez and co-workers reported an assay for the determination of tumor cells with poly(acrylic acid)-coated nanoceria as an oxidase mimic. When the nanoparticles were conjugated with folic acid, they could specifically recognize tumor cells, such as A-549 lung cancer cells, due to the elevated-expression of folate receptors on the cell surface. The targeting effect was based on the evidence that folate receptors are present in various tumors but absent in most normal tissue except choroid plexus, lung, thyroid and kidney.[120] The presence of the nanoparticles could then oxidize a colorless substrate to a colored product without H_2O_2. They also evaluated the selectivity using H9c2 cardiac myocytes as a control, showing good results.[81] Several advantages of the nanozyme-based assay were discussed, such as: (a) the nanozyme is more stable and robust, and is less expensive than HRP; (b) the nanozyme oxidizes the substrate without H_2O_2, eliminating the potential stability issue of H_2O_2; and (c) folic acid is used instead of an antibody, eliminating the potential stability issue of antibodies. Note that folate receptor is limited to cancer cells, and cannot differentiate the different cancer cell types. The affinity of folic acid to folate receptor is also lower than that of an antibody to the receptor.

In a subsequent study, they showed that for the substrate ampliflu, the oxidase-like activity of the nanoceria could be fine tuned by changing the reaction pH (Fig. 8).[90] Different from HRP/H_2O_2 at pH 4–7 and nanoceria at or below pH 5.0, nanoceria at pH 7 mediated mild and controlled oxidation of amplifu to a fluorescent product (resorufin) instead of the further oxidized nonfluorescent product (resazurin). This unique phenomenon was able to provide an assay format for long ELISA readout at neutral pH without the use of H_2O_2. The assay format was then successfully used to detect tumors by employing the nanozyme with protein G and specific antibodies (*i.e.*, folate receptor antibody for A549 cells and EpCAM antibody for MCF-7 cells).

2.2 Iron oxide-based nanomaterials

Iron oxide nanomaterials, especially magnetic iron oxide nanomaterials, have found broad use in many areas, such as the separation and capture of analytes, sensing and imaging.[57,121–132] They are usually considered chemically and biologically inert, so metal catalysts, enzymes, or antibodies are often conjugated for further functionalization. When magnetite nanoparticles were coated with small peptides, for example, they were shown to have specific tumor targeting activity for magnetic resonance imaging.[133] They have also been used for (bio)analysis, (bio)electrocatalysis, drug delivery, bacteria inactivation, *etc.*[122–126,128,130–132] Unexpectedly, Yan and co-workers have recently discovered that Fe_3O_4 magnetic nanoparticles (MNPs) actually exhibit an intrinsic peroxidase-like activity.[44,134] Since the pioneering study reported by Yan *et al.*,[44] a significant amount of research has been focused on imitating peroxidase activity with various nanomaterials and exploring the potential applications.[45–47,98,102,110–112,119,135–264] Here, we discuss the enzyme mimetic properties of iron oxide nanomaterials and their applications.

2.2.1 Iron oxide as peroxidase mimics. In nature, peroxidase, consisting of a large family of enzymes, catalyzes the oxidation of its substrate with peroxide (hydrogen peroxide in most cases) (Scheme 4). Through this catalysis, peroxidases play many critical roles in biological systems, such as detoxifying reactive oxygen species (*e.g.* glutathione peroxidase) and defending against pathogens (*e.g.* myeloperoxidase). In addition, peroxidase (especially HRP) has been widely used in bioanalytical and clinical chemistry, where it is usually employed as a conjugate to an antibody for enzymatically catalyzing colorimetric substrates for signaling or imaging. Recent studies from Yan's and others' groups have shown that certain nanomaterials can imitate peroxidase catalytic activity.[44–47,98,102,110–112,119,135–264]

In Yan's work, Fe_3O_4 MNPs with three different sizes (30, 50 and 300 nm) all oxidized TMB to the blue-colored product in the presence of H_2O_2 (Fig. 9).[44] The other two substrates tested (DAB and OPD) were also oxidized to their corresponding products, mimicking the activity of HRP. The catalytic activity of the nanozyme was size dependent, with smaller sized particles exhibiting higher activity. Like native HRP, the nanozyme performance varies with pH and temperature. However, compared with HRP, the Fe_3O_4 MNPs are much more robust as they remain stable and retain their catalytic activity after incubation at a range of temperatures (4–90 °C) and pH (0–12). The robustness of the

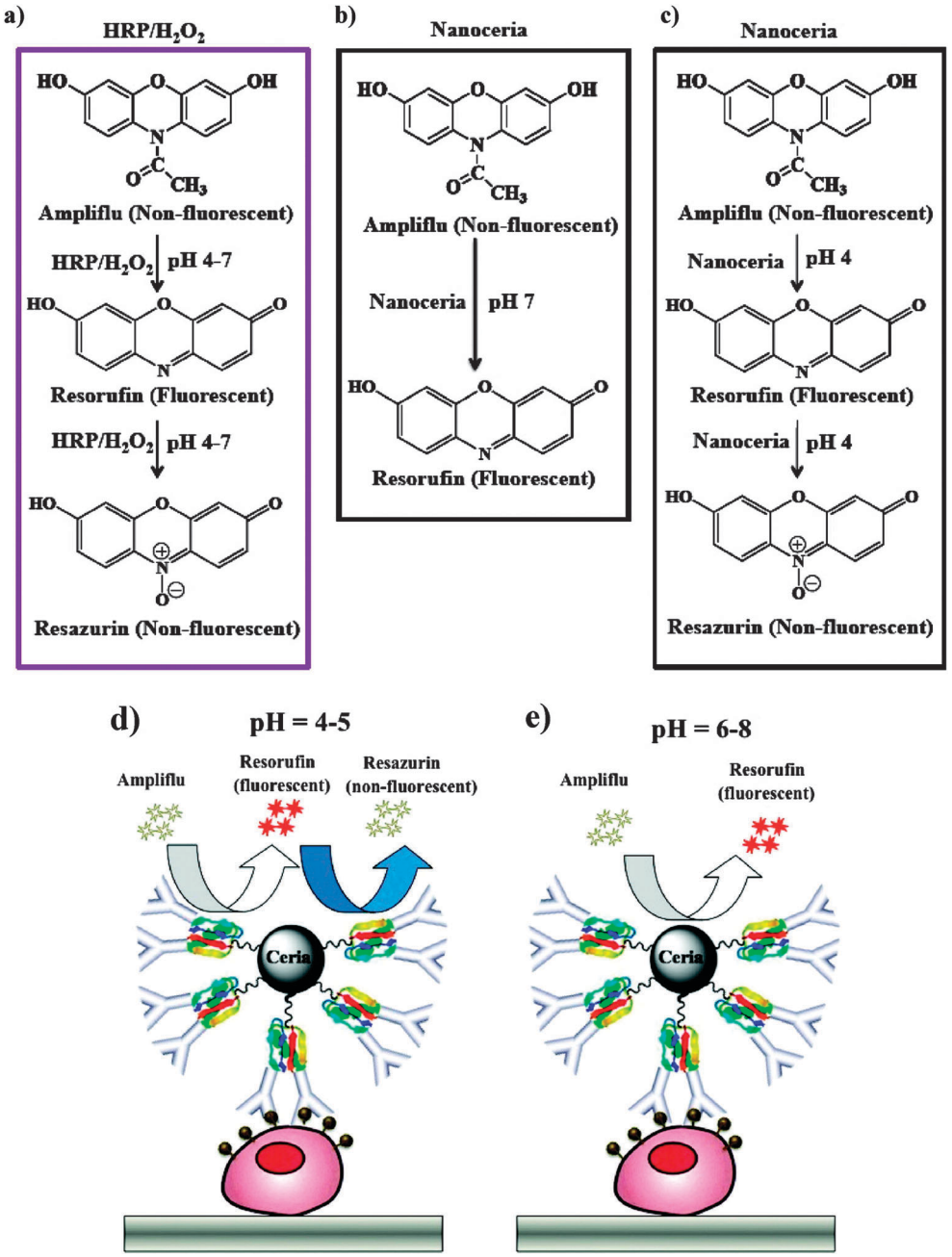

Fig. 8 Schematic showing the HRP/H_2O_2 and nanoceria mediated oxidation of ampliflu. (a) In the pH range 4–7, HRP/H_2O_2 oxidizes ampliflu to a nonfluorescent final product (resazurin). (b) In contrast, nanoceria oxidizes ampliflu to the intermediate oxidation fluorescent product (resorufin) at pH 7, (c) while at or below pH 5.0, nanoceria yields the terminal oxidized nonfluorescent product resazurin. (d, e) The ability of nanoceria to oxidize ampliflu to a stable fluorescent product in the pH range 6–8 will facilitate its use in ELISA without the use of H_2O_2. Reprinted with permission from ref. 90. Copyright (2011) American Chemical Society.

$$AH_2 + ROOH \xrightarrow{\text{Peroxidase}} A + ROH + H_2O \quad (4)$$

Scheme 4 The reaction catalyzed by peroxidase.

nanozyme, as well as its low cost, makes it suitable for a wide range of applications.[44]

In the study from Yan's group, it was suggested that the Fe_3O_4 MNP-based peroxidase activity is the result of a ping-pong mechanism (*i.e.*, no tertiary intermediate of an enzyme and its two substrates forms since one substrate is converted to the product and dissociates before the other one binds).[44] Their steady state kinetic measurements showed that the substrate concentration dependent Lineweaver–Burk (double-reciprocal) plots were parallel, characteristic of the ping-pong mechanism (Fig. 10). Native HRP also has a ping-pong catalytic mechanism. The Michaelis–Menten constants (*Km*, measuring the substrate's binding affinity) from the Lineweaver–Burk plots showed that the nanozyme had less affinity to hydrogen peroxide compared with HRP (154 mM for the nanozyme *vs.* 3.70 mM for HRP), but

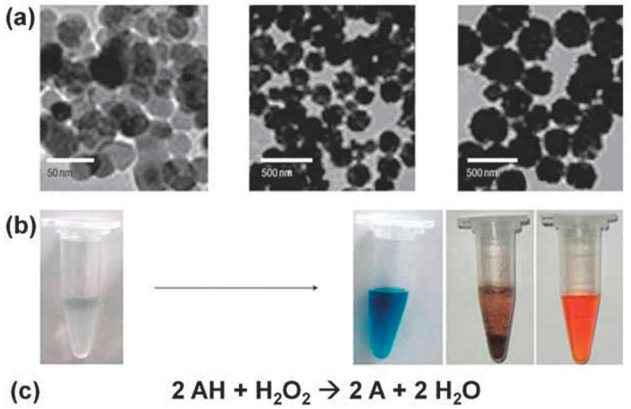

Fig. 9 Fe_3O_4 MNPs as nanozyme to mimic peroxidase. (a) TEM image of Fe_3O_4 MNPs with different sizes investigated. (b) The substrates, TMB, DAB and OPD, were catalytically oxidized to form colorimetric products with Fe_3O_4 MNPs. (c) The reaction catalyzed by Fe_3O_4 MNPs. Reprinted with permission from ref. 44. Copyright (2007) Nature Publishing Group.

had higher affinity to TMB compared with HRP (0.098 mM for the nanozyme *vs.* 0.434 mM for HRP). The calculated rate constant K_{cat} (measuring the overall catalytic rate) indicated that the Fe_3O_4 MNPs mimics reacted faster than native HRP towards both TMB and H_2O_2.

Soon after Yan's report, Wei and Wang developed novel sensing platforms for both H_2O_2 and glucose detection with Fe_3O_4 MNPs as peroxidase mimics.[45] The results of these initial studies stimulated rapidly expanding interests in the use of iron oxide nanomaterials as a peroxidase mimic. Among them, Fe_3O_4 (magnetite) nanomaterials have been the mostly extensively studied. In most cases, a substrate (such as ABTS or TMB) was used to examine the nanomaterials' peroxidase mimetic properties through the convenient colorimetric reaction in the presence of H_2O_2.[160–162,166,171,175,178,181,182,248] A previous study has suggested that TMB could be a better choice in certain cases since ABTS could be oxidized in the absence of peroxidase using H_2O_2 alone.[149] The nanomaterials' activity was also compared with HRP in some reports.[143,155] Wu *et al.* performed a detailed study to investigate the effects of aqueous–organic solvents on the activities of HRP and an Fe_3O_4-based nanozyme.[143,155] They showed that the relative catalytic activities of the nanozyme under given conditions were generally better than that of HRP.

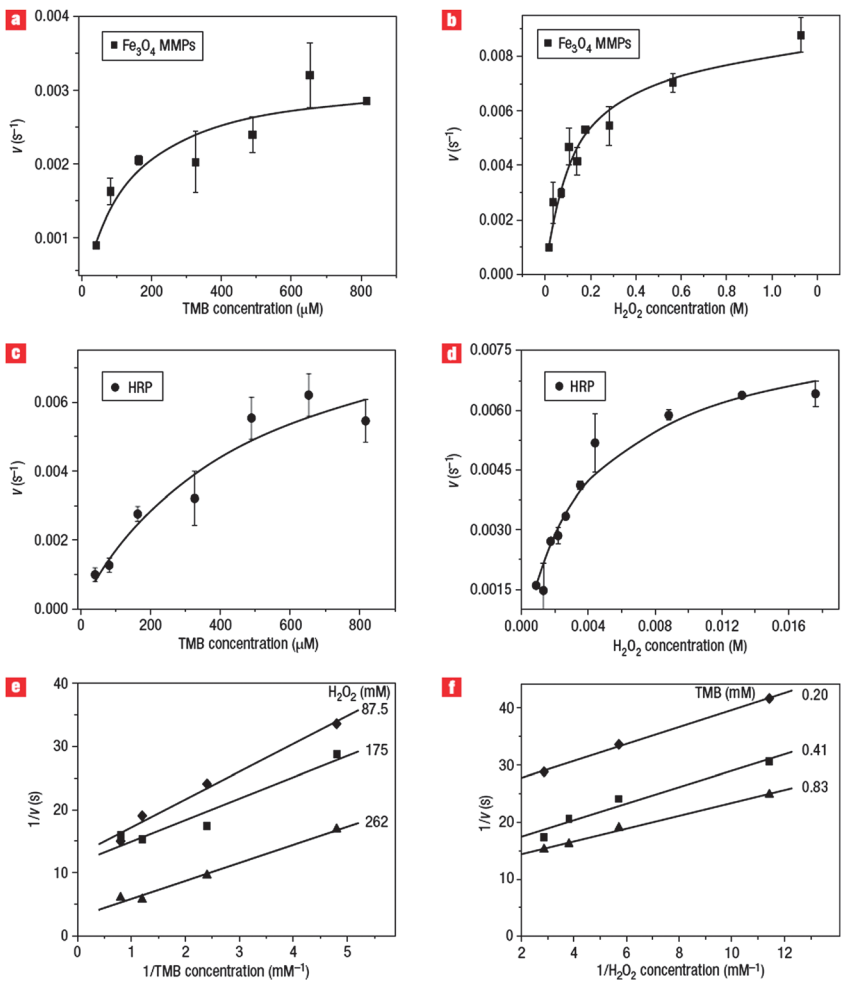

Fig. 10 Steady-state kinetic assay and catalytic mechanism of Fe_3O_4 MNPs as peroxidase mimic. Reprinted with permission from ref. 44. Copyright (2007) Nature Publishing Group.

Several studies have also been devoted to Fe_2O_3 (hematite) nanomaterials.[47,154,177,233,239] Very recently, magnetoferritin (Fe_2O_3 in ferritin) nanoparticles have been employed for targeting and visualizing tumor tissues.[47] The natural inorganic core of ferritin is hydrated iron oxide ferrihydrite, which has very low peroxidase mimic activity. To combat this lowered activity, the magnetic core was post-constructed by *in situ* oxidation of iron ions inside of the apo-ferritin, resulting in magnetoferritin nanoparticles with excellent peroxidase-like activity. In a recent comparison study of nanoparticles with similar size, Fe_3O_4 showed higher peroxidase mimetic activity than Fe_2O_3.[110] Though naturally-occurring hydrated iron oxide ferrihydrite has little activity, peroxidase mimetic activities have been found in certain iron oxide containing organelles, such as magnetosomes and ferruginous bodies.[210,235,241]

Doped ferrites, such as $MFeO_3$ (M = Bi, Eu) and MFe_2O_4 (M = Co, Mn, Zn), were also explored as peroxidase mimics.[180,197,212,216,223,231,257,264] For example, $CoFe_2O_4$ MNPs were used as a peroxidase mimic for the detection of H_2O_2 and glucose through chemiluminescence.[231] The performance was further improved by chitosan coating, which provided more monodispersed MNPs and a positive surface charge for affinity to luminol.[180]

The molecular level mechanisms responsible for iron oxide as peroxidase mimics have not been completely determined. They may adopt a Fenton and/or Haber–Weiss reaction mechanism though a mechanism similar to an authentic enzyme cannot be excluded.[151,228,265] In Tang and co-workers' study, they employed EPR measurements and a radical inhibition assay to elucidate the possible mechanism for catalytic degradation of organic pollutant by Fe_3O_4 MNPs-based nanozyme.[151] $HO^{\bullet -}$ and $O_2^{\bullet -}/HO_2^{\bullet}$ were detected using EPR, and the subsequent radical inhibition assay showed that $O_2^{\bullet -}/HO_2^{\bullet}$ was dominant. Combining with the fact that MNPs, rather than the leached ions, had catalytic activity, they proposed a mechanism as shown in Fig. 11.[151] Whether the proposed mechanism can be applied to other substrates should be studied in the future.

Since there is concern about whether the nanozymes' activity is from the nanomaterials or leached active species (such as iron ions for iron oxide-based nanozymes), it is important to investigate the activity of the leached ions.[44,45,144,220,257] Several studies confirmed that the nanozymes' activities originate from the intact nanomaterials and not the leachate.[44,45,220,257] For Fe_3O_4 MNP-based nanozymes, atomic absorption spectroscopy measurements indicated that small amounts of iron could be released from the Fe_3O_4 MNPs.[44,45] However, the number of leached ions was too low to explain the catalytic activity, further confirming that the observed activity was from intact MNPs rather than the leached ions. In Gao's work, however, they argued that the Fe_3O_4 MNPs catalyzed the polymerization of aniline *via* Fe ions.[144] This discrepancy may be due to the instability of the MNPs used and the pH of the reaction solution tested.

Applications

(a) H_2O_2 detection. H_2O_2 detection is of significant importance in many fields such as biology, medicine, environmental protection and the food industry. Since H_2O_2 is involved in the catalytic reaction of peroxidase and its mimics (Scheme 4), it is straightforward to measure H_2O_2 concentration through the color change of certain colorimetric substrates. In Wei and Wang's seminal report, a colorimetric platform for H_2O_2 determination was developed using ABTS as the substrate and Fe_3O_4 MNPs as the nanozyme.[45] The H_2O_2 mediated oxidation of ABTS produced a green colored product, which facilitated its colorimetric detection even by the naked eye. *Via* the proposed method, concentrations as low as 3 μM H_2O_2 were detected with a linear range from 5 μM to 100 μM. Later, H_2O_2 detection was demonstrated as a model in many follow-up studies (see Table 1). Besides ABTS, many other colorimetric substrates have been used, including 4-AAP-phenol, DPD, OPD and TMB. Tang *et al.* reported that their system for H_2O_2 detection showed good selectivity over several ions, ascorbic acid, glucose, *etc.*[203] They further determined H_2O_2 concentrations in rainwater, honey and milk samples.

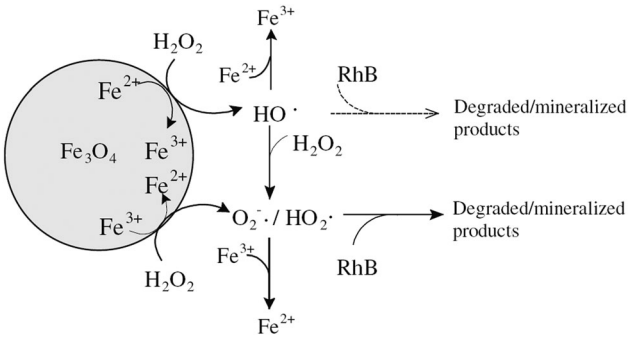

Fig. 11 A mechanism for the activation of H_2O_2 on the peroxidase-like Fe_3O_4 MNPs catalyst in the degradation of organic pollutants. Reprinted with permission from ref. 151. Copyright (2010) Elsevier.

If the substrate oxidation is associated with a fluorescent signaling change, a fluorometric approach to the determination of H_2O_2 can be used.[156,158,212] When fluorescent rhodamine B is oxidized by H_2O_2, it leads to fluorescence quenching. Based on this phenomenon, a selective sensor for H_2O_2 was developed.[158] The fluorescence of CdTe quantum dots is quenched upon oxidation as well, and can also be used for H_2O_2 determination.[156] A signal-on sensor was developed when non-fluorescent substrate BA was converted to its fluorescent product.[212] When luminol was employed as the substrate, its oxidation could result in chemiluminescence. A few studies based on chemiluminescent detection of H_2O_2 have been reported.[180,208,231]

Electrochemistry provides a convenient way for H_2O_2 detection with either natural HRP or its mimics.[138,141,159,161,167,174,183,199,201,204,206,219,220,238,239,249,266–268] Dong and co-workers fabricated the first electrochemical sensor for H_2O_2 detection using layer-by-layer assembly of Fe_3O_4 MNPs and poly(diallyldimethylammonium chloride) (PDDA) through electrostatic interactions on a tin-doped indium oxide (ITO) electrode.[138] The sensor had good sensitivity with a detection limit of 1.4 μM and was selective for H_2O_2 over ascorbic acid and uric acid. Compared with HRP, the nanozyme system showed several advantages, such as low cost, increased stability, sustainable

Table 1 H_2O_2 detection with peroxidase mimics[a]

Nanozyme	Method	Linear range	LOD	Comments	Ref.
Fe_3O_4 MNPs	Color.	5–100 μM	3 μM	Substrate: ABTS	45
Fe_3O_4 MNPs	Color.	0.5–150.0 μM	0.25 μM	Substrate: DPD H_2O_2 in rainwater, honey and milk was tested.	203
Fe_3O_4 MNPs	Color.	1–100 μM	0.5 μM	Substrate: TMB Fe_3O_4 was encapsulated in mesoporous silica.	160
Fe_3O_4 graphene oxide composites	Color.	1–50 μM	0.32 μM	Substrate: TMB	178
Fe-substituted SBA-15 microparticles	Color.	0.4–15 μM	0.2 μM	Substrate: TMB	163
Iron phosphate microflowers	Color.	10–50 μM	10 nM	Substrate: TMB	189
[FeIII(biuret-amide)] on mesoporous silica	Color.	0.1–5 mM	10 μM	Substrate: TMB	252
FeTe nanorods	Color.	0.1–5 μM	55 nM	Substrate: ABTS	254
Fe(III)-based coordination polymer	Color.	1–50 μM	0.4 μM	Substrate: TMB	258
CuO NPs	Color.	0.01–1mM	N/A	Substrate: 4-AAP and phenol	236
AuNPs	Color.	18–1100 μM	4 μM	Substrate: TMB Cysteamine was the ligand for AuNPs.	211
AuNC@BSA	Color.	0.5–20 μM	20 nM	Substrate: TMB	170
Au@Pt core–shell nanorods	Color.	45–1000 μM	45 μM	Substrate: OPD	119
Graphene oxide	Color.	0.05–100 μM	50 nM	Substrate: TMB	213
Hemin-graphene hybrid nanosheets	Color.	0.05–500 μM	20 nM	Substrate: TMB	222
Carbon nanodots	Color.	1–100 μM	0.2 μM	Substrate: TMB	230
Carbon nitride dots	Color.	1–100 μM	0.4 μM	Substrate: TMB	225
CoFe LDH nanoplates	Color.	1–20 μM	0.4 μM	Substrate: TMB	262
Carboxyl functionalized mesoporous polymer	Color.	1–8 μM	0.4 μM	Substrate: TMB	165
Pt–DNA complexes	Color.	0.979–17.6 mM	0.392 mM	Substrate: TMB 3.92 μM was detected with PVDF membrane.	237
Polyoxometalate	Color.	1–20 μM	0.4 μM	Substrate: TMB	247
Polyoxometalate	Color.	0.134–67 μM	0.134 μM	Substrate: TMB	186
Fe_3O_4 MNPs	Fluor.	10–200 nM	5.8 nM	Substrate: Rhodamine B Fluorescence of Rhodamine B was quenched.	158
$BiFeO_3$ NPs	Fluor.	20 nM–20 μM	4.5 nM	Substrate: BA Oxidation of BA gave fluorescence. H_2O_2 in rainwater was tested.	212
Fe_3O_4 MNPs	Fluor.	0.18–900 μM	0.18 μM	Fluorescence of CdTe QD was quenched.	156
$CoFe_2O_4$ NPs	CL	0.1–4 μM	0.02 μM	$CoFe_2O_4$ NPs form complexes with beta-CD.	208
$CoFe_2O_4$ NPs	CL	0.1–10 μM	10 nM	H_2O_2 in natural water was tested.	231
$CoFe_2O_4$ NPs with chitosan coating	CL	1 nM–4 μM	0.5 nM	$CoFe_2O_4$ NPs was coated with chitosan. H_2O_2 in natural water was tested.	180
Fe_3O_4 MNPs	E-chem	4.2–800 μM	1.4 μM		138
Fe_3O_4 microspheres-AgNP hybrids	E-chem	1.2–3500 μM	1.2 μM	H_2O_2 in disinfected FBS samples was tested.	268
Fe_3O_4 MNPs	E-chem	0–16 nM	1.6 nM	Fe_3O_4 was loaded on CNT.	159
Fe_3O_4 MNPs	E-chem	1–10 mM	N/A	Fe_3O_4 was entrapped in mesoporous carbon foam, and the composite was used to construct a carbon paste electrode. Not a linear response.	161
Fe_3O_4 MNPs	E-chem	20–6250 μM	2.5 μM	Fe_3O_4 MNPs and PDDA-graphene formed multilayer *via* layer-by-layer assembly. H_2O_2 in toothpaste was tested.	167
Fe_3O_4 nanofilms on TiN substrate	E-chem	1–700 μM	1 μM	H_2O_2 in Walgreens antiseptic/oral debriding	199
Fe_3O_4 MNPs	E-chem	0.2–2 mM	0.01 mM	agent, Crest whitening mouthwash solution, Diet coke and Gatorade was tested.	174
Fe_3O_4 MNPs	E-chem	0.1–6 mM	3.2 μM	Fe_3O_4 was on reduced graphene oxide.	201
Fe_2O_3 NPs	E-chem	20–140 μM	11 μM		239
Fe_2O_3 NPs	E-chem	20–300 μM	7 μM	Fe_2O_3 was modified with Prussian blue.	239
Iron oxide NPs/CNT	E-chem	0.099–6.54 mM	53.6 μM		141
FeS nano-sheet	E-chem	0.5–150 μM	92 nM		204
FeS needles	E-chem	5–140 μM	4.3 μM		238
FeSe NPs	E-chem	5–100 μM	3.0 μM		238
FeS	E-chem	10–130 μM	4.03 μM		249
Co_3O_4 NPs	E-chem	0.05–25 mM	0.01 mM		183
Hemin-graphene hybrid nanosheets	E-chem	0.5–400 μM	0.2 μM		222
Helical CNT	E-chem	0.5–115 μM	0.12 μM		220
LDH nanoflakes	E-chem	12–254 μM	2.3 μM		206
Calcined LDH	E-chem	1–100 μM	0.5 μM		219
CdS	E-chem	1–1900 μM	0.28 μM		251

[a] Color., Colorimetric; E-chem, electrochemical; Fluor., fluorometric; LOD, limit of detection.

electrocatalytic activity, and robustness to harsh environments.[138] Given the good selectivity of the sensors developed, the determination of H_2O_2 in real samples (such as toothpaste, Walgreens antiseptic/oral debriding agent, Crest whitening mouthwash solution, Diet coke and Gatorade) has been reported in several studies.[167,199]

Compared with colorimetric detection, fluorometric, chemiluminescent and electrochemical methods could provide better sensitivity as shown in several reports.[158,159,180,212]

(b) Glucose detection. Glucose detection is of great importance in clinical and food analysis and plays a critical role in the improvement of life quality.[269] Usually, glucose oxidase (GOx) is employed for glucose detection due to its high specificity and efficiency. The catalytic oxidation of glucose with molecular oxygen in the presence of GOx produces H_2O_2, which can be further determined by many analytical methods (such as HRP catalyzed colorimetric and electrochemical methods). The use of peroxidase mimics for glucose detection would be advantageous based on their high stability, low cost, *etc.*

For the first time, Wei and Wang developed a sensitive and selective colorimetric approach towards glucose detection by combining the catalytic oxidation reaction of glucose with GOx and the catalytic reaction of ABTS with Fe_3O_4 MNPs (Fig. 12).[45] With the developed approach, glucose concentrations as low as 30 μM were detected with a linear range from 50 μM to 1 mM. The system also showed excellent selectivity over other sugars such as fructose, lactose and maltose.

Similar to H_2O_2 detection (*vide supra*), numerous analytical approaches to glucose detection have been developed by varying the nanomaterials and substrates used (see Table 2). Several studies also reported novel methods for the determination of glucose concentration in real serum samples. For example, when PDDA-coated iron oxide nanoparticles (acting as nanozymes) were electrostatically assembled with GOx, the composites could be used for colorimetric sensing of glucose.[153] The sensing performance was validated by a commercial glucose meter.

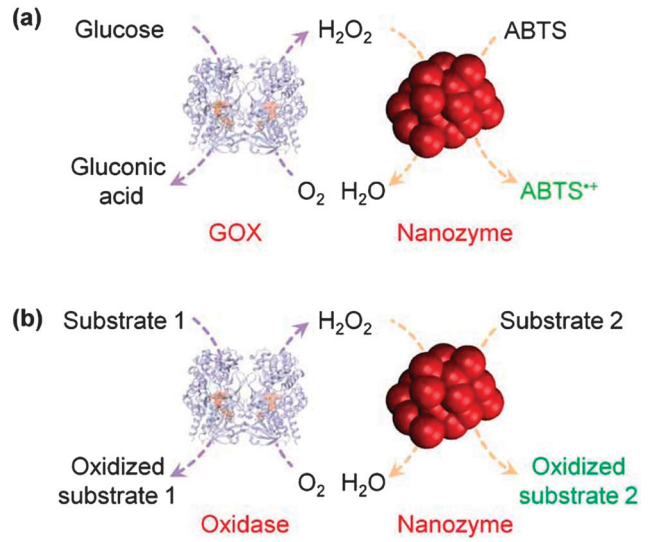

Fig. 12 (a) Nanozyme as peroxidase mimic for colorimetric sensing of H_2O_2 and glucose when combined with glucose oxidase. (b) The sensing format in (a) could be extended to other targets (substrate 1 here) when combined with a appropriate oxidase. Numerous transduction signals can be adopted for sensing (such as colorimetric, fluorometric and chemiluminescent signals when the corresponding substrates are used; and electrochemical signals when a nanozyme is immobilized on an electrode).

Moreover, the glucose concentrations in serum samples could be accurately and selectively detected over several other sugars, such as galactose, lactose, mannose, maltose, arabinose, cellobiose, raffinose and xylose. The glucose in urea was also determined.[178,257] There are many advantages to using nanozymes instead of GOx, such as stability, robustness and recyclability, which are addressed in several studies.[147,160]

The analytical strategy described above is easily adapted for other oxidases as well, as shown in Fig. 12b. Choline, cholesterol, galactose and xanthine have been successfully analyzed based on the above sensing strategy.[119,160,162,170,173,181]

(c) DNA detection. When double-stranded DNA's shielding against MNPs' mimicking activity was combined with PCR, a label-free colorimetric platform for DNA sensing was developed (Fig. 13).[169] The developed method was used for the selective detection of *Chlamydia trachomatis* pathogen using a human urine sample. One advantageous feature of the method is its simplicity, exemplified by achieving detection with the naked eye in 30 min.

(d) Aptasensors. Aptamers are selected ssDNA or ssRNA that can specifically bind to a target, and can be considered as nucleic acid versions of an antibody.[270] Therefore, aptamers have been extensively studied for the construction of aptasensors.[271–274] When nanozymes are introduced as signaling elements, new aptasensing platforms can be developed. Zhang *et al.* constructed a sandwich format for thrombin sensing using two antithrombin aptamers for capture and detection.[155] The detection aptamer was tagged with chitosan-modified Fe_3O_4 MNPs, which converts TMB into a colored product for colorimetric sensing. Using this method, they were able to achieve a linear detection range from 1 to 100 nM and a detection limit of 1 nM thrombin. In a study by Kong's group, aptamers and Fe_3O_4 MNPs were used to replace traditional small molecule electrochemical probes, resulting in a sensitive and reagentless electrochemical sensor for specific detection of thrombin (Fig. 14).[172] The sensor exhibits good sensitivity, with a linear range of 1.0 to 75 nM and a detection limit of 1 nM, and can also be regenerated.

(e) Immunoassay. Conjugating an antibody (or protein A) to a nanozyme, rather than a traditional enzyme like HRP, enables the use of nanozyme technology for a number of immunoassays (Table 3).[44,111,135,154,192,216,229,232,264] In Yan's pioneering work, two immunoassay formats were developed (Fig. 15a and b).[44] For the detection of hepatitis B virus surface antigen (preS1), the antigen was first adsorbed onto a plate. Anti-preS1 antibodies were then added for specific target recognition, followed by protein A-Fe_3O_4 MNP conjugates for signal development. This format was based on the traditional antigen-down immunoassay. In the second case, a modified sandwich assay was developed for detection of the myocardial infarction biomarker troponin I (TnI). The antigen was magnetically captured and separated from a blood sample using the antibody–Fe_3O_4 MNPs conjugate. This is different from a traditional sandwich assay, in which the antigen is captured by an antibody immobilized on a solid surface. The final sandwich format was formed between the

Table 2 Targets detection combining oxidases and peroxidase mimics[a]

Nanozyme	Method	Linear range	LOD	Comments	Ref.
Glucose					
Fe_3O_4 MNPs	Color.	50–1000 μM	30 μM	Substrate: ABTS Selectivity against sugars: fructose, lactose and maltose.	45
Fe_3O_4 MNPs with PDDA coating	Color.	39–100 μM	30 μM	Substrate: ABTS GOx was electrostatically assembled onto the Fe_3O_4@PDDA. Glucose in serum samples was tested. Compared with glucometer. Selectivity against sugars: galactose, lactose, mannose, maltose, arabinose, cellobiose, raffinose and xylose.	153
Fe_3O_4 MNPs	Color.	30–1000 μM	3 μM	Substrate: TMB Fe_3O_4 was encapsulated in mesoporous silica with GOx. Showing the recycle capability. Comparison between free MNPs *vs.* encapsulated MNPs.	160
Fe_3O_4 GO composites	Color.	2–200 μM	0.74 μM	Substrate: TMB Glucose in urine was tested.	178
Iron oxide NPs	Color.	31.2–250 μM	8.5 μM	Substrate: ABTS Iron oxide NPs was coated with glycine. More robust than HRP towards NaN_3 inhibition.	147
Iron oxide NPs	Color.	31.2–250 μM	15.8 μM	Substrate: ABTS Iron oxide NPs was coated with heparin. More robust than HRP towards NaN_3 inhibition.	147
Iron oxide NPs	Color.	0.12–4 μM	0.5 μM	Substrate: ABTS Iron oxide NPs was coated with APTES and MPTES.	168
$ZnFe_2O_4$	Color.	1.25–18.75 μM	0.3 μM	Substrate: TMB Glucose in urine was tested.	257
[FeIII(biuret-amide)] on mesoporous silica	Color.	20–300 μM	10 μM	Substrate: TMB Glucose in mice blood plasma was tested.	252
FeTe nanorods	Color.	1–100 μM	0.38 μM	Substrate: ABTS Glucose in spiked blood was tested.	254
Fe(III)-based coordination polymer	Color.	2–20 μM	1 μM	Substrate: TMB Glucose in serum was tested.	258
CuO NPs	Color.	0.1–8 mM	N/A	Substrate: 4-AAP and phenol	236
AuNPs	Color.	2.0–200 μM	0.5 μM	Substrate: TMB Cysteamine was the ligand for AuNPs.	211
Au@Pt core–shell nanorods	Color.	45–400 μM	45 μM	Substrate: OPD	119
Graphene oxide	Color.	1–20 μM	1 μM	Substrate: TMB Glucose in blood and fruit juice was tested.	213
Hemin–graphene hybrid nanosheets	Color.	0.05–500 μM	30 nM	Substrate: TMB	222
Carbon nanodots	Color.	1–500 μM	1 μM	Substrate: TMB Glucose in serum was tested.	230
Carbon nitride dots	Color.	1–5 μM	0.5 μM	Substrate: TMB	225
CoFe LDH nanoplates	Color.	1–10 mM	0.6 μM	Substrate: TMB	262
Fe_3O_4 MNPs	Fluor.	1.6–160 μM	1.0 μM	Fluorescence of CdTe QD was quenched. Glucose in serum was tested.	156
Fe_3O_4 MNPs with PDDA coating	Fluor.	3–9 μM	3 μM	GOx was electrostatically assembled onto the Fe_3O_4@PDDA. Oxidation of AU gave fluorescence. Glucose in serum was tested. Selectivity against sugars: arabinose, cellobiose, galactose, lactose, maltose, raffinose and xylose.	162
$BiFeO_3$ NPs	Fluor.	1–100 μM	0.5 μM	Oxidation of BA gave fluorescence. Glucose in serum was tested.	212
$CoFe_2O_4$ NPs	CL	0.1–10 μM	0.024 μM	Other sugars	231
$CoFe_2O_4$ NPs	CL	0.05–10 μM	10 nM	$CoFe_2O_4$ NPs were coated with chitosan.	180
Hemin-graphene hybrid nanosheets	E-chem	0.5–400 μM	0.3 μM	Glucose in serum was tested.	222
Fe_3O_4 MNPs	E-chem	6–2200 μM	6 μM	Glucose in serum was tested. Compared with clinical analyzer. Nafion for high selectivity against AA, UA, sucrose and lactose.	145
Fe_3O_4 MNPs	E-chem	0.5–10 mM	0.2 mM	Fe_3O_4 was encapsulated in mesoporous carbon with GOx, and the composite was used to construct a carbon paste electrode. Comparison between free MNPs *vs.* encapsulated MNPs.	161
Choline					
Fe_3O_4 MNPs with PDDA coating	Fluor.	20–100 μM	20 μM	Choline oxidase was electrostatically assembled onto the Fe_3O_4@PDDA. Oxidation of AU gave fluorescence.	162
Fe_3O_4 MNPs	E-chem	1 nM–10 mM (log)	0.1 nM	Fe_3O_4 and choline oxidase were immobilized together on electrode. Selectivity against AA and UA.	173

Table 2 (*continued*)

Nanozyme	Method	Linear range	LOD	Comments	Ref.
Cholesterol					
Fe_3O_4 MNPs	Color.	10–250 μM	5 μM	Substrate: TMB Fe_3O_4 was encapsulated in mesoporous silica with cholesterol oxidase. Showing the recycle capability. Comparison between free MNPs *vs.* encapsulated MNPs.	160
Au@Pt core–shell nanorods	Color.	30–300 μM	30 μM	Substrate: OPD	119
Galactose					
Fe_3O_4 MNPs	Color.	10–200 mg L^{-1}	5 mg L^{-1}	Substrate: ABTS Galactose in dried blood samples from normal people and patients was tested. Plates were used for sensing.	181
Fe_3O_4 MNPs with PDDA coating	Fluor.	2–80 μM	2 μM	Galactose oxidase was electrostatically assembled onto the Fe_3O_4@PDDA. Oxidation of AU gave fluorescence.	162
Xanthine					
AuNC@BSA	Color.	1–200 μM	0.5 μM	Substrate: TMB Xanthine in serum and urine samples was tested.	170

[a] Color., Colorimetric; E-chem, electrochemical; Fluor., fluorometric; LOD, limit of detection.

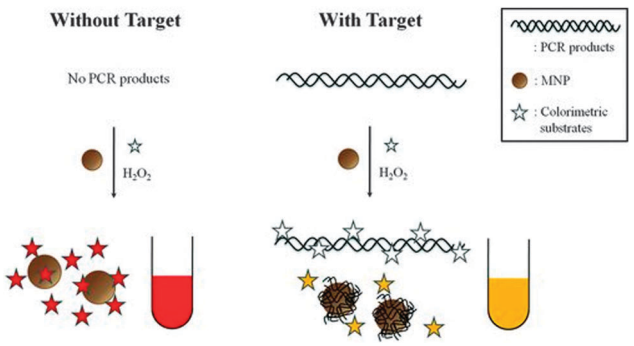

Fig. 13 Schematic illustration of a label-free colorimetric platform for DNA sensing based on target-induced shielding of nanozyme's activity. Reprinted with permission from ref. 169. Copyright (2011) John Wiley and Sons.

TnI/antibody-Fe_3O_4 MNPs complex and another capture antibody on a solid surface. The colorimetric signal was developed from the conversion of colorless TMB to its product. A slightly different format was developed in a later study for the detection of carcinoembryonic antigen (CEA) (Fig. 15c).[135] This format was very similar to a traditional sandwich assay, except that HRP was replaced with Fe_3O_4 MNPs.

Based on the MNPs' intrinsic peroxidase activity and the interaction of folic acid and its receptor, polyacrylic-acid coated iron oxide MNPs were successfully used to differentiate carcinoma cells (A549 cells) from non-carcinoma cells (H9c2).[192] The expression of the folic acid receptor in the A549 cells rather than H9c2 control cells was confirmed by flow cytometry, thus corroborating the nanozyme-based assay.[192]

(f) Immunostaining. Gu *et al.* demonstrated that ultra-small Fe_3O_4 MNPs were able to replace expensive enzymes (such as HRP) for immunohistochemical staining.[171] When dimercaptosuccinic acid-coated ultra-small Fe_3O_4 MNPs were conjugated with Nimotuzumab, a humanized monoclonal antibody for epidermal growth factor receptor (EGFR), the conjugates could specifically

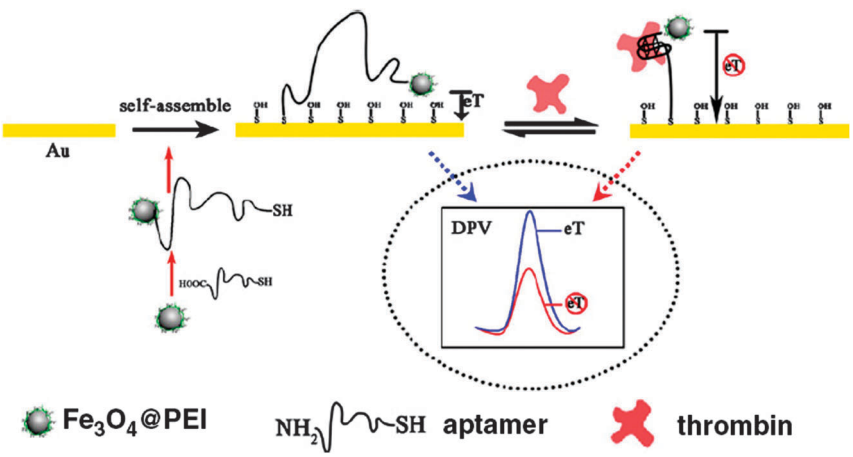

Fig. 14 An electrochemical aptasensor for reagentless protein detection. Reprinted with permission from ref. 172. Copyright (2011) Elsevier.

Table 3 Nanozyme as peroxidase mimics for immunoassay

Nanozyme	Target	Format	Comments	Ref.
Fe_3O_4 NPs with dextran coating	preS1 TnI	Antigen-down immunoassay Capture-detection sandwich immunoassay		44
Fe_3O_4 NPs with chitosan coating	mouse IgG CEA CEA	Antigen-down immunoassay Capture-detection sandwich immunoassay Sandwich immunoassay		135
Fe_2O_3 NPs with Prussian blue coating	IgG	Antigen-down immunoassay		154
Ferric nano-core residing in ferritin	Avidin Nitrated human ceruloplasmin	Antigen-down immunoassay Sandwich immunoassay	Avidin-biotin interaction	232
$Fe_{1-x}Mn_xFe_2O_4$ NPs with PMIDA coating	Mouse IgG	Antigen-down immunoassay	Both direct and indirect assay	216
$MnFe_2O_4$ NPs with citric acid coating	Sticholysin II	Antigen-down immunoassay		264
Au@Pt nanorods with PSS coating	Mouse IL-2	Sandwich immunoassay		111
Graphene oxide	PSA	Sandwich immunoassay	Clinical samples were tested	229

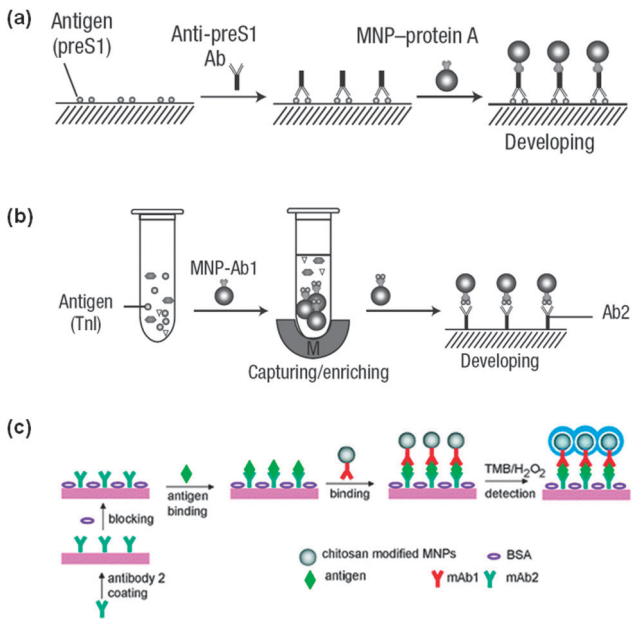

Fig. 15 Fe_3O_4 MNPs as nanozymes for immunoassay: (a) antigen-down immunoassay format; (b) capture-detection sandwich immunoassay format; and (c) sandwich immunoassay format; (a) and (b) reprinted with permission from ref. 44; copyright (2007) Nature Publishing Group; (c) reprinted with permission from ref. 135; copyright (2008) American Chemical Society.

detect EGFR over-expression on the membrane of esophageal cancer cells. In a more recent study, Yan and Liang's groups synthesized magnetoferritin nanoparticles (M-HFn) as novel reagents for targeting and visualizing tumor tissues (Fig. 16).[47] The M-HFn was prepared by encapsulating iron oxide nanoparticles inside the cavity of a recombinant human heavy-chain ferritin (HFn) protein cage. Since HFn binds directly to tumor cells *via* over-expressed transferrin receptor 1 (TfR1) proteins, no further conjugation is needed for targeting. Another advantage is that no additional contrast reagents are needed because the iron oxide nanoparticle cores act as peroxidase mimics and can catalyze the oxidation of peroxidase substrates to produce a colored product for the visualization of tumor tissues. They examined 474 clinical specimens from patients (247 clinical tumor tissue samples *vs.* 227 normal and lesion tissue control samples) with 9 types of cancer and verified that the nanozyme technology could distinguish cancerous cells from normal cells with 98% sensitivity and 95% specificity.[47]

(g) Detection of other substances. Besides the above mentioned targets, several other substances have been detected using peroxidase-like nanozymes. Reduced glutathione (GSH), an essential nutrient and an antioxidant, competitively inhibits ABTS catalytic oxidation by hydrogen peroxide and Fe_3O_4 MNPs-based nanozymes.[248] Since the inhibiting effects are dependent on GSH concentration, a simple approach was developed for GSH determination. The method has a linear range from 3.0 to 30.0 μM. This method was robust, having good selectivity over several thiols and good recovery. The method was also applied to detect GSH in lung adenocarcinoma epithelial cell lines (A549). Based on a similar design, melamine in dairy product was tested, where melamine was the competing agent against the nanozyme's substrate (ABTS).[150]

When Fe_3O_4 MNPs were entrapped within mesoporous carbon, a conductive nanocomposite was obtained. The nanocomposite was then used to construct highly efficient electrodes for sensing several phenolic compounds, which showed great promise for environmental monitoring.[161]

(h) Promotion of stem cell growth. In Huang's study, they investigated the effects of commercialized superparamagnetic iron oxide nanoparticles, Ferucarbotran (Resovist), on the proliferation of human mesenchymal stem cells (hMSCs).[140] Ferucarbotran was found to efficiently label hMSCs, and dramatically induced hMSCs proliferation. Since Ferucarbotran

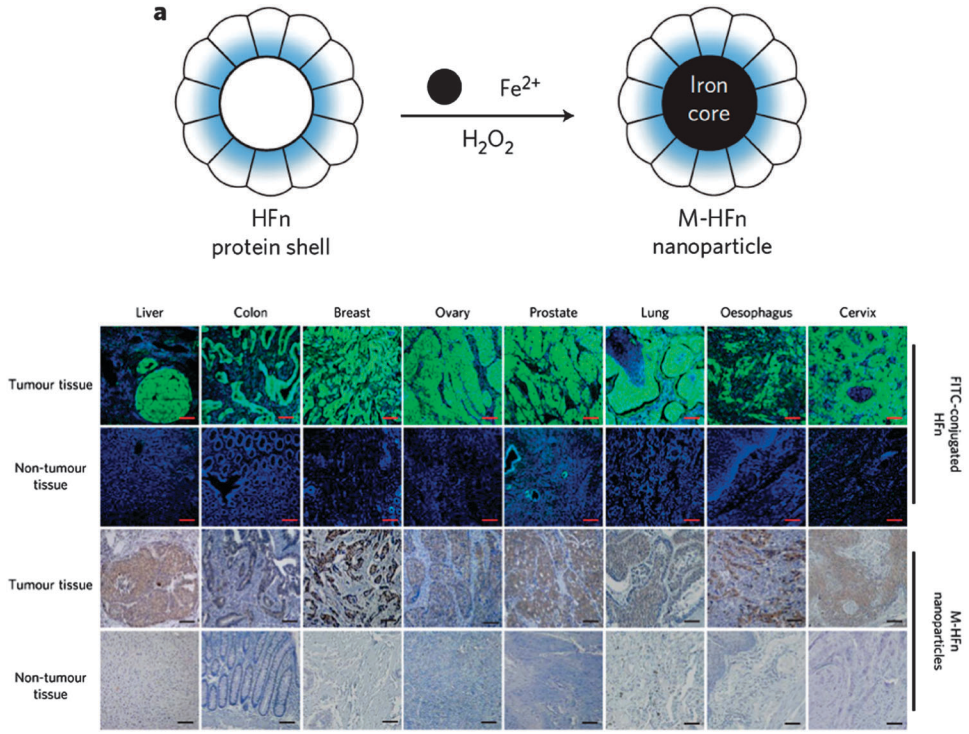

Fig. 16 Magnetoferritin nanoparticles as peroxidase mimic to target and visualize tumor tissues. Reprinted with permission from ref. 47. Copyright (2012) Nature Publishing Group.

exhibited *in vitro* and intracellular peroxidase-like activity, they proposed that the promotion of cell growth may be due to Ferucarbotran's ability to eliminate intracellular H_2O_2 through peroxidase mimetic activity (Fig. 17).[140] The study also showed that after internalization, Ferucarbotran was degraded into free iron ions, which then accelerated the cell cycle progression. A later study further confirmed the promoting effects of MNPs on MSCs proliferation.[195] Compared with the control groups with phosphate-buffered saline alone and magnetized MSCs, the MSCs sheet created by a new magnetite tissue engineering technology had greater angiogenesis in ischemic tissues. The mechanism was again attributed to the MNPs' peroxidase-like activity.

(i) Pollutant removal. The development of highly efficient, robust and low-cost catalysts for the removal of pollutants in wastewater is very important to our environment and health. The peroxidase-like activity of nanozymes has been explored for this purpose by several groups.[137,149,151,157,176,196,249,275] Model pollutants, such as phenol, rhodamine B, aniline, methylene blue and xylenol orange, have been tested. As high as 85% phenol removal was reported using ferromagnetic nanoparticles as the catalyst.[137] Using nanozymes as catalysts for pollutant removal has several distinct merits, such as low cost, easy preparation, high stability, low environmental impact, and recyclability.[137]

(j) Other applications. Dong *et al.* employed Fe_3O_4/Au nanocomposites to enhance the electricity generation from an electrogenic bacterium, *Shewanella oneidensis* MR-1 (Fig. 18).[263] The outer membrane c-type cytochromes act as molecular wires for electron transfer. When the *Shewanella oneidensis* MR-1

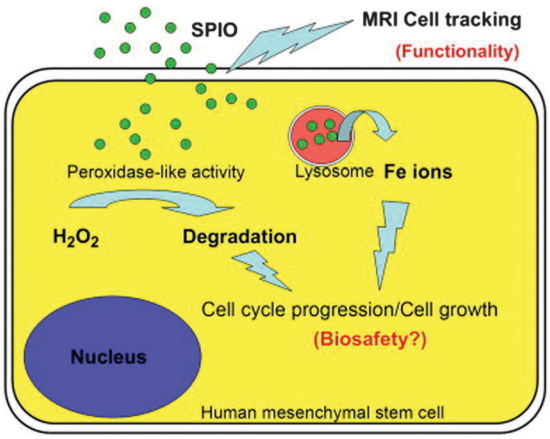

Fig. 17 Superparamagnetic iron oxide (SPIO) nanoparticles can promote cell growth due to their ability to diminish intracellular H_2O_2 through intrinsic peroxidase-like activity. Also, SPIO can accelerate cell cycle progression, which may be mediated by the free iron (Fe) released from lysosomal degradation. Reprinted with permission from ref. 140. Copyright (2009) Elsevier.

biofilm was co-immobilized onto a glassy carbon electrode with Fe_3O_4/Au nanocomposites, it exhibited a 22-fold increase in the current density compared with the biofilm without nanocomposites. The boosted efficiency was attributed to the unique properties of the nanocomposites. First, due to the peroxidase mimetic properties, the nanocomposites can participate in the electron transfer process; second, they lead to improved conductivity; third, the assembled nanocomposites provide a long-range pathway (instead of separated bacteria) for electron

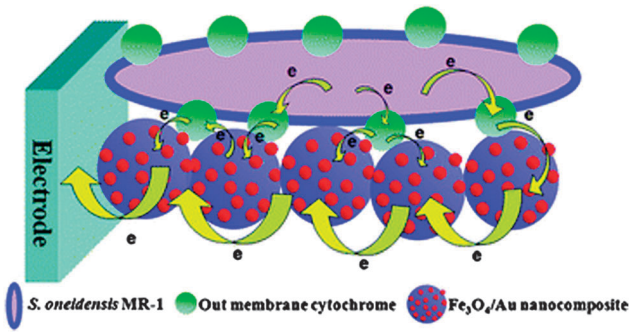

Fig. 18 Fe_3O_4/Au nanocomposites mediated efficient electron transfer between the electrogenic bacteria and electrode. Reprinted with permission from ref. 263. Copyright (2010) Royal Society of Chemistry.

propagation; and finally, they provide a more favorable, biocompatible environment for the proteinaceous electron transfer components needed for extracellular electron transfer.[263]

The peroxidase mimetic property was recently used for tracing ferrite nanoparticles *in vivo*.[190] By localizing MNPs within the main organs after intravenous injection, the biodistribution and organ clearance of MNPs were analyzed through MNP-mediated staining.

2.2.2 Iron oxide as both peroxidase and catalase mimics. Interestingly, Gu *et al.* recently found that iron oxide nanoparticles (both Fe_3O_4 and γ-Fe_2O_3) exhibited dual enzyme mimetic properties (*i.e.*, catalase and peroxidase mimics) (Fig. 19).[110] The study showed that the enzymatic activities were pH dependent, with catalase activity dominant at neutral conditions (pH = 7.4) while the peroxidase activity was dominant under acid conditions (pH = 4.8). Since the two nanoparticles had similar size and surface charge, they also made a side-by-side comparison of their performance. Fe_3O_4 MNPs alone (or with H_2O_2 as peroxidase mimic) showed higher cell toxicity when compared with γ-Fe_2O_3, which was attributed to Fe_3O_4 MNPs' higher activity for both mimics. More, the EPR measurements confirmed that hydroxyl radical was formed at acidic conditions, suggesting a Fenton-like mechanism for the peroxidase mimicking activity (Fig. 19a). No hydroxyl radical was detected at neutral conditions, suggesting a different mechanism for the catalase mimicking activity (Fig. 19b). They argued that at neutral or higher pH, the formation of $HO_2^{\bullet}$ was faster and it was then quickly ionized into $O_2^{\bullet -}$, further into O_2 by reacting with hydroxyl radical. The cellular toxicity of the nanozymes was due to the entrapment of the nanoparticles into acidic lysosomes, where hydroxyl radical was produced. They also suggested a potential protective role of the nanozymes. When they are entrapped within the cytosol, they can convert H_2O_2 into harmless products *via* catalase mimicking activity. Whether other peroxidase mimics have dual enzyme mimicking activities should be examined in the future to elucidate their mechanisms and explore the broad applications.

2.2.3 Iron oxide as oxidase mimics. In addition to nanoceria, other nanomaterials have recently been studied for oxidase mimetic properties. Fe_2O_3 nanowires were explored by Cao and Wang as a sensor for glucose detection using their oxidase-like activity.[114] The non-enzymatic glucose sensor was fabricated with a Fe_2O_3 nanowire

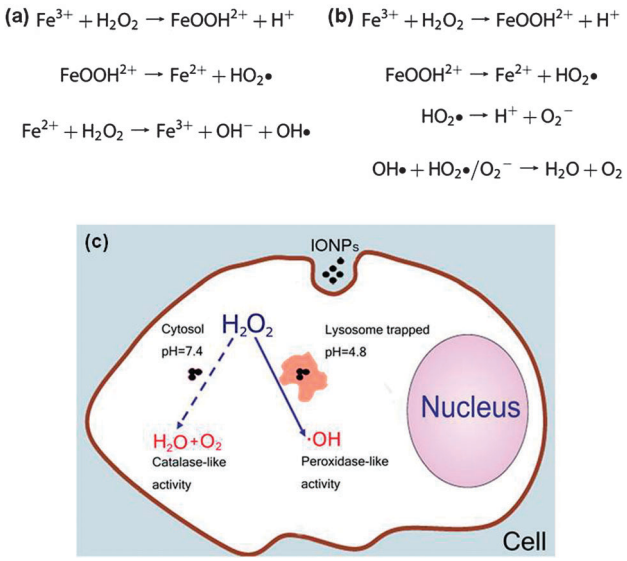

Fig. 19 Dual enzyme-like activities (*i.e.*, catalase and peroxidase mimics) of iron oxide nanoparticles. The nanoparticles may decompose H_2O_2 through catalase mimicking activity in neutral cytosol; however, they catalyzed H_2O_2 to produce hydroxyl radicals through peroxidase mimicking activity when trapped in acidic lysosomes. Reprinted with permission from ref. 110. Copyright (2012) American Chemical Society.

array.[114] Because it mimicked GOx behavior, the nanozyme sensor behaved as an oxidase mimic, rather than a peroxidase mimic as claimed. The sensing system had a linear range of 0.015 to 8 mM, with a detection limit of 6 μM towards glucose. More importantly, the system was able to detect glucose in serum samples with accurate performance. The system also showed good reproducibility and storage stability.

2.3 Other metal oxide-based nanomaterials

Many other metal oxide-based nanomaterials have also been explored to mimic several enzymes.[46,113,183,215,218,236,260]

2.3.1 Cobalt oxide as catalase and peroxidase mimics. Dual intrinsic enzyme mimicking activities (*i.e.*, catalase- and peroxidase-like activities) were observed for cubic Co_3O_4 nanoparticles.[183] The peroxidase mimicking activity was confirmed by catalytic oxidation of TMB. Kinetics studies showed that the nanozyme had higher affinity towards TMB but lower affinity towards H_2O_2 when compared with HRP. A further mechanism study suggested that the peroxidase-like activity was due to Co_3O_4 nanoparticles' ability for electron transfer between the substrate and H_2O_2 instead of hydroxyl radical. The catalase-like activity was also suggested based on the observation of increased oxygen generation in the presence of H_2O_2 and the nanozyme (Scheme 2). No mechanism for catalase-like activity was proposed. Since the peroxidase-like activity was not inhibited at high concentrations of H_2O_2, the cubic Co_3O_4 nanoparticles may actually imitate horseradish peroxidase C (HRP-C) properties, which exhibits weak catalase activity in addition to its peroxidase activity.

In another study, gillyflower-shaped Co_3O_4 nanoparticles were synthesized *via* an L-arginine-assisted hydrothermal approach and their peroxidase-like activity was tested.[260] When

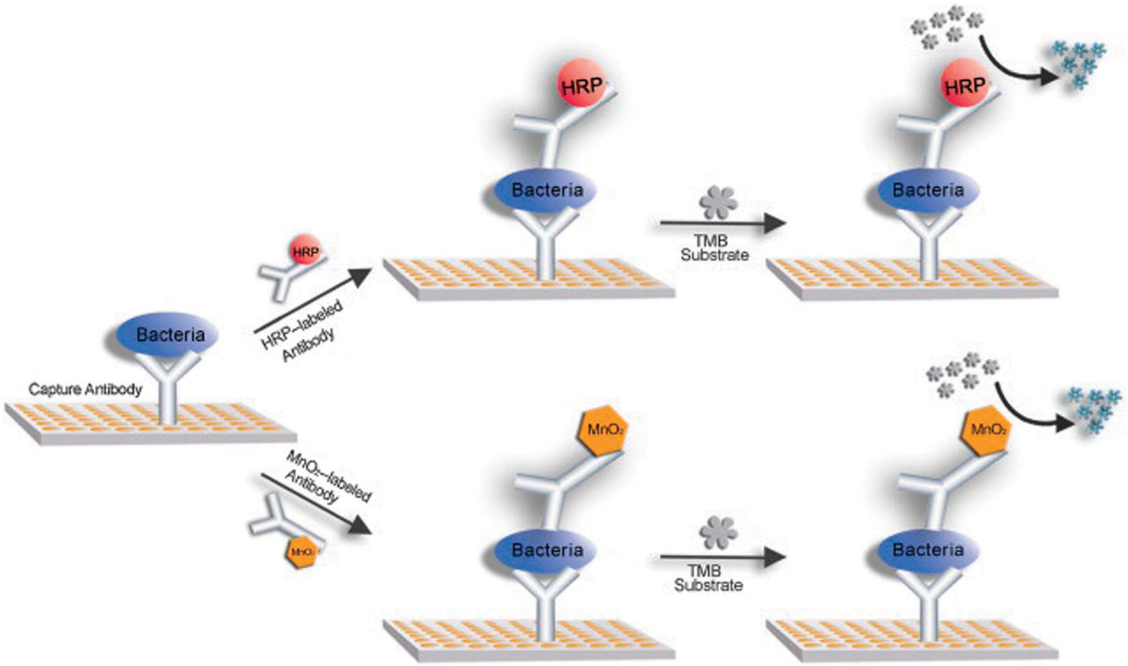

Fig. 20 MnO_2 NP as nanozyme to mimic oxidase for immunoassay. Reprinted with permission from ref. 113. Copyright (2012) Elsevier.

compared with commercially-available nanoparticles, superior peroxidase mimicking activity was achieved due to the unique gillyflower structures with larger specific surface area. Different from the above-mentioned cubic Co_3O_4 nanoparticles, hydroxyl radicals were involved in the suggested mechanism.

2.3.2 Copper oxide as oxidase mimics. Chen and co-workers found that commercially available 30 nm CuO nanoparticles showed peroxidase mimicking activity.[218] Compared with HRP and some other nanozymes, the CuO nanoparticles had the highest affinity to TMB. Later, they prepared water-soluble CuO nanoparticles *via* a quick-precipitation approach. Since the nanoparticles were smaller in size (6 nm) and had higher affinity towards H_2O_2, they showed higher peroxidase-like activity than the commercial ones.[236] A colorimetric assay for hydrogen peroxide and glucose was developed.

2.3.3 Manganese dioxide as oxidase mimics. MnO_2 nanomaterials with different morphologies (*i.e.*, nanosheets, nanospheres, nanosticks, nanocomplexes and nanowires) have also been studied to determine their oxidase mimicking activity.[113] Among them, MnO_2 nanowires had the highest and most stable activity, and were further used to label antibodies for an immunoassay of sulfate-reducing bacteria. A side-by-side study was carried out to compare the performance of the new nanozyme-based immunoassay to traditional HRP-based ELISA (Fig. 20).[113] Using a sandwich assay for the detection of a pathogen as an example, they showed that both the MnO_2 nanowire-ELISA and HRP-ELISA exhibited good sensitivity and high selectivity. However, the MnO_2 nanowire-ELISA was advantageous in several aspects: first, compared with HRP, the nanozyme was more stable, more robust but less expensive; second, the nanozyme oxidized the substrate without H_2O_2, eliminating the potential stability issue of H_2O_2.

2.3.4 Vanadium pentoxide as peroxidase mimics. V_2O_5 nanowires had catalytic activity towards peroxidase substrates (such as ABTS and TMB) in the presence of H_2O_2 as demonstrated in a study from Tremel's group.[215] They also showed that V_2O_5 nanowires exhibited similar kinetics but higher affinity towards both ABTS and H_2O_2 when compared with natural vanadium-dependent haloperoxidase (V-HPO). Based on structure similarity between V_2O_5 and V-HPO and EPR data, a reaction mechanism was proposed, in which a vanadium peroxo complex intermediate was involved (Fig. 21). The V_2O_5 based nanozymes could be re-used up to ten times and retained their activity in several organic solvents tested.

The excellent activity of the V_2O_5-based nanozymes was further demonstrated in a subsequent study, in which Tremel and co-workers reported that the V-HPO-like V_2O_5 nanowires prevented marine biofouling.[46] The long-term (60 day) *in situ* studies demonstrated that V_2O_5 nanowire-based nanozymes have excellent anti-biofouling capabilities (Fig. 22). The mechanism studies indicated that the anti-biofouling originated from HOBr and $^1O_2$ species. The as-prepared functional materials exerted a strong antibacterial activity against both Gram-negative and Gram-positive bacteria. Moreover, the nanozyme was even more inert than International Maritime Organization-approved antifouling products.

2.4 Metal-based nanomaterials

Metal nanomaterials can also be potential candidates for enzyme mimics, as indicated by numerous recent reports.[111,112,119,170,187,209,211,217,226,227,245]

2.4.1 Gold nanomaterials

2.4.1.1 Gold nanomaterials as oxidase mimics. Citrate-coated gold nanoparticles have been extensively studied for a variety of applications, such as biomedical assays, due to the routine synthesis and functionalization methods that have been

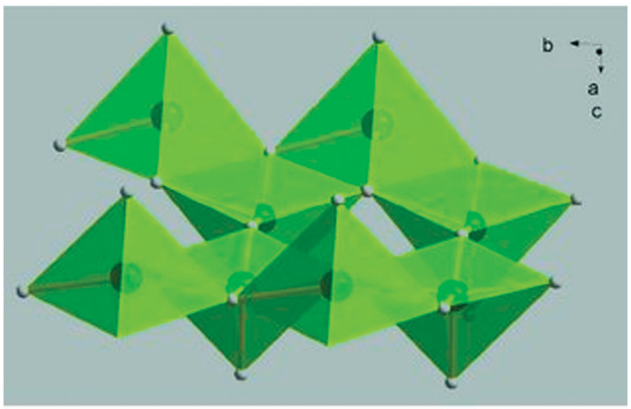

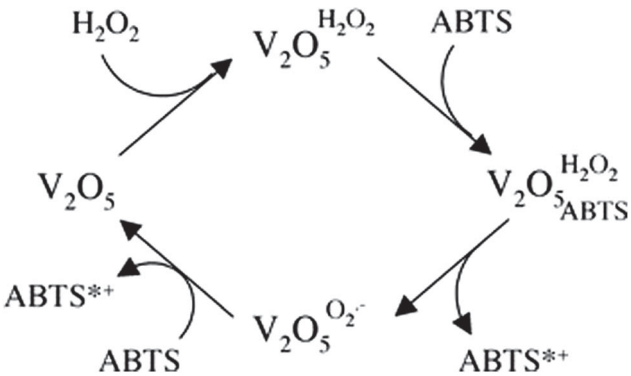

Fig. 21 The single layer structure of V_2O_5 and the proposed mechanism for its peroxidase-mimicking activity. Reprinted with permission from ref. 215. Copyright (2011) John Wiley and Sons.

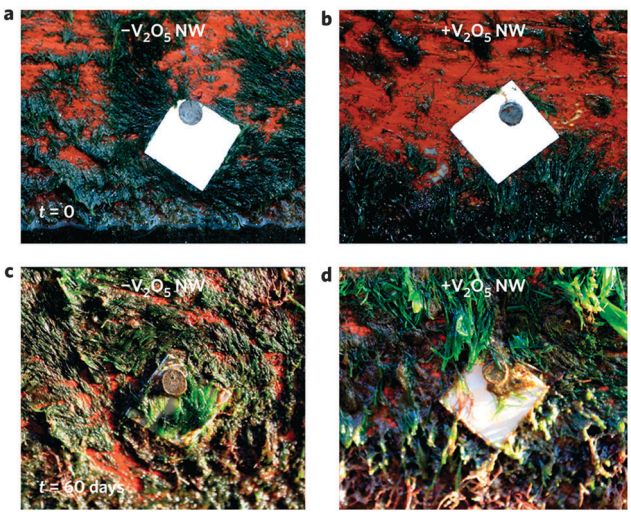

Fig. 22 Long-term *in situ* investigation showed that V_2O_5 nanowires based nanozymes had excellent anti-biofouling capability. Reprinted with permission from ref. 46. Copyright (2012) Nature Publishing Group.

developed. These nanomaterials have also been investigated for their catalytic activities. However, it was still surprising and remarkable when Rossi and co-workers showed that "naked" citrate-coated gold nanoparticles catalyzed the aerobic oxidation of glucose with dissolved oxygen.[40,42,276] The reaction was very similar to the reaction catalyzed by GOx, and suggested that gold nanoparticles could serve as a mimic for GOx (see Scheme 3a). Several other metal nanomaterials tested, such as Ag, Cu, Pd and Pt, did not show significant oxidase mimetic activity. Detailed mechanism studies were also carried out later by the same group.[42,276] Based on the experimental results, they proposed an Eley–Rideal mechanism for the catalysis. As suggested, glucose may first adsorb onto the gold nanoparticles; then an oxygen comes and reacts with the adsorbed glucose and forms the products (gluconic acids and H_2O_2). The gold nanozyme-based catalysis also followed Michaelis–Menten kinetics, and the results showed that native enzyme was 55 times more active than the nanozyme.

Inspired by these initial results, Fan *et al.* reported an interesting self-catalyzed, self-limiting system for controllable growth of gold nanoparticles (Fig. 23).[115] They further developed an innovative sensing strategy for DNA and microRNA detection based on the gold nanoparticles' intrinsic oxidase activity.[115,118] The different affinities of ssDNA and dsDNA towards gold nanoparticle seeds can be used to fine tune their growth, thus affecting their oxidase-like activity. Therefore, facilitated by the hybridization of the nucleic acids, nanozyme activity could be used to successfully detect target DNA or microRNA.[118] One appealing aspect of the strategy is that the final output signals are adaptable. When the system was coupled with HRP, colorimetric or chemiluminescent signals could be monitored. Without HRP, the plasmonic signals could be detected even at a single-nanoparticle level using dark field microscopy. The sensing system as a whole had single-base match differentiation capability.

2.4.1.2 Gold nanomaterials as peroxidase mimics. Gold nanoparticles with either positive or negative surface charges surprisingly showed peroxidase mimicking activity.[211,226] Chen and co-workers performed a systematic study to reveal the origin of the peroxidase-like activity seen from gold nanoparticles, confirming that the activity was indeed contributed by the gold nanoparticles.[187] The effects of surface modification on the activity were also examined, showing that the activities could be tuned by changing the affinities between the nanozymes and substrates. BSA (bovine serum albumin) encapsulated fluorescent gold nanoclusters were also used to mimic peroxidase.[170]

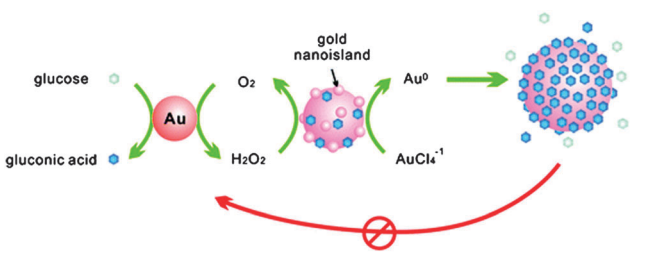

Fig. 23 Gold nanoparticles as nanozyme to mimic glucose oxidase. When glucose was oxidized, it produced H_2O_2, which would further promote the growth of gold seeds by reducing $HAuCl_4$ to Au^0. The system was self-limiting due to the presence of two negative feedback factors: size-dependent activity decrease of gold nanoparticles and product (gluconic acid)-induced surface passivation. Reprinted with permission from ref. 115. Copyright (2010) the American Chemical Society.

Mercury ions, which specifically enhance the peroxidase-like activity of gold nanoparticles compared with other metal ions, can also be detected using nanozyme technology.[226] Based on this phenomena, a colorimetric sensor for mercury ions was developed.

2.4.2 Platinum nanomaterials

2.4.2.1 Platinum nanomaterials as SOD mimics. Platinum nanoparticles encapsulated within apo-ferritin (PtNP@apo-ferritin) were synthesized and tested for their ability to detoxify reactive oxygen species.[277] The PtNP@apo-ferritin exhibited good SOD-like *in vitro* activity and long-term stability. The PtNP@apo-ferritin were uptaken by cells *via* a ferritin-receptor-mediated process and increased cell viability under externally induced stress.[277] Compared with ceria nanoparticles, the SOD-like activity of PtNP@apo-ferritin was lower on a weight basis as suggested by another study.[92]

2.4.2.2 Platinum nanomaterials as catalase and/or peroxidase mimics. 1–2 nm platinum nanoparticles within apo-ferritin (PtNP@apo-ferritin) were prepared and showed high stability.[112] Interestingly, the PtNP@apo-ferritin exhibited dual enzyme mimic behaviors (catalase and peroxidase), with both activities dependent on pH and temperature (Fig. 24). The study from Nie's research group indicated that the catalase-like activity were enhanced by increasing pH and temperature while the peroxidase-like activity had a maximum value at physiological temperature and slightly acidic conditions.[112] The catalytic activities were dependent on Pt content, with higher Pt content having better activities. Whether the PtNP@apo-ferritin from both reports also have triple enzyme mimicking activity should be investigated in the future.[112,277]

10 nm Pt nanocubes stabilized by cetyltrimethylammonium bromide (CTAB) were synthesized and exhibited peroxidase mimicking capability.[227] An Eley–Rideal mechanism for the catalysis was proposed as shown in Fig. 25. The catalytic activity was reduced when they formed aggregates, likely due to the decrease in surface area.[227]

2.4.3 Bimetal and other metal nanomaterials

2.4.3.1 Au@M (M = Bi, Pd and Pt) nanostructures as enzyme mimics. Chang and co-workers demonstrated that bismuth–gold nanoparticles exhibited peroxidase-like activity (Fig. 26).[245] They further developed a fluorescent signal-off assay for thrombin detection. The thrombin-induced signal decrease was due to the shielding of the peroxidase-like activity of bismuth–gold nanoparticles by thrombin triggered fibrinogen assemblies.

Wu, Yin and co-workers extended the previous studies to bimetal nanoparticles, *i.e.*, Au@Pt nanorods.[111,116,117,119] The

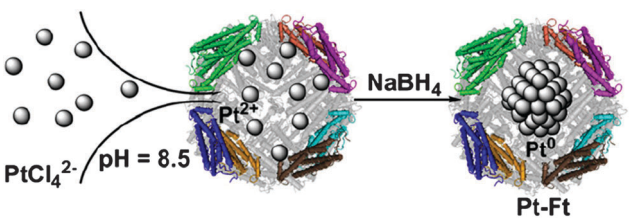

Fig. 24 Pt nanoparticles encapsulated within ferritin as dual enzyme mimics. Reprinted with permission from ref. 112. Copyright (2011) Elsevier.

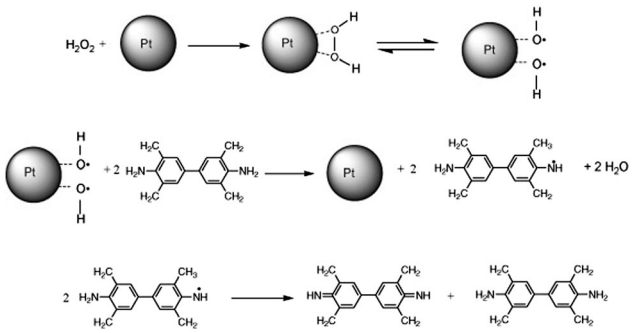

Fig. 25 Pt nanocubes as peroxidase mimics and the possible mechanism. Reprinted with permission from ref. 227. Copyright (2011) Elsevier.

Au@Pt nanorods showed multiple enzyme mimetic capabilities. The oxidase and peroxidase mimetic properties were confirmed by the oxidation of colorimetric substrates OPD and TMB in the absence and presence of hydrogen peroxide, respectively.[111] The catalase-like activity was confirmed by EPR spectroscopic studies.[111] An immunoassay for mouse interleukin 2 was developed by exploring the Au@Pt nanorods' dual enzyme mimicking activity using a 96-well plate format (Fig. 27). Further, they have shown that the Au@Pt nanorods also have ascorbate oxidase-like activities, which was used to eliminate the ascorbate interference towards glucose detection.[119]

2.4.3.2 AgM (M = Au, Pd and Pt) nanostructures as enzyme mimics. Another study from Wu, Yin and co-workers showed that a series of silver-based bimetallic alloy nanostructures, *i.e.*, AgM (M = Au, Pd and Pt), were able to oxidize colorimetric substrates to the corresponding products with H_2O_2, displaying peroxidase-like activity.[209] As expected, ascorbic acid was able to inhibit the oxidation of a substrate (OPD) in the presence of these silver nanozymes due to its natural antioxidant properties. Exploiting this phenomena, a method for determining ascorbic acid concentration was developed using these silver-based bimetallic nanozymes. The method has a linear range from 9 to 45 μM and a detection limit of 6.7 μM.

2.5 Carbon-based nanomaterials

Carbon-based nanomaterials, such as fullerene, carbon nanotubes (CNTs) and graphene, are showing great promise in various applications.[278] They have also received considerable attention from the nanozyme community due to their ability to mimic the activity of natural enzymes.[200,201,213,214,220–222,224,225,229,230,234]

2.5.1 Fullerene and derivatives as SOD mimics. Since its discovery, fullerene and its derivatives have attracted considerable attention in many research fields.[279] Early studies have shown that [60]fullerene (*i.e.*, C_{60}) could be considered as a radical sponge due to its unique chemical reactivity towards radicals.[280] However, fullerenes without any modifications are insoluble in water, which makes them unlikely to interact with biomolecules in aqueous solution. The ongoing efforts in developing water-soluble fullerene derivatives *via* chemical modification strategies have led to several intriguing discoveries, such as their interactions with biomolecules and enzyme-like activities.[54,55,281,282]

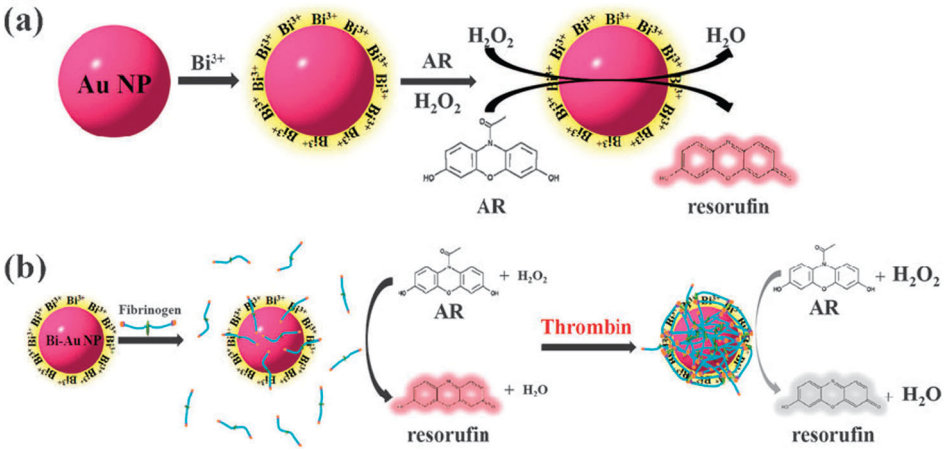

Fig. 26 Bismuth–gold nanoparticles as a peroxidase mimic and the application for thrombin detection. Reprinted with permission from ref. 245. Copyright (2012) Royal Chemistry Society.

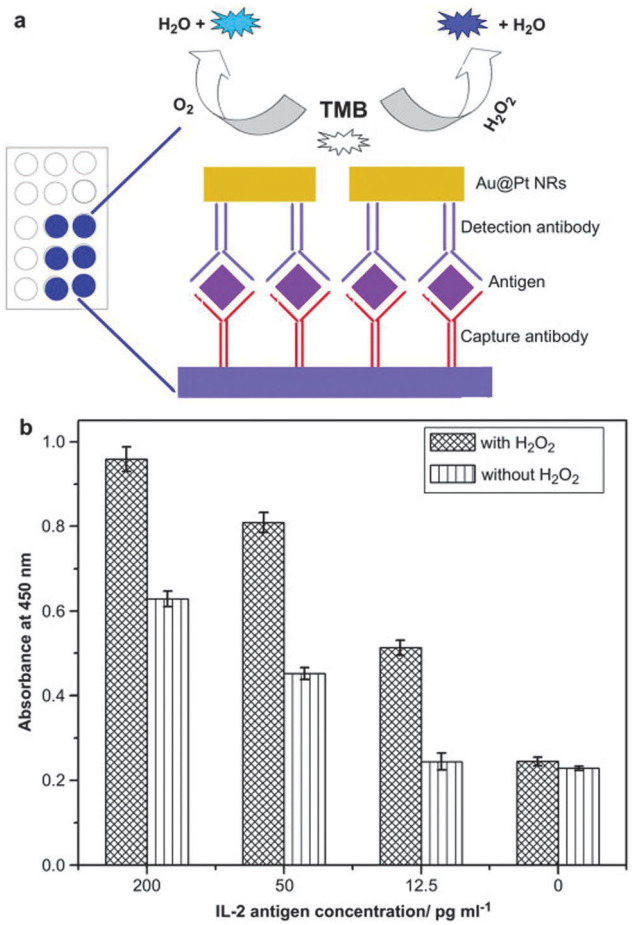

Fig. 27 Au@Pt nanorods as oxidase and peroxidase mimic and the application for immunoassay. Reprinted with permission from ref. 111. Copyright (2011) Elsevier.

In their initial studies, Choi and co-workers investigated the neuroprotective effects of two polyhydroxylated fullerenes ($C_{60}(OH)_{12}$ and $C_{60}(OH)_nO_m$, n = 18–20, m = 3–7 hemiketal groups). They found that both derivatives retained the free radical scavenging capability of native C_{60} and significantly reduced excitotoxic and apoptotic death of cultured cortical neurons.[35] Based on mass spectrum and ERP measurements, potential mechanisms for the excellent neuroprotective effects were suggested. First, the fullerenes were able to accept multiple free radicals and thus detoxify them by forming adducts; and second, the formed adducts were diamagnetic (*i.e.*, not radical species) and thus non-harmful. However, no SOD mimetic activity was suggested at that time.

In subsequent studies, more consistent results with *tris*-malonic acid derivatives of C_{60} ($C_{60}[C(COOH)_2]_3$, rather than polyhydroxylated C_{60}) showed fullerene derivatives could be effective neuroprotective antioxidants both *in vitro* and *in vivo*.[36,38,283] The superoxide radical quenching activities were demonstrated for both regioisomers of $C_{60}[C(COOH)_2]_3$ with C_3 and D_3 symmetry. $C_{60}[C(COOH)_2]_3$ with C_3 symmetry (C_{60}-C_3) showed higher activities than $C_{60}[C(COOH)_2]_3$ with $D3$ symmetry (C_{60}-D_3), which was attributed to C_{60}-C_3's polar nature and resultant better cell membrane penetrating ability. Moreover, detailed studies with EPR and other techniques confirmed the SOD mimetic property of C_{60}-C_3 (Fig. 28).[38] Unlike polyhydroxylated fullerenes, Ali and co-workers demonstrated that the C_{60}-C_3's SOD mimetic activity was due to the catalytic dismutation of superoxide rather than stoichiometric scavenging.[38] The catalytic mechanism was experimentally validated by several observations, such as the lack of structural modifications to C_{60}-C_3, absence of detectable paramagnetic products, generation of hydrogen peroxide and regeneration of oxygen.[38] They also carried out semi-empirical quantum-mechanical calculations to model the interactions between the superoxide radical substrate and the C_{60}-C_3 nanozyme. The electron distribution map results indicated that, with the help of protons from the carboxyl groups and/or surrounding water molecules, the electron-deficient regions on C_{60}-C_3 electrostatically drew the substrate anions toward the C_{60}-C_3 surface and directed them for further dismutation (Fig. 28).[38] Later, they carried out a more detailed structure-activity study to build a relationship between neuroprotection by carboxyfullerenes and their affinity toward superoxide radicals.[284] The computational model demonstrated

that the activity was closely related to both the number and distribution of carboxyl groups on the fullerene ball.

To compare C_{60}-C_3's performance with native and other artificial enzymes', kinetics studies have been performed.[38] Based on a xanthine oxidase/cytochrome *c* assay, the rate constant of C_{60}-*C*3 at pH = 7.4 was calculated to be 2.2×10^6 M^{-1} s^{-1}. This rate was comparable to several manganese-containing mimics, though it was 100-fold lower than native SOD.[38] Further, using the same ping-pong mechanism of native SOD, a kinetics model was proposed and fit well with experimental results. Further work from Gozin and co-workers showed C_{60}-C_3 nanozyme and human serum albumin could form a non-covalent complex with a binding constant of 1.2×10^7 M^{-1}.[285] The SOD mimetic activity of the complex was found to be nearly identical to free C_{60}-C_3 nanozyme.

Applications. Fullerene derivative-based SOD mimics have showed protective roles in many redox-active biological processes, such as neuroprotection and anti-aging.[36,38,283,286]

(a) Neuroprotection. Using carboxyfullerenes as an effective neuroprotective agent was among the first bioactivity studies of nanozymes in the literature.[35,36,283] Dugan *et al.* first reported that carboxyfullerenes acted as novel free radical scavengers and effectively reduced excitotoxic and apoptotic death of cultured cortical neurons.[35] Their subsequent studies showed that the C_{60}-C_3 nanozyme was more effective towards neuron protection than other fullerene derivatives and could be further extended to other neurodegenerative disorders, including Parkinson's disease.[36,283] Using SOD2 knockout mice as an *in vivo* model, which lack the mitochondrial manganese SOD (MnSOD), Ali and co-workers found that both utero and post-natal survival were improved following C_{60}-C_3 treatment. For the live-born SOD2 knockout mice pups, as long as 300% life span was observed with daily injections of C_{60}-C_3. They also showed that some of the C_{60}-C_3 localized to mitochondria. Together, these results suggest that C_{60}-C_3 acts as a biologically active SOD mimic *in vivo*, and holds great promise for functional replacement of MnSOD.[38] In a more detailed study, the neuroprotective activities of six different carboxyfullerene based SOD mimics were evaluated experimentally and qualitatively correlated with their superoxide affinity (Fig. 29).[284] Among the six candidates, the C_{60}-C_3 nanozyme exhibited the highest efficacy, which was consistent with previous results.[36] The structure-activity relationships were revealed by computer-assistant molecular modeling, indicating that the activities were tuned by both the number of carboxyl groups and their distribution on the fullerene.

(b) Anti-aging. Research has suggested that aging is associated closely with several key redox processes, such as detoxification of reactive oxygen species and the cellular response to oxidatively-damaged macromolecules.[286] Quick and co-workers' excellent study demonstrated that the C_{60}-C_3-based SOD mimic not only improved wild-type mice's cognition ability but also extended their lifespan. Their fixed brain slice imaging results showed that age-related oxidative damage in all brain regions tested was significantly reduced after the nanozyme chronic treatment (Fig. 30). Using spin-trapping EPR measurements, they have convincingly demonstrated that the nanozyme was mitochondrially active (since mitochondria are the major cellular source of reactive oxygen species), and could reverse age-associated mitochondrial free radical production. The effects of the nanozyme on age-related loss of spatial learning and memory were also evaluated, showing the nanozyme's potential for rescuing age-related cognitive impairment in mice.

2.5.2 CNTs, graphene and derivatives as peroxidase mimics. The peroxidase-like activity of CNTs was reported by

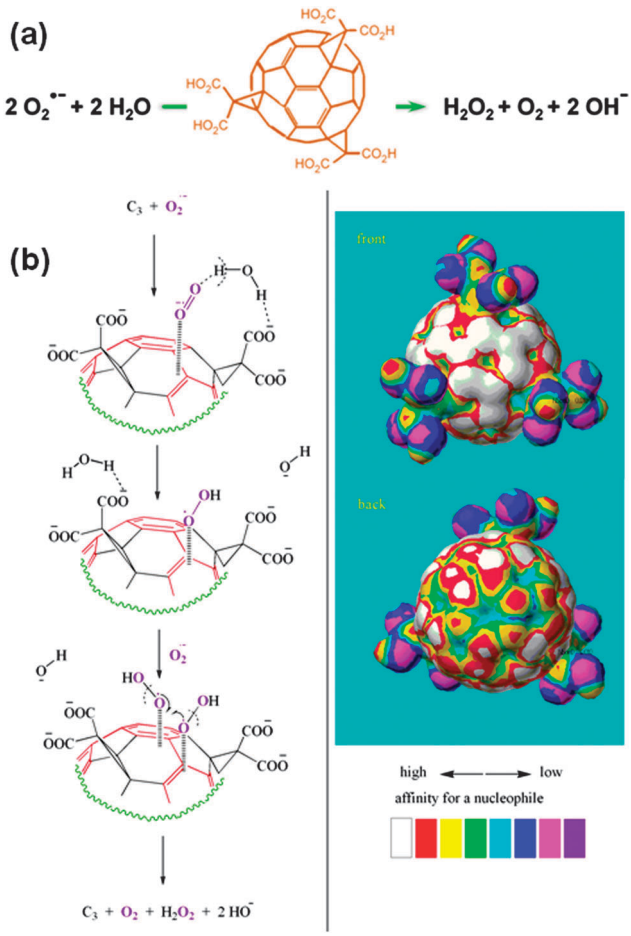

Fig. 28 (a) $C_{60}[C(COOH)_2]_3$ with C_3 symmetry (C_{60}-C_3) as nanozyme to mimic SOD and (b) the proposed catalytic mechanism. Reprinted with permission from ref. 38. Copyright (2004) Elsevier.

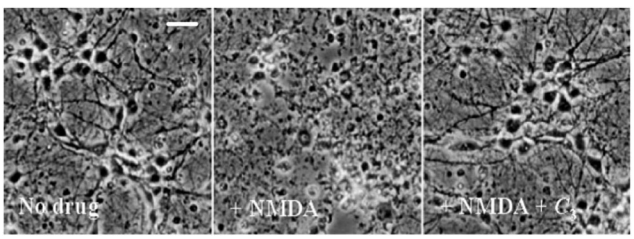

Fig. 29 Neuroprotection by carboxyfullerenes in NMDA receptor-mediated excitotoxic injury. Reprinted with permission from ref. 284. Copyright (2008) Elsevier.

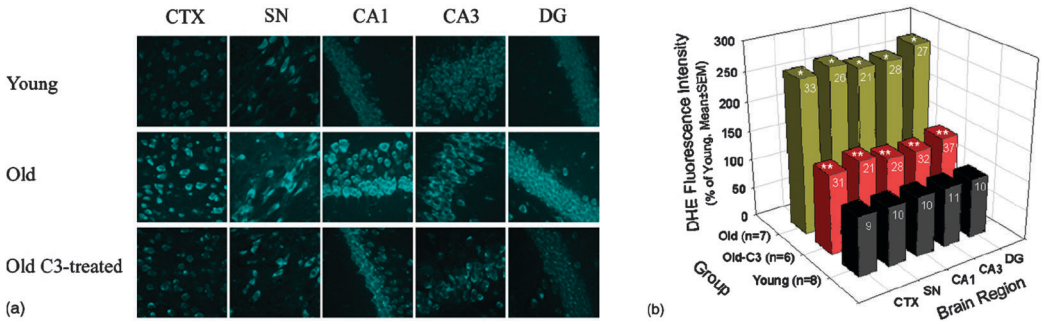

Fig. 30 Reduction of age-associated brain oxidative stress by the C_{60}-C_3 based SOD mimic. Reprinted with permission from ref. 286. Copyright (2008) Elsevier.

several groups recently.[214,220] The intrinsic peroxidase-like activity of single-walled carbon nanotubes (SWNTs) was investigated by Qu *et al.*[214] Similar to HRP, its activity was pH, temperature and H_2O_2 dependent. After removal of cobalt from SWNTs by sonication in concentrated sulfuric and nitric acids, the treated SWNTs still retained similar catalytic activity, which confirmed that the catalytic activity was due to SWNTs rather than trace amounts of metal catalyst.[214] However, Fe content did affect the activity of helical CNTs, as shown by Zhu's study.[220] They showed that higher Fe content resulted in better catalytic activity. Although they showed helical CNTs had better catalytic performance than multi-walled carbon nanotubes (MWNTs), no direct comparison between helical CNTs and SWNTs was made. More systematic studies are needed to understand the discrepancy between these studies.[214,220] The *Km* from kinetics studies showed that the helical CNTs had a higher affinity towards TMB (0.020 mM for helical CNTs *vs.* 0.4 mM for HRP) but a lower affinity towards H_2O_2 when compared with HRP (41.42 mM for helical CNTs *vs.* 3.7 mM for HRP).[220] The helical CNTs exhibited better affinity towards H_2O_2 than Fe_3O_4 NPs (41.42 mM for helical CNTs *vs.* 154 mM for Fe_3O_4 NPs). No molecular mechanism was proposed for the CNTs' peroxidase mimicking activity.

Graphene oxide was also found to possess intrinsic peroxidase mimicking activity by Qu *et al.*[213] Due to its very high surface-to-volume ratio as well as high affinity towards organic substrates, graphene oxide showed a higher affinity towards TMB than HRP (*Km*, 0.0237 mM for graphene oxide *vs.* 0.275 mM for HRP), but a lower affinity towards H_2O_2 than HRP (*Km*, 3.99 mM for graphene oxide *vs.* 0.214 mM for HRP). Dong and co-workers synthesized a functionalized graphene with hemin as a peroxidase mimic for the first time (Fig. 31).[221] The functional hybrid nanosheets were formed through π–π interactions between graphene and hemin. The intrinsic peroxidase-like activity, originating mainly from the hemin, was indicated by the conversion of TMB, ABTS and OPD to their colored product. The kinetics studies showed the catalytic reaction of the graphene/hemin-based nanozyme had a ping-pong mechanism, which was consistent with HRP and other carbon-based nanozymes. However, different from CNT and graphene oxide, the graphene/hemin-based nanozyme had a higher affinity towards H_2O_2 but a lower affinity towards TMB when compared with HRP.[222] Further experimental, as well as computational, studies are needed to explain the difference. Later results from Quan's and Wang's groups indicate that other nanomaterials can complex with graphene, resulting in enhanced peroxidase mimetic activity due to synergetic effects.[200,201,224] No molecular mechanism was suggested for either graphene- or graphene oxide-based nanozymes.

Other forms of carbon, such as nanodots, nanoparticles and nitrogen doped nanodots, were also explored to mimic peroxidase's activity.[225,230,234]

Applications

(a) H_2O_2 and glucose detection. As summarized in Table 1, carbon-based nanozymes as peroxidase mimics were also used for detection of H_2O_2 and glucose.

(b) Metal ions detection. When the synergic effects of CNTs' and magnetic silica nanoparticles' peroxidase-like activities were combined with copper-based click chemistry, a signal-on, highly sensitive and selective sensor toward copper(II) ions was developed (Fig. 32).[194] With a high selectivity against several other metal ions and a detection limit of 1 μM, the current method

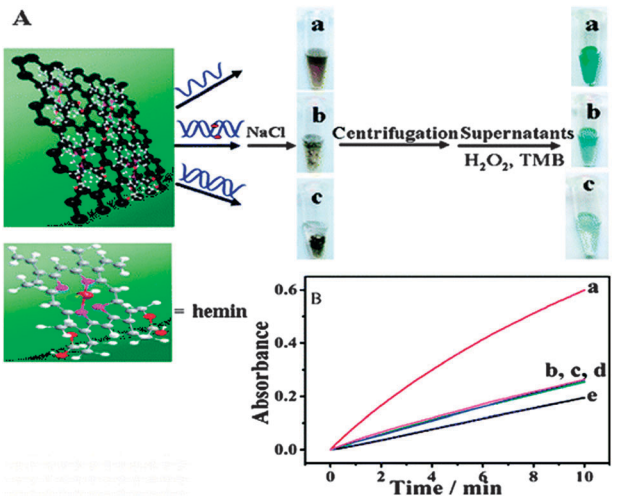

Fig. 31 Functionalized graphene with hemin as peroxidase mimic. The hybrid nanosheets were synthesized through π–π interactions between graphene and hemin. The nanosheets had intrinsic peroxidase-like activity, originating from the hemin. Based on the unique capability of differentiating ssDNA and dsDNA, the nanosheets were further used for colorimetric detection of single-nucleotide polymorphisms in disease-associated DNA. Reprinted with permission from ref. 221. Copyright (2011) American Chemical Society.

meets the EPA detection limit requirement (20 μM) for copper ion monitoring. However, one potential challenge for practical use is that the click chemistry reaction takes 24 h.[194]

(c) DNA detection. Most of the DNA detection methods are based on the different affinities of ssDNA and dsDNA towards nanozymes (such as CNTs and graphene).[169,200,214,221,224] For example, compared with dsDNA, ssDNA has a higher affinity towards hemin-modified graphene and can stabilize it against salt-induced aggregation. Thus, after centrifugation, a majority of the hemin-modified graphene remains in the supernatant, which exhibits high nanozyme activity. Combining this principle and DNA hybridization, a target DNA and a single base mismatch DNA can be readily differentiated (Fig. 31).[221] The proposed method has been successfully used for label-free colorimetric detection of single nucleotide polymorphisms. CNT-based nanozymes operate under the same principle and have also been investigated for single nucleotide polymorphism analysis.[214] Liu *et al.* demonstrated that the adsorption of ssDNA onto a gold nanoparticle-modified graphene surface could inhibit its peroxidase-like activity.[200,224] When ssDNA was released from the graphene surface by either hybridizing with its complementary ssDNA or cleavage with an enzyme, the peroxidase-like activity of the graphene was restored, providing a sensing mechanism for either DNA or enzyme-activity (Fig. 33).

(d) Aptasensors. Further studies have established that ssDNA can be adsorbed onto a graphene surface while dsDNA cannot. When ssDNA is adsorbed onto a graphene surface, it can significantly affect the graphene's properties, such as inhibiting its peroxidase-like activity as described above. Based on this phenomena, a novel sensing strategy for insulin was developed by exploring the different affinities of an anti-insulin aptamer and the insulin–aptamer complex towards a graphene–gold nanoparticle hybrid.[200]

(e) Immunoassay. Qu and co-workers reported electrochemical and colorimetric platforms for the detection of PSA (a cancer biomarker) by using graphene oxide's peroxidase-like activity.[229] To efficiently capture and separate PSA from the sample, magnetic beads conjugated with anti-PSA (Ab1) were used. The presence of PSA induced the formation of a magnetic bead-Ab1/PSA/Ab2-graphene oxide sandwich complex. After magnetic separation, a homogeneous solution of Ab2-graphene oxide converted a substrate (hydroquinone) to a brown colored product. The hydroquinone is electrochemically active, so it can also be electrochemically detected by square wave voltammograms. Both the colorimetric and electrochemical signals were inversely correlated with PSA concentration. A cutoff concentration of 4 ng mL^{-1} for prostate cancer diagnosis can be easily monitored by the current colorimetric method. Under optimal conditions, PSA can be electrochemically detected with a linear range from 0.1 to 10 ng mL^{-1}. The electrochemical method showed good selectivity against human immunoglobulin G, BSA, α-1-fetoprotein and lysozyme. More impressively, when the method was applied to 8 clinical serum samples, the results were consistent with ones obtained using a commercial ELISA method, showing great promise for future applications (Fig. 34).

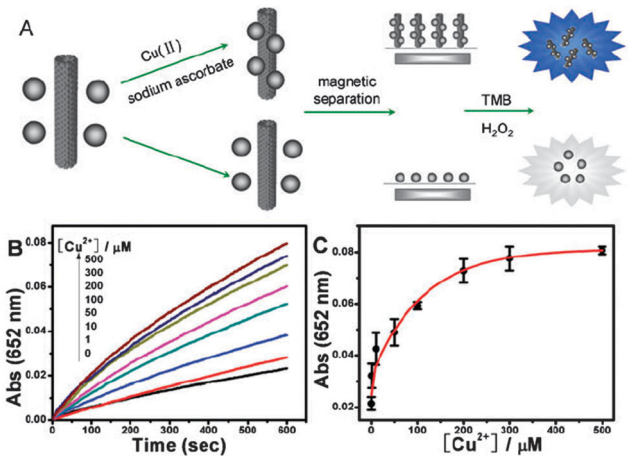

Fig. 32 Detection of copper ions using magnetic silica nanoparticles clicked on multi-walled carbon nanotubes. Reprinted with permission from ref. 194. Copyright (2010) Royal Society of Chemistry.

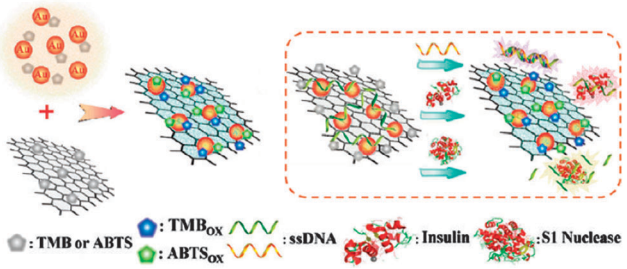

Fig. 33 Schematic illustration of a versatile and label-free colorimetric biosensing platform based on the switchable interface of gold nanoparticle-modified graphene hybrid. Reprinted with permission from ref. 200. Copyright (2012) American Chemical Society.

2.6 Other nanomaterials

Inspired by the great progress in the development of peroxidase-mimicking nanomaterials described above, additional materials have been explored to investigate their potential enzyme-like activities.[163,165,180,186,188,189,196–198,204,206,212,216,219,223,231,237,238,242,247,249,251,252,254,257,258,262,264]

2.6.1 Other iron-based nanomaterials as peroxidase mimics. Other iron-based nanomaterials have also received considerable attention for their peroxidase mimicking capability.[163,180,189,196,197,204,212,216,223,231,238,249,252,254,257,258,264] Ju *et al.* prepared FeS nanosheets by a micelle-assisted approach and studied their peroxidase mimetic activities (Fig. 35).[204] Due to their large specific area, these FeS nanosheets showed better performance than spherical FeS nanomaterials and were used to develop an amperometric sensor for H_2O_2 detection. FeS peroxidase-like activity was also reported by other groups.[238,249] A recent study showed that FeS nanoneedles had better activity than FeSe spherical nanoparticles.[238] FeTe nanorods, with a larger specific surface area compared with Fe_3O_4 MNPs, showed enhanced activity as

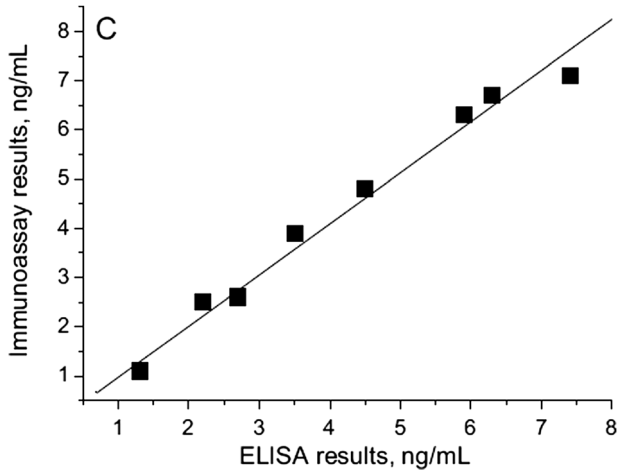

Fig. 34 Comparison of the PSA concentrations in serum samples determined with the proposed immunoassay and the ELISA method. Reprinted with permission from ref. 229. Copyright (2011) Elsevier.

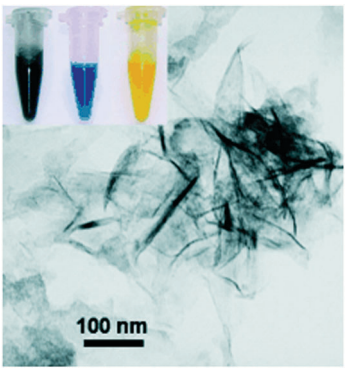

Fig. 35 FeS nanosheets as nanozyme to mimic peroxidase. The nanosheets were characterized by TEM imaging and the peroxidase-like activity was confirmed through oxidation of TMB (inset). Reprinted with permission from ref. 204. Copyright (2009) John Wiley and Sons.

well.[254] These results together suggest that the surface area of nanomaterials plays a crucial role in their catalytic activities.

A few other iron based nanomaterials were also reported, such as γ-FeOOH nanosheets on graphene,[196] iron-substituted SBA-15 microparticles,[163] [FeIII(biuret-amide)],[252] Fe(III)-based coordination polymer nanoparticles,[258] and iron phosphate microflowers,[189] illustrating the growing interest and efforts for developing new nanozyme mimics.

2.6.2 Others nanomaterials as peroxidase mimics. Nanostructured layered double hydroxide (LDH) was shown to have peroxidase mimicking activities and then used for constructing electrochemical and colorimetric sensors.[206,219,262] Sun and co-workers recently showed that both polyoxometalate and carboxyl-functionalized mesoporous polymers also have good peroxidase-mimicking activities.[165,247] CuS concave superstructures were formed *via* a solvothermal approach and were shown to have a 2-fold higher peroxidase mimetic activity than CuS microspheres.[242]

Most of these nanozymes were confirmed by the reaction with colorimetric substrates in the presence of hydrogen peroxide.

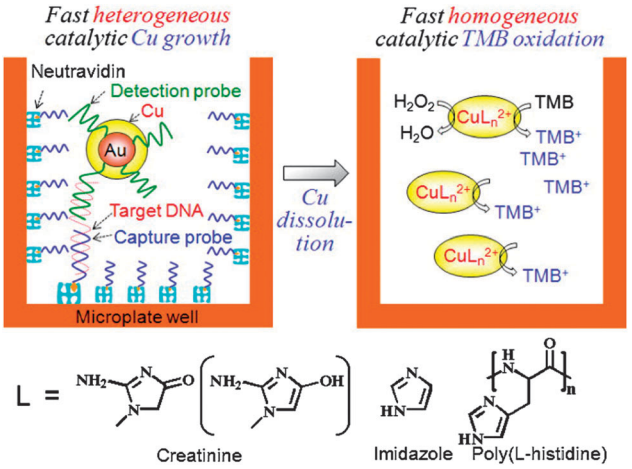

Fig. 36 DNA detection using a peroxidase-like copper-creatinine complex. Reprinted with permission from ref. 198. Copyright (2011) Elsevier.

Usually, hydrogen peroxide and/or glucose detection were demonstrated as potential applications. Singh *et al.* proposed a different approach to DNA detection using a peroxidase-like copper–creatinine complex (Fig. 36).[198] In the presence of a target DNA, a sandwich structure is formed and a copper shell is grown onto the DNA–gold nanoparticle conjugate probes. The copper is then released as free ions and is further complexed with creatinine to form a nanozyme for generating colorimetric signals. This proposed method has a detection limit two orders of magnitude lower than the HRP-based DNA detection (0.1 pM *vs.* 1 nM).

3. Tuning nanozyme activity

Like natural enzymes, the nanozymes' activities can be tuned by many factors. Below, several important factors are summarized and reviewed.

3.1 Size

Many properties of nanomaterials are size-dependent. Unsurprisingly, it is possible to tune the activity of nanozymes by controlling their sizes, which has been demonstrated in many studies.[44,81,115,136,177,182,217,236,287] In most cases, smaller nanoparticles have higher activity than the larger ones, likely due to a higher surface to volume ratio.[44,136] For example, Peng and co-workers investigated the size-dependent peroxidase-like catalytic activity of Fe_3O_4 MNPs.[136] By comparing Fe_3O_4 MNPs with different diameters, they showed that the nanozymes' activity increased with the reduced nanoparticle size.

3.2 Shape and morphology

The shape and morphology of nanozyme also play critical roles in tuning their catalytic activities.[113,142,166,177,184,242] In Wan's report, manganese oxide nanomaterials with different shapes (sheet, sphere, wire, complex, stick) were synthesized and their oxidase-like activities were compared.[113] Though the nanospheres and nanowires exhibited the highest activities, the nanospheres were

not stable, and only the manganese oxide nanowires were used for further bioanalysis. Liu *et al.* carried out a detailed study to understand the shape and morphology effects of Fe_3O_4 MNPs on their peroxidase mimetic activities (Fig. 37a).[166] Compared with triangular plates and octahedrons, the highest activity was seen from spheres, and was attributed to their higher specific surface area. For the triangular plates and the octahedrons, which had similar size and surface area, the difference in activity was due to their surface atom arrangements. The more active {220} planes of the triangular plates were responsible for their higher activities when compared with the octahedrons, with {111} planes.

3.3 Surface coating and modification

The nanozymes' surface coatings provide them not only enhanced stability but also functional groups for further bioconjugation.[44,81,85,90,95,111,113,119,140,142,147,153–155,162,175,180,187,190,192,233,264,287,288] Thus, coatings have been used to further tune the nanozymes' activities. Usually, the surface coating shields the catalytic nanozyme core from the substrate, which in turn decreases its activity. A number of factors can be used to tune the coating and hence the activity, such as the thickness and size of the coating layer and the packing density of the modifying groups.[44] For example, the peroxidase activity of Fe_3O_4 MNPs decreased when they were coated with SiO_2, 3-aminopropyltriethoxysilane, polyethylene glycol or dextran.[44] Among the coatings, the dextran-modified Fe_3O_4 MNPs exhibited the highest performance. For a given polymer coating (such as polyethylene glycol or dextran), the coating's molecular weight and thickness are inversely correlated with the activity. Certain coatings can also enhance the catalytic activity of the nanozymes. For example, it has been shown that the Fe_2O_3 MNPs with a Prussian blue coating exhibit activity correlated with coating levels, *i.e.*, a higher content of Prussian blue results in higher nanozyme activity.[154,233]

Wang *et al.* carried out a comparison of peroxidase-like gold nanoparticles with different coatings, *i.e.*, unmodified, amino-modified and citrate-modified coatings, to evaluate nanozyme activity (Fig. 37b).[187] For both substrates tested (ABTS and TMB), unmodified gold nanoparticles showed superior catalytic activity compared to amino- and citrate-modified nanoparticles. Using ABTS as a substrate, amine-modified nanozymes showed higher activity than citrate-modified nanozymes, while the trend was reversed for the TMB substrate. These results reveal that (a) superficial gold atoms were a contributing factor to the nanozyme activity and (b) the charge characteristics of the coating and the substrates played an important role in the activity. The use of interactions between the substrate and the coating to tune the nanozyme's activity was also confirmed in several independent studies.[119,147,180]

3.4 Composition

He *et al.* showed that for AgM bimetallic alloy-based peroxidase nanozymes, the activity could be fine-tuned by gradually changing the ratio of the two metals (Fig. 37c).[209] They suggested that the composition-dependent activity was from the electronic structure due to alloying. Doping approaches were also used to modulate the nanozymes' activities.[91,102] For nanoceria-based SOD mimics, the catalytic activity was reduced with titanium doping.[102] The reduced activity is likely due to the fact that TiO_2 nanoparticles have no SOD activity. To provide further insights into the mechanism of nanoceria's biological activity, the effects of samarium doping was also investigated. The samarium doping decreased

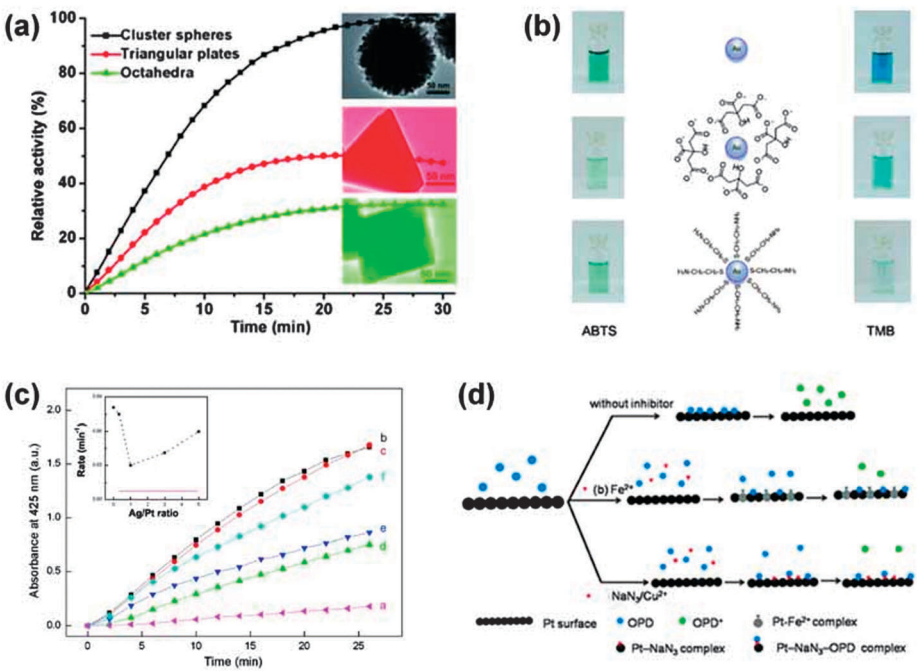

Fig. 37 Tuning nanozymes' activity by controlling nanomaterials' shapes (a), surface coatings (b), compositions (c), and adding inhibitors (d): (a) reprinted with permission from ref. 166; copyright (2010) John Wiley and Sons; (b) reprinted with permission from ref. 187; copyright (2012) John Wiley and Sons; (c) reprinted with permission from ref. 209; copyright (2010) American Chemical Society; and (d) reprinted with permission from ref. 116; copyright (2011) Royal Society of Chemistry.

Ce^{3+} but did not affect the oxygen vacancy content. The finding that gradual samarium doping progressively reduced the nanozymes' activity established that Ce^{3+}/Ce^{4+} redox reactions were responsible for the outstanding biological properties of nanoceria.[91]

3.5 Activators and inhibitors

For natural enzymes, an activator increases the enzymatic activity while an inhibitor decreases the activity when binding to the enzyme. Researchers have also sought activators and inhibitors to tailor the catalytic activity of nanozymes.[95,116] Singh *et al.* showed that phosphate (instead of sulfate or carbonate) anions could arrest "Ce" in the +3 state, and thus increase the catalase-like activity of nanoceria.[95] Wu and co-workers performed a screening study to select candidates that could inhibit the oxidase-like activity of Au@Pt nanorods (Fig. 37d).[116] They found that Fe^{2+} was an irreversible inhibitor while Cu^{2+} and NaN_3 were reversible inhibitors. They also showed that Hg^{2+} was an efficient inhibitor and established a detection method for Hg^{2+} based on the inhibition phenomena.

3.6 Forming hybrids

The catalytic activity of Fe_3O_4 MNPs was also investigated by electrochemistry.[289] Using a synthetic protocol, dumbell-like Au–Fe_3O_4 MNPs were obtained and compared against Fe_3O_4 MNPs. The dumbell-like Au–Fe_3O_4 MNPs showed enhanced hydrogen peroxide reduction activity compared with Fe_3O_4 MNPs alone, which was attributed to the polarization effects from Au to Fe_3O_4.[289] In another independent study, it was shown that Fe_3O_4 MNPs' electrochemical activity toward hydrogen peroxide sensing was enhanced and tuned by silver nanoparticles.[268]

3.7 Other factors

Other factors, such as pH and temperature, can also affect and tune the catalytic activity of nanozymes.[44,45,90,110,112]

4. Comparison, challenges and perspective

In this section, a brief comparison of nanozymes, other artificial enzymes, natural enzymes, organic catalysts, and nanomaterial-based catalysts is presented to address the advantages and disadvantages of each type of catalyst. As shown in Table 4, besides the several distinct advantages shared with other artificial enzymes, nanozymes are unique due to their nanoscale sizes. Shrinking the size of materials to the nanoscale size regime results in very interesting and useful properties, such as the plasmonic properties of noble metal nanoparticles and the superparamagnetic properties of iron oxide nanoparticles. Also, nanoscale materials have a sufficiently large area for conjugating multiple ligands for biorecognition.

Despite the above mentioned advantages, there are numerous challenges to be addressed in the field (Table 4).

(a) Compared with natural enzymes and organic catalysts, the efficiency of most nanozymes are still lower. Therefore, the development of high performance nanozymes will be a hot topic for future research.[290] In certain circumstances, though the nanozyme's core is highly active, additional coatings and bioconjugation can decrease the activity dramatically. Thus, novel surface coating and bioconjugation techniques are required to maximize the performance of nanozymes.

(b) Though selective detection protocols have been established for sensing important targets, the nanozymes themselves have limited selectivity. For example, the selective detection of glucose was mainly due to GOx, rather than the MNP nanozymes. Therefore, the design and development of nanozymes with high (asymmetric) selectivity towards given substrates will be one of the greatest challenges to be tackled.

(c) There are various types of natural enzymes and organic catalysts, which together can catalyze almost all of the important reactions. However, most of the nanozymes' catalytic reactions are based on redox type reactions (*vide supra*) except a few which are based on hydrolytic reactions.[37,39,291–296] The development of nanozymes for new types of reactions will be another hot topic in this field.

(d) The toxicity of nanomaterials is currently receiving significant attention from both academia and the public due to their potential environmental, health and safety concerns.[297,298] Likewise, nanozymes are facing the same challenges. For example, to develop a nanozyme as a novel therapeutic reagent, it must pass the strict safety and efficacy requirements of the regulatory agencies (such as the US Food and Drug Administration). Nevertheless, it is encouraging that several iron oxide nanoparticle-based reagents, such as Resovist, have been approved for clinical use. More effort is needed to translate the fundamental and leading scientific results for practical applications.

(e) In certain cases, natural enzymes are working together as enzyme clusters. The functional assemblies of several nanozymes together will provide new paradigms with combined (and enhanced) properties due to the synergic effects of different components.[299]

(f) Most of the catalytic activity seen from current nanozymes is due to the surface atoms (sites). The inside core may also play a critical role. Moreover, the activity may be further tuned by manipulating the inside core. For example, it would be interesting to re-examine the activities of fullerene-based nanozymes after doping certain (metal) atoms inside.

(g) Most of the nanozymes used are not atomically uniform in size (one exception is fullerene-based nanozymes). Therefore, ongoing research will focus on improving synthetic protocols to obtain high quality nanozymes with uniform size and atomically precise structures. A related issue is how to rationally design a nanozyme for a specific requirement (function).[300] Based on advanced computation, researchers now are able to construct novel protein nano-assemblies with atomic level accuracy, showing the great promise of computation-assisted rational design.[301] Due to the complex nature of nanozymes' rational design, close collaboration will be needed from researchers in multiple areas. As a subdiscipline of nanomaterials, nanozymes share all the advantages and challenges of other nanomaterial-based catalysts, as shown in Table 4. Since the primary goal of nanozymes research is to develop more efficient artificial alternatives to natural enzymes, nanozyme research will find its unique niche in nanomedicine, biotechnology and related areas.

Table 4 Comparison between nanozymes and others[a]

		Advantages	Challenges
Artificial enzymes	Nanozymes	(1) Low cost	(1) Low efficiency
		(2) Easy for mass-production	(2) Low specificity
		(3) Robustness to harsh environments	(3) Low selectivity
		(4) High stability	(4) Limited catalytic reactions
		(5) Long-term storage	(5) The exact mechanism
		(6) Tunable activity	(6) Atomic precise structure and 3D structural information
		(7) *Size-* (*shape-*, *structure-*, *composition-*) *dependent properties*	(7) *Rational design of the nanozymes*
		(8) *Other functions besides catalysis* (*i.e.*, *the unique functions from the nanoscaled materials, such as magnetic properties for recycling, and plasmonic properties for sensing*)	(8) *Bio-directed* (*bio-encoded*) *synthesis*
		(9) *Large surface area for further modification* (*such as bioconjugation*) *compared with molecular and bulk materials*	(9) *Delivery and administration for nanomedicine*
		(10) *Self-assembly*	(10) *Potential nano-toxicity*
			(11) *Limited types of nanozymes*
	Others	(1) Low cost	(1) Low efficiency
		(2) Easy mass-production	(2) Low specificity
		(3) Robustness to harsh environments	(3) Low selectivity
		(4) High stability	(4) Limited catalytic reactions
		(5) Long-term storage	(5) The exact mechanism
		(6) Tunable activity	(6) Atomic precise structure and 3D structural information
		(7) *Established methods for preparation and characterization*	(7) Rational design of the artificial enzymes
		(8) *Uniform size and defined structures of molecular mimics*	(8) *Separation and recycle*
		(9) *Smaller size* (*compared with nanozymes*)	
Nanomaterial-based catalysts		(1) Low cost	(1) Low efficiency
		2) Easy for mass-production	(2) Low specificity
		(3) Robustness to harsh environments	(3) Low selectivity
		(4) High stability	(4) Limited catalytic reactions
		(5) Long-term storage	(5) The exact mechanism
		(6) Tunable activity	(6) Atomic precise structure and 3D structural information
		(7) Size-(shape-, structure-, composition-)dependent properties	(7) Biocompatibility
		(8) Other functions besides catalysis (*i.e.*, the unique functions from the nanoscaled materials, such as magnetic properties for recycling, and plasmonic properties for sensing)	(8) Biological functions
		(9) Large surface area for further modification (such as bioconjugation) compared with molecular and bulk materials	
		(10) Self-assembly	
Natural enzymes		(1) High catalytic efficiency	(1) High cost
		(2) High substrate specificity	(2) Hard for mass-production
		(3) High (enantio)selectivity	(3) Time-consuming separation and purification
		(4) Sophisticated three-dimensional structures	(4) Limited stability
		(5) Wide range of catalytic reactions	(5) Hard for long-term storage
		(6) Tunable activity	(6) Hard for harsh environment (such as industrial catalysis)
		(7) Good biocompatibility	
		(8) Gene manipulation	
Organic catalysts		(1) High efficiency	(1) Lower efficiency and less specificity compared with natural enzymes
		(2) Asymmetric selectivity	(2) Some of them are toxic
		(3) Atomic precise structures	(3) Some of the precursor materials are resource-limited (such as Pd and Pt for metal complex catalysts)
		(4) Wide range of catalytic reactions	
		(5) Wide range of applications	
		(6) Industrial standards	

[a] The items (in italic font) are unique for nanozymes compared with other artificial enzymes.

The different kinds of catalysts including nanozymes will find their unique places in various applications based on their own advantages and disadvantages. Most nanozyme-based catalysis is heterogeneous while molecular (such as organic catalysts and enzymes) catalysis is homogeneous. Combining the two will provide complementary means to address unmet challenges. For example, two (or even more) kinds of catalysts could be used together for sensitive and selective sensing and concurrent tandem catalysis.[45,302]

5. Conclusions

This review highlights the recent progress in the field of nanomaterial-based artificial enzymes, which are defined as ''nanozymes''. As discussed, though the area of nanozymes is still in its infancy, it has developed substantially as a part of the artificial enzyme field. The research in this field is highly active, as evidenced by the rapidly growing number of publications. Future breakthroughs in nanozyme technology will lead to a new wave of novel biocatalysts for wide applications by overcoming the above-mentioned and other potential challenges.

Abbreviations

4-AAP	4-aminoatipyrine
ABTS	2,2′-azino-bis(3-ethylbenzothiazoline-6-sulfonic acid)
AgNP	silver nanoparticle
AuNC	gold nanocluster
AuNP	gold nanoparticle
BA	benzoic acid
BSA	bovine serum albumin
CEA	carcinoembryonic antigen
CNT	carbon nanotube
DAB	diazoaminobenzene
DOPA	dopamine
DPD	*N*,*N*-diethyl-*p*-phenylenediamine sulfate
dsDNA	double-stranded DNA
ELISA	enzyme-linked immunosorbent assay
EPR	electron paramagnetic resonance
HPNP	2-hydroxypropyl-4-nitrophenylphosphate
HRP	horseradish peroxidase
LDH	layered double hydroxide
NMDA	*N*-methyl-D-aspartate
MNPs	magnetic nanoparticles
NPs	nanoparticles
OPD	*o*-phenylenediamine
PDDA	poly(diallyldimethylammonium chloride)
PLGA	poly(D,L-lactic-co-glycolic acid)
PMIDA	*N*-(phosphonomethyl)iminodiacetic acid
PSA	prostate-specific antigen
PSS	poly(styrenesulfonate)
PVDF	polyvinylidene difluoride
SBA-15	Santa Barbara Amorphous type material
SOD	superoxide dismutase
ssDNA	single-stranded DNA
TMB	3,3′,5,5′-tetramethylbenzidine

Acknowledgements

This work was supported by the National Natural Science Foundation of China (No. 21190040) and 973 Project (Nos. 2009CB930100 and 2010CB933600). We would like to thank Professors Shaojun Dong and Shuming Nie for their insightful discussions and suggestions, Dr Brad Kairdolf, Dr Bingling Li and Gang Wu for the carefully proofreading of the manuscript, and the anonymous reviewers for their critical and insightful comments.

References

1 R. Breslow and L. E. Overman, *J. Am. Chem. Soc.*, 1970, **92**, 1075–1077.
2 R. Breslow, *Artificial enzymes*, Wiley-VCH, Weinheim, 2005.
3 A. J. Kirby and F. Hollfelder, *From enzyme models to model enzymes*, Royal Society of Chemistry, Cambridge, 2009.
4 Y. Aiba, J. Sumaoka and M. Komiyama, *Chem. Soc. Rev.*, 2011, **40**, 5657–5668.
5 R. P. Bonarlaw and J. K. M. Sanders, *J. Am. Chem. Soc.*, 1995, **117**, 259–271.
6 G. P. Royer and I. M. Klotz, *J. Am. Chem. Soc.*, 1969, **91**, 5885–5886.
7 X. Zhang, H. P. Xu, Z. Y. Dong, Y. P. Wang, J. Q. Liu and J. C. Shen, *J. Am. Chem. Soc.*, 2004, **126**, 10556–10557.
8 D. J. Cram and J. M. Cram, *Science*, 1974, **183**, 803–809.
9 J. M. Lehn and C. Sirlin, *J. Chem. Soc., Chem. Commun.*, 1978, 949–951.
10 Z. Y. Dong, Y. G. Wang, Y. Z. Yin and J. Q. Liu, *Curr. Opin. Colloid Interface Sci.*, 2011, **16**, 451–458.
11 G. Wulff and A. Sarhan, *Angew. Chem., Int. Ed. Engl.*, 1972, **11**, 341–342.
12 T. Takagish and I. M. Klotz, *Biopolymers*, 1972, **11**, 483–491.
13 T. Pan and O. C. Uhlenbeck, *Biochemistry*, 1992, **31**, 3887–3895.
14 R. R. Breaker and G. F. Joyce, *Chem. Biol.*, 1994, **1**, 223–229.
15 A. Tramontano, K. D. Janda and R. A. Lerner, *Science*, 1986, **234**, 1566–1570.
16 S. J. Pollack, J. W. Jacobs and P. G. Schultz, *Science*, 1986, **234**, 1570–1573.
17 Y. Lu, N. Yeung, N. Sieracki and N. M. Marshall, *Nature*, 2009, **460**, 855–862.
18 R. Breslow, *Chem. Soc. Rev.*, 1972, **1**, 553–580.
19 M. P. Mertes and K. B. Mertes, *Acc. Chem. Res.*, 1990, **23**, 413–418.
20 R. Breslow, *Acc. Chem. Res.*, 1995, **28**, 146–153.
21 Y. Murakami, J. Kikuchi, Y. Hisaeda and O. Hayashida, *Chem. Rev.*, 1996, **96**, 721–758.
22 R. Breslow and S. D. Dong, *Chem. Rev.*, 1998, **98**, 1997–2011.
23 D. P. Riley, *Chem. Rev.*, 1999, **99**, 2573–2587.
24 M. C. Feiters, A. E. Rowan and R. J. M. Nolte, *Chem. Soc. Rev.*, 2000, **29**, 375–384.
25 P. Molenveld, J. F. J. Engbersen and D. N. Reinhoudt, *Chem. Soc. Rev.*, 2000, **29**, 75–86.
26 C. M. Thomas and T. R. Ward, *Chem. Soc. Rev.*, 2005, **34**, 337–346.
27 T. Darbre and J. L. Reymond, *Acc. Chem. Res.*, 2006, **39**, 925–934.
28 F. Gloaguen and T. B. Rauchfuss, *Chem. Soc. Rev.*, 2009, **38**, 100–108.
29 S. Friedle, E. Reisner and S. J. Lippard, *Chem. Soc. Rev.*, 2010, **39**, 2768–2779.
30 K. P. Bhabak and G. Mugesh, *Acc. Chem. Res.*, 2010, **43**, 1408–1419.
31 X. Huang, X. M. Liu, Q. A. Luo, J. Q. Liu and J. C. Shen, *Chem. Soc. Rev.*, 2011, **40**, 1171–1184.
32 G. Wulff and J. Q. Liu, *Acc. Chem. Res.*, 2012, **45**, 239–247.

33 J. Barber, *Chem. Soc. Rev.*, 2009, **38**, 185–196.
34 G. Mugesh and H. B. Singh, *Chem. Soc. Rev.*, 2000, **29**, 347–357.
35 L. L. Dugan, J. K. Gabrielsen, S. P. Yu, T. S. Lin and D. W. Choi, *Neurobiol. Dis.*, 1996, **3**, 129–135.
36 L. L. Dugan, D. M. Turetsky, C. Du, D. Lobner, M. Wheeler, C. R. Almli, C. K. F. Shen, T. Y. Luh, D. W. Choi and T. S. Lin, *Proc. Natl. Acad. Sci. U. S. A.*, 1997, **94**, 9434–9439.
37 L. Pasquato, F. Rancan, P. Scrimin, F. Mancin and C. Frigeri, *Chem. Commun.*, 2000, 2253–2254.
38 S. S. Ali, J. I. Hardt, K. L. Quick, J. S. Kim-Han, B. F. Erlanger, T. T. Huang, C. J. Epstein and L. L. Dugan, *Free Radical Biol. Med.*, 2004, **37**, 1191–1202.
39 F. Manea, F. B. Houillon, L. Pasquato and P. Scrimin, *Angew. Chem., Int. Ed.*, 2004, **43**, 6165–6169.
40 M. Comotti, C. Della Pina, R. Matarrese and M. Rossi, *Angew. Chem., Int. Ed.*, 2004, **43**, 5812–5815.
41 R. W. Tarnuzzer, J. Colon, S. Patil and S. Seal, *Nano Lett.*, 2005, **5**, 2573–2577.
42 P. Beltrame, M. Comotti, C. Della Pina and M. Rossi, *Appl. Catal., A*, 2006, **297**, 1–7.
43 J. P. Chen, S. Patil, S. Seal and J. F. McGinnis, *Nat. Nanotechnol.*, 2006, **1**, 142–150.
44 L. Z. Gao, J. Zhuang, L. Nie, J. B. Zhang, Y. Zhang, N. Gu, T. H. Wang, J. Feng, D. L. Yang, S. Perrett and X. Yan, *Nat. Nanotechnol.*, 2007, **2**, 577–583.
45 H. Wei and E. Wang, *Anal. Chem.*, 2008, **80**, 2250–2254.
46 F. Natalio, R. Andre, A. F. Hartog, B. Stoll, K. P. Jochum, R. Wever and W. Tremel, *Nat. Nanotechnol.*, 2012, **7**, 530–535.
47 K. L. Fan, C. Q. Cao, Y. X. Pan, D. Lu, D. L. Yang, J. Feng, L. N. Song, M. M. Liang and X. Y. Yan, *Nat. Nanotechnol.*, 2012, **7**, 459–464.
48 Z. L. Wang, H. Y. Liu, S. H. Yang, T. Wang, C. Liu and Y. C. Cao, *Proc. Natl. Acad. Sci. U. S. A.*, 2012, **109**, 12387–12392.
49 X. N. Hu, J. B. Liu, S. Hou, T. Wen, W. Q. Liu, K. Zhang, W. W. He, Y. L. Ji, H. X. Ren, Q. Wang and X. C. Wu, *Sci. China, Ser. G: Phys., Mech. Astron.*, 2011, **54**, 1749–1756.
50 H. X. Ju, X. J. Zhang and J. Wang, *Nanobiosensing: Principles, Development and Application*, Springer, New York, 2011.
51 A. Karakoti, S. Singh, J. M. Dowding, S. Seal and W. T. Self, *Chem. Soc. Rev.*, 2010, **39**, 4422–4432.
52 J. X. Xie, X. D. Zhang, H. Wang, H. Z. Zheng and Y. M. Huang, *TrAC, Trends Anal. Chem.*, 2012, **39**, 114–129.
53 I. Celardo, J. Z. Pedersen, E. Traversa and L. Ghibelli, *Nanoscale*, 2011, **3**, 1411–1420.
54 E. Nakamura and H. Isobe, *Acc. Chem. Res.*, 2003, **36**, 807–815.
55 S. Bosi, T. Da Ros, G. Spalluto and M. Prato, *Eur. J. Med. Chem.*, 2003, **38**, 913–923.
56 S. J. Guo and E. K. Wang, *Acc. Chem. Res.*, 2011, **44**, 491–500.
57 Y. H. Xu and E. K. Wang, *Electrochim. Acta*, 2012, **84**, 62–73.
58 G. A. Silva, *Nat. Rev. Neurosci.*, 2006, **7**, 65–74.
59 I. Batinic-Haberle, J. S. Reboucas and I. Spasojevic, *Antioxid. Redox Signaling*, 2010, **13**, 877–918.
60 B. Perez-Lopez and A. Merkoci, *Trends Food Sci. Technol.*, 2011, **22**, 625–639.
61 M. Solomon and G. G. M. D'Souza, *Curr. Opin. Pediatr.*, 2011, **23**, 215–220.
62 Y. J. Song, W. L. Wei and X. G. Qu, *Adv. Mater.*, 2011, **23**, 4215–4236.
63 J. P. Lei and H. X. Ju, *Chem. Soc. Rev.*, 2012, **41**, 2122–2134.
64 D. Salvemini, D. P. Riley and S. Cuzzocrea, *Nat. Rev. Drug Discovery*, 2002, **1**, 367–374.
65 T. Ueno, S. Abe, N. Yokoi and Y. Watanabe, *Coord. Chem. Rev.*, 2007, **251**, 2717–2731.
66 A. Dhakshinamoorthy, S. Navalon, M. Alvaro and H. Garcia, *ChemSusChem*, 2012, **5**, 46–64.
67 J. Morimoto, Y. Hayashi, K. Iwasaki and H. Suga, *Acc. Chem. Res.*, 2011, **44**, 1359–1368.
68 N. A. Kotov, *Science*, 2010, **330**, 188–189.
69 F. Esch, S. Fabris, L. Zhou, T. Montini, C. Africh, P. Fornasiero, G. Comelli and R. Rosei, *Science*, 2005, **309**, 752–755.
70 F. S. Hong, *Biol. Trace Elem. Res.*, 2002, **87**, 191–200.
71 G. A. Silva, *Nat. Nanotechnol.*, 2006, **1**, 92–94.
72 M. Das, S. Patil, N. Bhargava, J. F. Kang, L. M. Riedel, S. Seal and J. J. Hickman, *Biomaterials*, 2007, **28**, 1918–1925.
73 C. Korsvik, S. Patil, S. Seal and W. T. Self, *Chem. Commun.*, 2007, 1056–1058.
74 J. L. Niu, A. Azfer, L. M. Rogers, X. H. Wang and P. E. Kolattukudy, *Cardiovasc. Res.*, 2007, **73**, 549–559.
75 S. Patil, A. Sandberg, E. Heckert, W. Self and S. Seal, *Biomaterials*, 2007, **28**, 4600–4607.
76 E. G. Heckert, A. S. Karakoti, S. Seal and W. T. Self, *Biomaterials*, 2008, **29**, 2705–2709.
77 A. S. Karakoti, N. A. Monteiro-Riviere, R. Aggarwal, J. P. Davis, R. J. Narayan, W. T. Self, J. McGinnis and S. Seal, *J. Mater. Sci.*, 2008, **60**, 33–37.
78 E. J. Park, J. Choi, Y. K. Park and K. Park, *Toxicology*, 2008, **245**, 90–100.
79 J. M. Perez, A. Asati, S. Nath and C. Kaittanis, *Small*, 2008, **4**, 552–556.
80 T. Xia, M. Kovochich, M. Liong, L. Madler, B. Gilbert, H. B. Shi, J. I. Yeh, J. I. Zink and A. E. Nel, *ACS Nano*, 2008, **2**, 2121–2134.
81 A. Asati, S. Santra, C. Kaittanis, S. Nath and J. M. Perez, *Angew. Chem., Int. Ed.*, 2009, **48**, 2308–2312.
82 S. Babu, R. Thanneeru, T. Inerbaev, R. Day, A. E. Masunov, A. Schulte and S. Seal, *Nanotechnology*, 2009, **20**, 085713.
83 J. Colon, L. Herrera, J. Smith, S. Patil, C. Komanski, P. Kupelian, S. Seal, D. W. Jenkins and C. H. Baker, *Nanomed.: Nanotechnol., Biol. Med.*, 2009, **5**, 225–231.
84 S. M. Hirst, A. S. Karakoti, R. D. Tyler, N. Sriranganathan, S. Seal and C. M. Reilly, *Small*, 2009, **5**, 2848–2856.
85 A. S. Karakoti, S. Singh, A. Kumar, M. Malinska, S. Kuchibhatla, K. Wozniak, W. T. Self and S. Seal, *J. Am. Chem. Soc.*, 2009, **131**, 14144–14145.
86 J. Colon, N. Hsieh, A. Ferguson, P. Kupelian, S. Seal, D. W. Jenkins and C. H. Baker, *Nanomed.: Nanotechnol., Biol. Med.*, 2010, **6**, 698–705.
87 C. Mandoli, F. Pagliari, S. Pagliari, G. Forte, P. Di Nardo, S. Licoccia and E. Traversa, *Adv. Funct. Mater.*, 2010, **20**, 1617–1624.

88 T. Pirmohamed, J. M. Dowding, S. Singh, B. Wasserman, E. Heckert, A. S. Karakoti, J. E. S. King, S. Seal and W. T. Self, *Chem. Commun.*, 2010, **46**, 2736–2738.
89 S. Singh, A. Kumar, A. Karakoti, S. Seal and W. T. Self, *Mol. BioSyst.*, 2010, **6**, 1813–1820.
90 A. Asati, C. Kaittanis, S. Santra and J. M. Perez, *Anal. Chem.*, 2011, **83**, 2547–2553.
91 I. Celardo, M. De Nicola, C. Mandoli, J. Z. Pedersen, E. Traversa and L. Ghibelli, *ACS Nano*, 2011, **5**, 4537–4549.
92 A. Clark, A. P. Zhu, K. Sun and H. R. Petty, *J. Nanopart. Res.*, 2011, **13**, 5547–5555.
93 M. Horie, K. Nishio, H. Kato, K. Fujita, S. Endoh, A. Nakamura, A. Miyauchi, S. Kinugasa, K. Yamamoto, E. Niki, Y. Yoshida, Y. Hagihara and H. Iwahashi, *J. Biochem.*, 2011, **150**, 461–471.
94 L. Kong, X. Cai, X. H. Zhou, L. L. Wong, A. S. Karakoti, S. Seal and J. F. McGinnis, *Neurobiol. Dis.*, 2011, **42**, 514–523.
95 S. Singh, T. Dosani, A. S. Karakoti, A. Kumar, S. Seal and W. T. Self, *Biomaterials*, 2011, **32**, 6745–6753.
96 X. H. Zhou, L. L. Wong, A. S. Karakoti, S. Seal and J. F. McGinnis, *PLoS One*, 2011, **6**, 10.
97 S. Das, S. Singh, J. M. Dowding, S. Oommen, A. Kumar, T. X. T. Sayle, S. Saraf, C. R. Patra, N. E. Vlahakis, D. C. Sayle, W. T. Self and S. Seal, *Biomaterials*, 2012, **33**, 7746–7755.
98 X. Jiao, H. J. Song, H. H. Zhao, W. Bai, L. C. Zhang and Y. Lv, *Anal. Methods*, 2012, **4**, 3261–3267.
99 X. Y. Liu, W. Wei, Q. Yuan, X. Zhang, N. Li, Y. G. Du, G. H. Ma, C. H. Yan and D. Ma, *Chem. Commun.*, 2012, **48**, 3155–3157.
100 F. Pagliari, C. Mandoli, G. Forte, E. Magnani, S. Pagliari, G. Nardone, S. Licoccia, M. Minieri, P. Di Nardo and E. Traversa, *ACS Nano*, 2012, **6**, 3767–3775.
101 V. Shah, S. Shah, H. Shah, F. J. Rispoli, K. T. McDonnell, S. Workeneh, A. Karakoti, A. Kumar and S. Seal, *PLoS One*, 2012, **7**, 13.
102 A. P. Zhu, K. Sun and H. R. Petty, *Inorg. Chem. Commun.*, 2012, **15**, 235–237.
103 L. Alili, M. Sack, C. von Montfort, S. Giri, S. Das, K. S. Carroll, K. Zanger, S. Seal and P. Brenneisen, *Antioxid. Redox Signaling*, 2013, 130124061130004, DOI: 10.1089/ars.2012.4831.
104 K. Chaudhury, K. N. Babu, A. K. Singh, S. Das, A. Kumar and S. Seal, *Nanomed.: Nanotechnol., Biol. Med.*, 2013, **9**, 439.
105 S. Chigurupati, M. R. Mughal, E. Okun, S. Das, A. Kumar, M. McCaffery, S. Seal and M. P. Mattson, *Biomaterials*, 2013, **34**, 2194–2201.
106 S. Giri, A. Karakoti, R. P. Graham, J. L. Maguire, C. M. Reilly, S. Seal, R. Rattan and V. Shridhar, *PLoS One*, 2013, **8**, e54578.
107 S. M. Hirst, A. Karakoti, S. Singh, W. Self, R. Tyler, S. Seal and C. M. Reilly, *Environ. Toxicol.*, 2013, **28**, 107–118.
108 M. S. Wason, J. Colon, S. Das, S. Seal, J. Turkson, J. Zhao and C. H. Baker, *Nanomed.: Nanotechnol., Biol. Med.*, 2013, **9**, 558.
109 N. Pourkhalili, A. Hosseini, A. Nili-Ahmadabadi, S. Hassani, M. Pakzad, M. Baeeri, A. Mohammadirad and M. Abdollahi, *World J. Diabetes*, 2011, **2**, 204–210.
110 Z. W. Chen, J. J. Yin, Y. T. Zhou, Y. Zhang, L. Song, M. J. Song, S. L. Hu and N. Gu, *ACS Nano*, 2012, **6**, 4001–4012.
111 W. W. He, Y. Liu, J. S. Yuan, J. J. Yin, X. C. Wu, X. N. Hu, K. Zhang, J. B. Liu, C. Y. Chen, Y. L. Ji and Y. T. Guo, *Biomaterials*, 2011, **32**, 1139–1147.
112 J. Fan, J. J. Yin, B. Ning, X. C. Wu, Y. Hu, M. Ferrari, G. J. Anderson, J. Y. Wei, Y. L. Zhao and G. J. Nie, *Biomaterials*, 2011, **32**, 1611–1618.
113 Y. Wan, P. Qi, D. Zhang, J. J. Wu and Y. Wang, *Biosens. Bioelectron.*, 2012, **33**, 69–74.
114 X. Cao and N. Wang, *Analyst*, 2011, **136**, 4241–4246.
115 W. J. Luo, C. F. Zhu, S. Su, D. Li, Y. He, Q. Huang and C. H. Fan, *ACS Nano*, 2010, **4**, 7451–7458.
116 J. B. Liu, X. N. Hu, S. Hou, T. Wen, W. Q. Liu, X. Zhu and X. C. Wu, *Chem. Commun.*, 2011, **47**, 10981–10983.
117 K. Zhang, X. N. Hu, J. B. Liu, J. J. Yin, S. A. Hou, T. Wen, W. W. He, Y. L. Ji, Y. T. Guo, Q. Wang and X. C. Wu, *Langmuir*, 2011, **27**, 2796–2803.
118 X. X. Zheng, Q. Liu, C. Jing, Y. Li, D. Li, W. J. Luo, Y. Q. Wen, Y. He, Q. Huang, Y. T. Long and C. H. Fan, *Angew. Chem., Int. Ed.*, 2011, **50**, 11994–11998.
119 J. B. Liu, X. N. Hu, S. Hou, T. Wen, W. Q. Liu, X. Zhu, J. J. Yin and X. C. Wu, *Sens. Actuators, B*, 2012, **166–167**, 708–714.
120 J. Sudimack and R. J. Lee, *Adv. Drug Delivery Rev.*, 2000, **41**, 147–162.
121 N. A. Frey, S. Peng, K. Cheng and S. H. Sun, *Chem. Soc. Rev.*, 2009, **38**, 2532–2542.
122 L. H. Zhang, B. F. Liu and S. J. Dong, *J. Phys. Chem. B*, 2007, **111**, 10448–10452.
123 J. F. Zhai, M. H. Huang, Y. M. Zhai and S. J. Dong, *J. Mater. Chem.*, 2008, **18**, 923–928.
124 Y. M. Zhai, J. F. Zhai, D. Wen, M. Zhou, L. H. Zhang and S. J. Dong, *Electrochem. Commun.*, 2008, **10**, 1172–1175.
125 S. J. Guo, J. Li and E. Wang, *Chem.–Asian J.*, 2008, **3**, 1544–1548.
126 S. J. Guo, D. Li, L. M. Zhang, J. Li and E. K. Wang, *Biomaterials*, 2009, **30**, 1881–1889.
127 S. Guo, S. Dong and E. Wang, *Chem.–Eur. J.*, 2009, **15**, 2416–2424.
128 Y. M. Zhai, J. F. Zhai, Y. L. Wang, S. J. Guo, W. Ren and S. J. Dong, *J. Phys. Chem. C*, 2009, **113**, 7009–7014.
129 Y. M. Zhai, J. F. Zhai and S. J. Dong, *Chem. Commun.*, 2010, **46**, 1500–1502.
130 Y. M. Zhai, L. Han, P. Wang, G. P. Li, W. Ren, L. Liu, E. K. Wang and S. J. Dong, *ACS Nano*, 2011, **5**, 8562–8570.
131 Y. M. Zhai, L. H. Jin, P. Wang and S. J. Dong, *Chem. Commun.*, 2011, **47**, 8268–8270.
132 Y. Du, B. L. Li, S. J. Guo, Z. X. Zhou, M. Zhou, E. K. Wang and S. J. Dong, *Analyst*, 2011, **136**, 493–497.
133 J. Xie, K. Chen, H. Y. Lee, C. J. Xu, A. R. Hsu, S. Peng, X. Y. Chen and S. H. Sun, *J. Am. Chem. Soc.*, 2008, **130**, 7542–7543.

134 J. M. Perez, *Nat. Nanotechnol.*, 2007, **2**, 535–536.
135 L. Z. Gao, J. M. Wu, S. Lyle, K. Zehr, L. L. Cao and D. Gao, *J. Phys. Chem. C*, 2008, **112**, 17357–17361.
136 F. F. Peng, Y. Zhang and N. Gu, *Chin. Chem. Lett.*, 2008, **19**, 730–733.
137 J. B. Zhang, J. Zhuang, L. Z. Gao, Y. Zhang, N. Gu, J. Feng, D. L. Yang, J. D. Zhu and X. Y. Yan, *Chemosphere*, 2008, **73**, 1524–1528.
138 L. H. Zhang, Y. M. Zhai, N. Gao, D. Wen and S. J. Dong, *Electrochem. Commun.*, 2008, **10**, 1524–1526.
139 H. M. Fan, J. B. Yi, Y. Yang, K. W. Kho, H. R. Tan, Z. X. Shen, J. Ding, X. W. Sun, M. C. Olivo and Y. P. Feng, *ACS Nano*, 2009, **3**, 2798–2808.
140 D. M. Huang, J. K. Hsiao, Y. C. Chen, L. Y. Chien, M. Yao, Y. K. Chen, B. S. Ko, S. C. Hsu, L. A. Tai, H. Y. Cheng, S. W. Wang, C. S. Yang and Y. C. Chen, *Biomaterials*, 2009, **30**, 3645–3651.
141 Y. Q. Miao, H. Wang, Y. Y. Shao, Z. W. Tang, J. Wang and Y. H. Lin, *Sens. Actuators, B*, 2009, **138**, 182–188.
142 S. Nath, C. Kaittanis, V. Ramachandran, N. S. Dalal and J. M. Perez, *Chem. Mater.*, 2009, **21**, 1761–1767.
143 Q. Wu, J. Rong, Z. Shan, H. Y. Chen and W. S. Yang, *Chin. J. Biotechnol.*, 2009, **25**, 1976–1982.
144 C. H. Yang, J. J. Du, Q. Peng, R. R. Qiao, W. Chen, C. Xu, Z. G. Shuai and M. Y. Gao, *J. Phys. Chem. B*, 2009, **113**, 5052–5058.
145 L. Q. Yang, X. L. Ren, F. Q. Tang and L. Zhang, *Biosens. Bioelectron.*, 2009, **25**, 889–895.
146 X. Y. Ye, Z. M. Liu, Z. G. Wang, X. J. Huang and Z. K. Xu, *Mater. Lett.*, 2009, **63**, 1810–1813.
147 F. Q. Yu, Y. Z. Huang, A. J. Cole and V. C. Yang, *Biomaterials*, 2009, **30**, 4716–4722.
148 S. X. Zhang, X. L. Zhao, H. Y. Niu, Y. L. Shi, Y. Q. Cai and G. B. Jiang, *J. Hazard. Mater.*, 2009, **167**, 560–566.
149 X. L. Zuo, C. Peng, Q. Huang, S. P. Song, L. H. Wang, D. Li and C. H. Fan, *Nano Res.*, 2009, **2**, 617–623.
150 N. Ding, N. Yan, C. L. Ren and X. G. Chen, *Anal. Chem.*, 2010, **82**, 5897–5899.
151 N. Wang, L. H. Zhu, D. L. Wang, M. Q. Wang, Z. F. Lin and H. Q. Tang, *Ultrason. Sonochem.*, 2010, **17**, 526–533.
152 N. Wang, L. H. Zhu, M. Q. Wang, D. L. Wang and H. Q. Tang, *Ultrason. Sonochem.*, 2010, **17**, 78–83.
153 C. J. Yu, C. Y. Lin, C. H. Liu, T. L. Cheng and W. L. Tseng, *Biosens. Bioelectron.*, 2010, **26**, 913–917.
154 X. Q. Zhang, S. W. Gong, Y. Zhang, T. Yang, C. Y. Wang and N. Gu, *J. Mater. Chem.*, 2010, **20**, 5110–5116.
155 Z. X. Zhang, Z. J. Wang, X. L. Wang and X. R. Yang, *Sens. Actuators, B*, 2010, **147**, 428–433.
156 Y. Gao, G. N. Wang, H. Huang, J. J. Hu, S. M. Shah and X. G. Su, *Talanta*, 2011, **85**, 1075–1080.
157 J. Z. Jiang, J. Zou, L. H. Zhu, L. Huang, H. P. Jiang and Y. X. Zhang, *J. Nanosci. Nanotechnol.*, 2011, **11**, 4793–4799.
158 Z. L. Jiang, L. Kun, H. X. Ouyang, A. H. Liang and H. S. Jiang, *J. Fluoresc.*, 2011, **21**, 2015–2020.
159 S. Z. Kang, H. Chen and J. Mu, *Solid State Sci.*, 2011, **13**, 142–145.
160 M. I. Kim, J. Shim, T. Li, J. Lee and H. G. Park, *Chem.–Eur. J.*, 2011, **17**, 10700–10707.
161 M. I. Kim, Y. Ye, B. Y. Won, S. Shin, J. Lee and H. G. Park, *Adv. Funct. Mater.*, 2011, **21**, 2868–2875.
162 C. H. Liu and W. L. Tseng, *Anal. Chim. Acta*, 2011, **703**, 87–93.
163 S. Liu, J. Q. Tian, L. Wang, Y. L. Luo, G. H. Chang and X. P. Sun, *Analyst*, 2011, **136**, 4894–4897.
164 S. Liu, J. Q. Tian, J. F. Zhai, L. Wang, W. B. Lu and X. P. Sun, *Analyst*, 2011, **136**, 2037–2039.
165 S. Liu, L. Wang, J. F. Zhai, Y. L. Luo and X. P. Sun, *Anal. Methods*, 2011, **3**, 1475–1477.
166 S. H. Liu, F. Lu, R. M. Xing and J. J. Zhu, *Chem.–Eur. J.*, 2011, **17**, 620–625.
167 X. X. Liu, H. Zhu and X. R. Yang, *Talanta*, 2011, **87**, 243–248.
168 Y. P. Liu and F. Q. Yu, *Nanotechnology*, 2011, **22**, 8.
169 K. S. Park, M. I. Kim, D. Y. Cho and H. G. Park, *Small*, 2011, **7**, 1521–1525.
170 X. X. Wang, Q. Wu, Z. Shan and Q. M. Huang, *Biosens. Bioelectron.*, 2011, **26**, 3614–3619.
171 Y. H. Wu, M. J. Song, Z. A. Xin, X. Q. Zhang, Y. Zhang, C. Y. Wang, S. Y. Li and N. Gu, *Nanotechnology*, 2011, **22**, 8.
172 S. Zhang, G. L. Zhou, X. L. Xu, L. L. Cao, G. H. Liang, H. Chen, B. H. Liu and J. L. Kong, *Electrochem. Commun.*, 2011, **13**, 928–931.
173 Z. X. Zhang, X. L. Wang and X. R. Yang, *Analyst*, 2011, **136**, 4960–4965.
174 Z. X. Zhang, H. Zhu, X. L. Wang and X. R. Yang, *Microchim. Acta*, 2011, **174**, 183–189.
175 H. L. Zhu, Y. Hu, G. X. Jiang and G. Q. Shen, *Eur. Food Res. Technol.*, 2011, **233**, 881–887.
176 M. Y. Zhu and G. W. Diao, *J. Phys. Chem. C*, 2011, **115**, 18923–18934.
177 K. N. Chaudhari, N. K. Chaudhari and J. S. Yu, *Catal. Sci. Technol.*, 2012, **2**, 119–124.
178 Y. L. Dong, H. G. Zhang, Z. U. Rahman, L. Su, X. J. Chen, J. Hu and X. G. Chen, *Nanoscale*, 2012, **4**, 3969–3976.
179 A. K. Dutta, S. K. Maji, A. Mondal, B. Karmakar, P. Biswas and B. Adhikary, *Sens. Actuators, B*, 2012, **173**, 724–731.
180 Y. W. Fan and Y. M. Huang, *Analyst*, 2012, **137**, 1225–1231.
181 M. I. Kim, J. Shim, T. Li, M. A. Woo, D. Cho, J. Lee and H. G. Park, *Analyst*, 2012, **137**, 1137–1143.
182 J. W. Lee, H. J. Jeon, H. J. Shin and J. K. Kang, *Chem. Commun.*, 2012, **48**, 422–424.
183 J. S. Mu, Y. Wang, M. Zhao and L. Zhang, *Chem. Commun.*, 2012, **48**, 2540–2542.
184 N. Puvvada, P. K. Panigrahi, D. Mandal and A. Pathak, *RSC Adv.*, 2012, **2**, 3270–3273.
185 C. I. Wang, W. T. Chen and H. T. Chang, *Anal. Chem.*, 2012, **84**, 9706–9712.
186 J. J. Wang, D. X. Han, X. H. Wang, B. Qi and M. S. Zhao, *Biosens. Bioelectron.*, 2012, **36**, 18–21.
187 S. Wang, W. Chen, A. L. Liu, L. Hong, H. H. Deng and X. H. Lin, *ChemPhysChem*, 2012, **13**, 1199–1204.
188 W. Wang, X. P. Jiang and K. Z. Chen, *Chem. Commun.*, 2012, **48**, 6839–6841.

189 W. Wang, X. P. Jiang and K. Z. Chen, *Chem. Commun.*, 2012, **48**, 7289–7291.
190 J. Zhuang, K. L. Fan, L. Z. Gao, D. Lu, J. Feng, D. L. Yang, N. Gu, Y. Zhang, M. M. Liang and X. Y. Yan, *Mol. Pharmaceutics*, 2012, **9**, 1983–1989.
191 Q. B. Wang, J. P. Lei, S. Y. Deng, L. Zhang and H. X. Ju, *Chem. Commun.*, 2013, **49**, 916–918.
192 C. Kaittanis, S. Santra and J. M. Perez, *J. Am. Chem. Soc.*, 2009, **131**, 12780–12791.
193 L. H. Zhang, S. J. Guo and S. J. Dong, *J. Biomed. Nanotechnol.*, 2009, **5**, 586–590.
194 Y. J. Song, K. G. Qu, C. Xu, J. S. Ren and X. G. Qu, *Chem. Commun.*, 2010, **46**, 6572–6574.
195 M. Ishii, R. Shibata, Y. Numaguchi, T. Kito, H. Suzuki, K. Shimizu, A. Ito, H. Honda and T. Murohara, *Arterioscler., Thromb., Vasc. Biol.*, 2011, **31**, 2210–2215.
196 C. Peng, B. W. Jiang, Q. Liu, Z. Guo, Z. J. Xu, Q. Huang, H. J. Xu, R. Z. Tai and C. H. Fan, *Energy Environ. Sci.*, 2011, **4**, 2035–2040.
197 W. B. Shi, H. Wang and Y. M. Huang, *Luminescence*, 2011, **26**, 547–552.
198 A. Singh, S. Patra, J. A. Lee, K. H. Park and H. Yang, *Biosens. Bioelectron.*, 2011, **26**, 4798–4803.
199 J. Yang, H. Xiang, L. Shuai and S. Gunasekaran, *Anal. Chim. Acta*, 2011, **708**, 44–51.
200 M. Liu, H. M. Zhao, S. Chen, H. T. Yu and X. Quan, *ACS Nano*, 2012, **6**, 3142–3151.
201 Y. P. Ye, T. Kong, X. F. Yu, Y. K. Wu, K. Zhang and X. P. Wang, *Talanta*, 2012, **89**, 417–421.
202 H. M. Deng, W. Shen, Y. F. Peng, X. J. Chen, G. S. Yi and Z. Q. Gao, *Chem.–Eur. J.*, 2012, **18**, 8906–8911.
203 Q. Chang, K. J. Deng, L. H. Zhu, G. D. Jiang, C. Yu and H. Q. Tang, *Microchim. Acta*, 2009, **165**, 299–305.
204 Z. H. Dai, S. H. Liu, J. C. Bao and H. X. Ju, *Chem.–Eur. J.*, 2009, **15**, 4321–4326.
205 A. Kaushik, P. R. Solanki, A. A. Ansari, G. Sumana, S. Ahmad and B. D. Malhotra, *Sens. Actuators, B*, 2009, **138**, 572–580.
206 Y. L. Wang, S. H. Chen, F. Ni, F. Gao and M. G. Li, *Electroanalysis*, 2009, **21**, 2125–2132.
207 C. L. Du, W. Du, B. Wang, W. Y. Feng, Z. Wang and Y. L. Zhao, *Chin. J. Anal. Chem.*, 2010, **38**, 902–908.
208 S. H. He, W. B. Shi, X. D. Zhang, J. A. Li and Y. M. Huang, *Talanta*, 2010, **82**, 377–383.
209 W. W. He, X. C. Wu, J. B. Liu, X. N. Hu, K. Zhang, S. A. Hou, W. Y. Zhou and S. S. Xie, *Chem. Mater.*, 2010, **22**, 2988–2994.
210 L. L. Hu, T. Song, Q. F. Ma, C. F. Chen, W. D. Pan, C. L. Xie, L. Nie and W. H. Yang, in *8th International Conference on the Scientific and Clinical Applications of Magnetic Carriers*, American Institute of Physics, Melville, 2010, pp. 369–374.
211 Y. Jv, B. X. Li and R. Cao, *Chem. Commun.*, 2010, **46**, 8017–8019.
212 W. Luo, Y. S. Li, J. Yuan, L. H. Zhu, Z. D. Liu, H. Q. Tang and S. S. Liu, *Talanta*, 2010, **81**, 901–907.
213 Y. J. Song, K. G. Qu, C. Zhao, J. S. Ren and X. G. Qu, *Adv. Mater.*, 2010, **22**, 2206–2210.
214 Y. J. Song, X. H. Wang, C. Zhao, K. G. Qu, J. S. Ren and X. G. Qu, *Chem.–Eur. J.*, 2010, **16**, 3617–3621.
215 R. Andre, F. Natalio, M. Humanes, J. Leppin, K. Heinze, R. Wever, H. C. Schroder, W. E. G. Muller and W. Tremel, *Adv. Funct. Mater.*, 2011, **21**, 501–509.
216 D. Bhattacharya, A. Baksi, I. Banerjee, R. Ananthakrishnan, T. K. Maiti and P. Pramanik, *Talanta*, 2011, **86**, 337–348.
217 H. Y. Chen, Y. Li, F. B. Zhang, G. L. Zhang and X. B. Fan, *J. Mater. Chem.*, 2011, **21**, 17658–17661.
218 W. Chen, J. Chen, A. L. Liu, L. M. Wang, G. W. Li and X. H. Lin, *ChemCatChem*, 2011, **3**, 1151–1154.
219 L. Cui, H. S. Yin, J. Dong, H. Fan, T. Liu, P. Ju and S. Y. Ai, *Biosens. Bioelectron.*, 2011, **26**, 3278–3283.
220 R. J. Cui, Z. D. Han and J. J. Zhu, *Chem.–Eur. J.*, 2011, **17**, 9377–9384.
221 Y. J. Guo, L. Deng, J. Li, S. J. Guo, E. K. Wang and S. J. Dong, *ACS Nano*, 2011, **5**, 1282–1290.
222 Y. J. Guo, J. Li and S. J. Dong, *Sens. Actuators, B*, 2011, **160**, 295–300.
223 L. L. Ju, Z. Y. Chen, L. Fang, W. Dong, F. G. Zheng and M. R. Shen, *J. Am. Ceram. Soc.*, 2011, **94**, 3418–3424.
224 M. Liu, H. M. Zhao, S. Chen, H. T. Yu and X. Quan, *Chem. Commun.*, 2012, **48**, 7055–7057.
225 S. Liu, J. Q. Tian, L. Wang, Y. L. Luo and X. P. Sun, *RSC Adv.*, 2012, **2**, 411–413.
226 Y. J. Long, Y. F. Li, Y. Liu, J. J. Zheng, J. Tang and C. Z. Huang, *Chem. Commun.*, 2011, **47**, 11939–11941.
227 M. Ma, Y. Zhang and N. Cu, *Colloids Surf., A*, 2011, **373**, 6–10.
228 H. Y. Niu, D. Zhang, S. X. Zhang, X. L. Zhang, Z. F. Meng and Y. Q. Cai, *J. Hazard. Mater.*, 2011, **190**, 559–565.
229 F. L. Qu, T. Li and M. H. Yang, *Biosens. Bioelectron.*, 2011, **26**, 3927–3931.
230 W. B. Shi, Q. L. Wang, Y. J. Long, Z. L. Cheng, S. H. Chen, H. Z. Zheng and Y. M. Huang, *Chem. Commun.*, 2011, **47**, 6695–6697.
231 W. B. Shi, X. D. Zhang, S. H. He and Y. M. Huang, *Chem. Commun.*, 2011, **47**, 10785–10787.
232 Z. W. Tang, H. Wu, Y. Y. Zhang, Z. H. Li and Y. H. Lin, *Anal. Chem.*, 2011, **83**, 8611–8616.
233 H. Wang and Y. M. Huang, *J. Hazard. Mater.*, 2011, **191**, 163–169.
234 X. H. Wang, K. G. Qu, B. L. Xu, J. S. Ren and X. G. Qu, *Nano Res.*, 2011, **4**, 908–920.
235 V. Borelli, E. Trevisan, F. Vita, C. Bottin, M. Melato, C. Rizzardi and G. Zabucchi, *J. Toxicol. Environ. Health, Part A*, 2012, **75**, 603–623.
236 W. Chen, J. Chen, Y. B. Feng, L. Hong, Q. Y. Chen, L. F. Wu, X. H. Lin and X. H. Xia, *Analyst*, 2012, **137**, 1706–1712.
237 X. Chen, X. D. Zhou and J. M. Hu, *Anal. Methods*, 2012, **4**, 2183–2187.
238 A. K. Dutta, S. K. Maji, D. N. Srivastava, A. Mondal, P. Biswas, P. Paul and B. Adhikary, *ACS Appl. Mater. Interfaces*, 2012, **4**, 1919–1927.
239 A. K. Dutta, S. K. Maji, D. N. Srivastava, A. Mondal, P. Biswas, P. Paul and B. Adhikary, *J. Mol. Catal. A: Chem.*, 2012, **360**, 71–77.
240 G. Guan, L. Yang, Q. Mei, K. Zhang, Z. Zhang and M. Y. Hang, *Anal. Chem.*, 2012, **84**, 9492–9497.

241 F. F. Guo, W. Yang, W. Jiang, S. Geng, T. Peng and J. L. Li, *Environ. Microbiol.*, 2012, **14**, 1722–1729.
242 W. W. He, H. M. Jia, X. X. Li, Y. Lei, J. Li, H. X. Zhao, L. W. Mi, L. Z. Zhang and Z. Zheng, *Nanoscale*, 2012, **4**, 3501–3506.
243 M. I. Kim, J. Shim, H. J. Parab, S. C. Shin, J. Lee and H. G. Park, *J. Nanosci. Nanotechnol.*, 2012, **12**, 5914–5919.
244 Y. Y. Li, C. Qin, C. Chen, Y. C. Fu, M. Ma and Q. J. Xie, *Sens. Actuators, B*, 2012, **168**, 46–53.
245 C. W. Lien, C. C. Huang and H. T. Chang, *Chem. Commun.*, 2012, **48**, 7952–7954.
246 S. Liu, J. Q. Tian, L. Wang and X. P. Sun, *Sens. Actuators, B*, 2012, **165**, 44–47.
247 S. Liu, J. Q. Tian, L. Wang, Y. W. Zhang, Y. L. Luo, H. Y. Li, A. M. Asiri, A. O. Al-Youbi and X. P. Sun, *ChemPlusChem*, 2012, **77**, 541–544.
248 Y. H. Ma, Z. Y. Zhang, C. L. Ren, G. Y. Liu and X. G. Chen, *Analyst*, 2012, **137**, 485–489.
249 S. K. Maji, A. K. Dutta, P. Biswas, D. N. Srivastava, P. Paul, A. Mondal and B. Adhikary, *Appl. Catal., A*, 2012, **419**, 170–177.
250 S. K. Maji, A. K. Dutta, S. Dutta, D. N. Srivastava, P. Paul, A. Mondal and B. Adhikary, *Appl. Catal., B*, 2012, **126**, 265–274.
251 S. K. Maji, A. K. Dutta, D. N. Srivastava, P. Paul, A. Mondal and B. Adhikary, *J. Mol. Catal. A: Chem.*, 2012, **358**, 1–9.
252 B. Malvi, C. Panda, B. B. Dhar and S. Sen Gupta, *Chem. Commun.*, 2012, **48**, 5289–5291.
253 Y. Nangia, B. Kumar, J. Kaushal and C. R. Suri, *Anal. Chim. Acta*, 2012, **751**, 140–145.
254 P. Roy, Z. H. Lin, C. T. Liang and H. T. Chang, *Chem. Commun.*, 2012, **48**, 4079–4081.
255 A. D. Ryabov, R. Cerón-Camacho, O. Saavedra-Díaz, M. A. Denardo, A. Ghosh, R. Le Lagadec and T. J. Collins, *Anal. Chem.*, 2012, **84**, 9096–9100.
256 J. H. Shi, L. Z. Tong, D. M. Liu and H. Yang, *J. Nanopart. Res.*, 2012, **14**, 9.
257 L. Su, J. Feng, X. M. Zhou, C. L. Ren, H. H. Li and X. G. Chen, *Anal. Chem.*, 2012, **84**, 5753–5758.
258 J. Q. Tian, S. Liu, Y. L. Luo and X. P. Sun, *Catal. Sci. Technol.*, 2012, **2**, 432–436.
259 G. Q. Xie, P. X. Xi, H. Y. Liu, F. J. Chen, L. Huang, Y. J. Shi, F. P. Hou, Z. Z. Zeng, C. W. Shao and J. Wang, *J. Mater. Chem.*, 2012, **22**, 1033–1039.
260 J. F. Yin, H. Q. Cao and Y. X. Lu, *J. Mater. Chem.*, 2012, **22**, 527–534.
261 W. Zhang, X. Y. Liu, D. Walsh, S. Y. Yao, Y. Kou and D. Ma, *Small*, 2012, **8**, 2948–2953.
262 Y. W. Zhang, J. Q. Tian, S. Liu, L. Wang, X. Y. Qin, W. B. Lu, G. H. Chang, Y. L. Luo, A. M. Asiri, A. O. Al-Youbi and X. P. Sun, *Analyst*, 2012, **137**, 1325–1328.
263 L. Deng, S. J. Guo, Z. J. Liu, M. Zhou, D. Li, L. Liu, G. P. Li, E. K. Wang and S. J. Dong, *Chem. Commun.*, 2010, **46**, 7172–7174.
264 V. Figueroa-Espi, A. Alvarez-Paneque, M. Torrens, A. J. Otero-Gonzalez and E. Reguera, *Colloids Surf., A*, 2011, **387**, 118–124.
265 S. Shin, H. Yoon and J. Jang, *Catal. Commun.*, 2008, **10**, 178–182.
266 J. B. Jia, B. Q. Wang, A. G. Wu, G. J. Cheng, Z. Li and S. J. Dong, *Anal. Chem.*, 2002, **74**, 2217–2223.
267 C. L. Guo, Y. H. Song, H. Wei, P. C. Li, L. Wang, L. L. Sun, Y. J. Sun and Z. Li, *Anal. Bioanal. Chem.*, 2007, **389**, 527–532.
268 Z. L. Liu, B. Zhao, Y. Shi, C. L. Guo, H. B. Yang and Z. A. Li, *Talanta*, 2010, **81**, 1650–1654.
269 K. Wang, J. J. Xu, D. C. Sun, H. Wei and X. H. Xia, *Biosens. Bioelectron.*, 2005, **20**, 1366–1372.
270 A. D. Ellington and J. W. Szostak, *Nature*, 1990, **346**, 818–822.
271 H. Wei, B. L. Li, J. Li, E. K. Wang and S. J. Dong, *Chem. Commun.*, 2007, 3735–3737.
272 B. L. Li, Y. Du, H. Wei and S. J. Dong, *Chem. Commun.*, 2007, 3780–3782.
273 B. L. Li, H. Wei and S. J. Dong, *Chem. Commun.*, 2007, 73–75.
274 Y. Wang, H. Wei, B. Li, W. Ren, S. Guo, S. Dong and E. Wang, *Chem. Commun.*, 2007, 5220–5222.
275 Y. M. Zhai, J. F. Zhai, M. Zhou and S. J. Dong, *J. Mater. Chem.*, 2009, **19**, 7030–7035.
276 P. Beltrame, M. Comotti, C. Della Pina and M. Rossi, *J. Catal.*, 2004, **228**, 282–287.
277 L. B. Zhang, L. Laug, W. Munchgesang, E. Pippel, U. Gosele, M. Brandsch and M. Knez, *Nano Lett.*, 2010, **10**, 219–223.
278 S. J. Guo and S. J. Dong, *Chem. Soc. Rev.*, 2011, **40**, 2644–2672.
279 H. W. Kroto, J. R. Heath, S. C. Obrien, R. F. Curl and R. E. Smalley, *Nature*, 1985, **318**, 162–163.
280 P. J. Krusic, E. Wasserman, P. N. Keizer, J. R. Morton and K. F. Preston, *Science*, 1991, **254**, 1183–1185.
281 H. Tokuyama, S. Yamago, E. Nakamura, T. Shiraki and Y. Sugiura, *J. Am. Chem. Soc.*, 1993, **115**, 7918–7919.
282 A. S. Boutorine, H. Tokuyama, M. Takasugi, H. Isobe, E. Nakamura and C. Helene, *Angew. Chem., Int. Ed. Engl.*, 1995, **33**, 2462–2465.
283 L. L. Dugan, E. G. Lovett, K. L. Quick, J. Lotharius, T. T. Lin and K. L. O'Malley, *Parkinsonism Relat. Disord.*, 2001, **7**, 243–246.
284 S. S. Ali, J. I. Hardt and L. L. Dugan, *Nanomed.: Nanotechnol., Biol. Med.*, 2008, **4**, 283–294.
285 B. Belgorodsky, L. Fadeev, V. Ittah, H. Benyamini, S. Zelner, D. Huppert, A. B. Kotlyar and M. Gozin, *Bioconjugate Chem.*, 2005, **16**, 1058–1062.
286 K. L. Quick, S. S. Ali, R. Arch, C. Xiong, D. Wozniak and L. L. Dugan, *Neurobiol. Aging*, 2008, **29**, 117–128.
287 T. Rhadfi, J. Y. Piquemal, L. Sicard, F. Herbst, E. Briot, M. Benedetti and A. Atlamsani, *Appl. Catal., A*, 2010, **386**, 132–139.
288 D. Zhu, J. J. Luo, X. Y. Rao, J. J. Zhang, G. F. Cheng, P. G. He and Y. Z. Fang, *Anal. Chim. Acta*, 2012, **711**, 91–96.
289 Y. M. Lee, M. A. Garcia, N. A. F. Huls and S. H. Sun, *Angew. Chem., Int. Ed.*, 2010, **49**, 1271–1274.
290 U. T. Bornscheuer, G. W. Huisman, R. J. Kazlauskas, S. Lutz, J. C. Moore and K. Robins, *Nature*, 2012, **485**, 185–194.
291 P. Pengo, S. Polizzi, L. Pasquato and P. Scrimin, *J. Am. Chem. Soc.*, 2005, **127**, 1616–1617.
292 P. Pengo, L. Baltzer, L. Pasquato and P. Scrimin, *Angew. Chem., Int. Ed.*, 2007, **46**, 400–404.

293 R. Bonomi, F. Selvestrel, V. Lombardo, C. Sissi, S. Polizzi, F. Mancin, U. Tonellato and P. Scrimin, *J. Am. Chem. Soc.*, 2008, **130**, 15744–15745.
294 Z. M. Zhang, Q. A. Fu, X. Q. Li, X. Huang, J. Y. Xu, J. C. Shen and J. Q. Liu, *JBIC, J. Biol. Inorg. Chem.*, 2009, **14**, 653–662.
295 D. Zaramella, P. Scrimin and L. J. Prins, *J. Am. Chem. Soc.*, 2012, **134**, 8396–8399.
296 G. Pieters and L. J. Prins, *New J. Chem.*, 2012, **36**, 1931–1939.
297 M. Mahmoudi, K. Azadmanesh, M. A. Shokrgozar, W. S. Journeay and S. Laurent, *Chem. Rev.*, 2011, **111**, 3407–3432.
298 M. Horie, H. Kato, K. Fujita, S. Endoh and H. Iwahashi, *Chem. Res. Toxicol.*, 2012, **25**, 605–619.
299 O. I. Wilner, Y. Weizmann, R. Gill, O. Lioubashevski, R. Freeman and I. Willner, *Nat. Nanotechnol.*, 2009, **4**, 249–254.
300 R. Bhandari, R. Coppage and M. R. Knecht, *Catal. Sci. Technol.*, 2012, **2**, 256–266.
301 N. P. King, W. Sheffler, M. R. Sawaya, B. S. Vollmar, J. P. Sumida, I. Andre, T. Gonen, T. O. Yeates and D. Baker, *Science*, 2012, **336**, 1171–1174.
302 V. Köhler, Y. M. Wilson, M. Dürrenberger, D. Ghislieri, E. Churakova, T. Quinto, L. Knörr, D. Häussinger, F. Hollmann, N. J. Turne and T. R. Ward, *Nat. Chem.*, 2012, **5**, 93–99.